DOCTOR OF PHILOSOPHY

Regulation of dorsal raphe serotonergic neurons by histamine

Panetta, Kara Marie

Award date:
2014

Regulation of dorsal raphe serotonergic neurons by histamine

By

Kara Marie Panetta

BSc, Cell Biology (Hons)

University of St Andrews

A thesis submitted in candidature

for the degree of Doctor of Philosophy

University of Dundee

November 2013

Table of contents

List of figures

List of tables

Abbreviations

5-HT	Serotonin (5-hydroxytryptamine)
5-HTP	5-hydroxytryptophan
8-OH-DAT	8-hydroxy-2-(di-n-propy- lamino) tetralin
aCSF	Artificial cerebrospinal fluid
AMPA	α-Amino-3-hydroxy-5-methyl-4 isoxazolepropionic acid
ANCOVA	Analysis of covariance
ANOVA	Analysis of variance
AP	Action potential
ATP	Adenosine triphosphate
cAMP	Cyclic adenosine monophosphate
cGMP	Cyclic guanosine 3',5'-monophosphate
CNS	Central nervous sytem
CRF	Corticotropin releasing factor
CT	Circadian time
CV	Coefficient of variation
DAG	Diacylglycerol
DMSO	Dimethyl sulfoxide
DOI	2,5-dimethoxy-4-iodoamphetamine
DR	Dorsal raphe
DRC	Dorsal raphe caudal
DRD	Dorsal raphe dorsal
DRI	Dorsal raphe interfascicular
DRN	Dorsal raphe nucleus
DRV	Dorsal raphe ventral
DRVL	Dorsal raphe ventrolateral

ECS	Extracellular recording solution
EEG	Electroencephalogram
EMG	Electromyography
FDA	Food and drugs agency
FFT	Fast Fourier transform
GABA	gamma-aminobutyric acid
GAD	Glutamic acid decarboxylase
GDP-βS	Guanosine 5’-[β-thio]diphosphate
GPCR	G-protein coupled receptor
GEE	General estimating equation
GTP	Guanosine triphosphate
HBCD	Hydroxypropyl beta-cyclodextrin
HDC	Histidine decarboxylase
HNMT	Neuronal histamine N-methyltransferase
IC	Inhibitory concentration
ICS	Intracellular solution
ICV	Intracerebroventricular
IEI	Inter-event interval
i.p.	Intraperotineal
IP_3	Inositol triphosphate
IPSC	Inhibitory postsynaptic potential
i.v.	Intravenous
KO	Knock out
LDT	Laterodorsal tegmentum
LC	Locus coeruleus
LSD	Lysergic acid diethylamide
MAO	Monoamine oxidase

MC	Methyl cellulose
MCH	Melanin-concentrating hormone
MDL 100907	(R)-(+)-α-(2,3-Dimethoxyphenyl)-1-[2-(4 fluorophenyl)ethyl]-4 piperidinemethanol
mIPSC	Miniature inhibitory postsynaptic current
mlf	Medial longitudinal fasciculus
MnPO	Median preoptic nucelus
MnR	Median raphe
NBQX	2,3-dihydroxy-6-nitro-7-sulfamoyl-benzo[f]quinoxaline-2,3-dione
NC-IUPHAR	The Receptor Nomenclature Committee of the International Union of Pharmacology
NREM	Non-rapid eye movement
NVS	National veterinary supplies
OX	Orexin
pCPA	p-chlorophenylalanine
PE	Phenylephrine
PDT	Pedunculopontine tegmentum
PFC	Prefrontal cortex
PGO	Ponto-geniculo-occipital
PLC	Phospholipase C
QX-314	N-(2,6-Dimethylphenylcarbamoylmethyl) triethylammonium
REM	Rapid eye movement
RMS	Root mean square
SB 242084	6-Chloro-5-methyl-1-[[2-[(2-methyl-3-pyridyl)oxy]-5-pyridyl]carbamoyl]- indoline
SEM	Standard error of the mean
SERT	Selective serotonin transport

sIPSC	Spontaneous inhibitory postsynaptic current
SLD	Sublaterodorsal nucleus
SN	Substantia nigra
SWS	Slow-wave sleep
THIP	4,5,6,7-tetrahydroisoxazolo-[5,4-c]-pyridin-3-ol hydrochloride
TTX	Tetrodotoxin
TPH	Tryptophan hydroxylase
TRPC	Transient receptor potential channel
TMN	Tuberomammillary nucleus
VGLUT	Vesicular glutamate transporter
VLPAG	Ventrolateral periaqueductal gray
VLPO	Ventrolateral preoptic nucleus
VTA	Ventral tegmentum area
WT	Wild type
xscp	Decussion of the superior cerebellar peduncle

Acknowledgements

The completion of my PhD thesis represents the end of one of the most challenging and rewarding periods of my life. The journey has taught me so much more than I could have ever imagined, including the importance of maintaining a good work-life balance. I take this opportunity to thank the many wonderful people who have helped and supported me over these last four years.

First I would like to thank my academic supervisors, Dr Delia Belelli and Professor Jeremy Lambert, for giving me the opportunity to carry out these studies and for all of their support and guidance. I would like to thank my industrial supervisor, Dr Keith Wafford for all of his help and encouragement especially during the most difficult final few months. I would also like to thank my monitoring committee chaired by Professor Tim Hales for providing excellent advice regarding experiments and my thesis.

Many thanks have to go to Dr Murray Herd, Dr Ben Gunn, Dr Edward McGuire, Dr Elizabeth Mitchell, Dr Michelle Cooper, Dr Adam Brown, Mr Scott Greig, Mrs Linda Cunningham, Dr Stephen Humble, Mr Harry Donaldson, Mrs Lyn Dyer, Dr Elaine Shanks and Dr Keith Phillips. All of these incredible people have helped to teach me the techniques I have used and also helped with the many technical, theoretical and administrative problems I encountered.

Special thanks must go to Dr Lori-An Etherington, Dr Joanne Wallace, Dr Olivia Monteiro and Miss Casmira Brazaitis for their love and laughter throughout the most difficult points of my PhD. I will be eternally grateful for their friendship. I would like to thank all of my family and friends for putting up with me during the ups and downs of my PhD, especially my parents, in-laws, brother and my sisters. Also thank you to all of my friends from home. Particular thanks must go my husband, Alan. Without his unwavering love, support and encouragement this would not have been possible. Lastly I must thank my loved ones who didn't get to see me finish, my grandmother Eileen Glass, my grandfather Walter Dudgeon and my friend Stuart Campbell. I know how proud they would be.

Candidate's declaration

I declare that I am the author of this thesis and that it is a true record of the work performed by me. The thesis has not been previously submitted for application for a higher degree. All sources of information used in the preparation of this thesis have consulted and are cited correctly. This work has been carried out in the Centre for Neuroscience, Division of Medical Sciences, University of Dundee, under the supervision of Dr Delia Belelli and Prof. Jeremy Lambert. This work was also carried out in Eli Lilly, Surrey under the supervision of Dr Keith Wafford.

Signed,

Kara Panetta

Supervisor's declaration

We certify that Kara Panetta has completed 9 terms of experimental research with an industrial placement and that she has fulfilled the conditions of Ordinance 39, University of Dundee, such that she is eligible to submit the following thesis in application for the degree of Doctor of Philosophy.

Doctor Delia Belelli

Professor Jeremy Lambert

Doctor Keith Wafford

Abstract

Neural control of the sleep-wake cycle results from the complex interaction of neurotransmitters systems, which arise from anatomically and chemically defined brain structures. Serotonergic neurons located in the dorsal raphe nucleus (DRN) are currently accepted to be wake-promoting however their precise regulation by other neurotransmitter systems during the sleep-wake cycle is currently unknown. The main aim of this study was to utilise *in vitro* and *in vivo* electrophysiological techniques in order to elucidate the intra-raphe regulation of serotonergic neurons.

In vitro, single-unit recordings from putative serotonin (5-HT) neurons revealed that these neurons fired spontaneously in acute brain slices taken from mice. Initial pharmacological investigations revealed that putative 5-HT neurons in the DRN were under regulatory control by α_1-adrenoreceptors, 5-HT_2 receptors, orexin receptors and histamine receptors. *In vitro*, patch-clamp studies were performed in order to extend the investigation of 5-HT_2, orexin and histamine receptors further in the hope of understanding the cellular mechanisms responsible for their actions. Most interestingly, histamine produced a large inward current, depolarisation and excitation of putative 5-HT neurons in the DRN. Histamine was shown to mediate its effects predominantly via the H_1 receptor subtype and furthermore this receptor was observed to be constitutively active in the acute brain slice.

In vivo, single unit recordings from putative 5-HT neurons were performed in order to assess the role of the H_1 receptor further. Recordings were made from the DRN of anaesthetised, head-restrained rats. Pharmacological inhibition of H_1 receptors reduced the firing of putative 5-HT neurons, confirming the functional activity of these receptors in the intact brain. In order to investigate the significance of H_1 receptor blockade on the sleep-wake cycle, electroencephalogram (EEG) recordings were performed. EEG recordings revealed that blocking H_1 receptors caused a significant increase in the amount of non-rapid eye movement (NREM) sleep. The data reported here could have important clinical implications in the discovery of novel sleep therapies which target the serotonergic and/or the histaminergic system.

Chapter 1:

Introduction

1.1 The sleep-wake cycle

Sleep is a universal phenomenon which has been observed in almost every animal species studied. In humans it is essential for our cognitive and physical wellbeing (Alhola & Polo-Kantola, 2007; Neu *et al*., 2010), however a precise understanding of how and why we sleep is far from complete. Sleep is defined behaviourally by a number of criteria including: reduced motor activity, decreased response to stimulation, stereotypic postures, and relative ease of reversibility (distinguishing it from coma, hibernation and anaesthesia) (Rechtschaffen & Siegal, 2000). The transition from waking to sleep is accompanied by obvious changes to the electrical activity of the brain, most commonly recorded by electroencephalogram (EEG) (Figure 1, top). During wakefulness the cortical EEG displays high-frequency, low amplitude waves however as an individual "falls" asleep the EEG transitions progressively into slow-frequency, high voltage waves representing non-rapid eye movement or slow-wave sleep (NREM or SWS) (Dement & Kleitman, 1957). The high-frequency, low amplitude activity is associated with behavioural activation and is often referred to as "desynchronised" activity, whereas the slow-frequency, high amplitude EEG activity reflects the synchronous alternation between firing and inactivity of a large population of neurons in the brain and is often referred to as "synchronised" activity (Steriade, 1994). The changes to the EEG are observed in humans and rodents however the timing is noticeably different. In humans the changes take anywhere from 10 seconds to a minute, whereas in rodents these changes can occur over a few seconds or less (Merica & Fortune, 2004; Tanaka *et al*., 2000). During NREM sleep the EEG is characterised by progressively slower frequencies and higher amplitude activities, moving from theta waves (4-8Hz) through to delta waves (0.5-4Hz). In humans NREM sleep is divided into 4 stages (I, II, III and IV: corresponding to the depth of sleep) whereas in rodents it is divided into 2 stages (NREM-1 and NREM-2), mimicking stages I-II and III-IV, respectively (Wafford & Ebert, 2008). In humans a typical NREM bout lasts from 40 minutes to an hour, whereas in rodents this is much shorter, typically lasting for a few minutes. Across four mammalian species including human and rat, the duration of sleep bouts positively correlated with the metabolic rate *per* unit body mass (Lo *et al*., 2004). The EEG then transitions from NREM into REM sleep, with lower voltage, higher frequency activity. During REM sleep, there is a complete loss of skeletal muscle tone, except those used for eye movements and breathing. REM sleep is most often accompanied by active dreaming however less lively

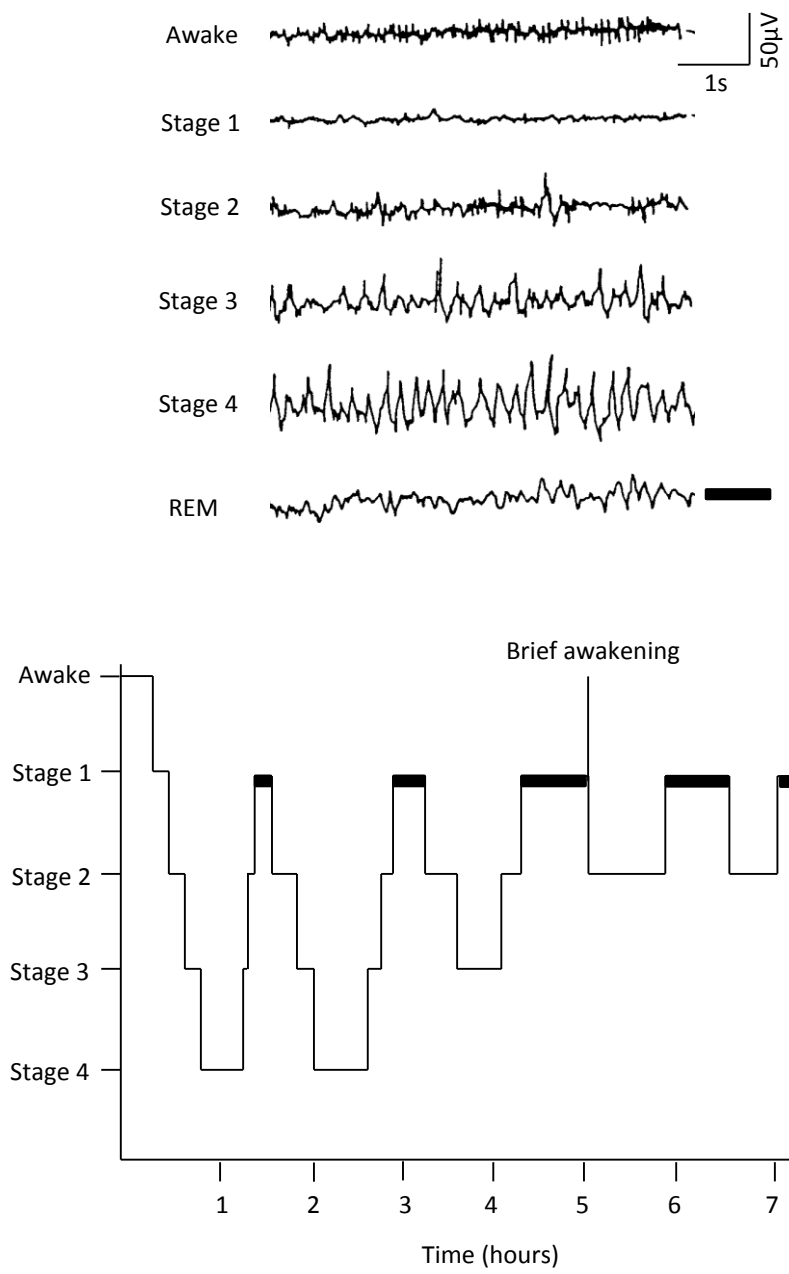

Figure 1.0 Sleep-wake parameters and measurements. Top: Electroencephalogram (EEG) activity of the brain during each stage of sleep: awake (high-frequency, low amplitude waves), stage 1 (theta waves), stage 2 (sleep spindles), stage 3 (0.5-4Hz waves), stage 4 (delta waves), REM (higher-frequency, low amplitude). Bottom: Sleep architecture over 7 hours showing the transition from wakefulness through to REM sleep. Note brief awakenings can occur. Adapted from Wafford *et al*, 2008 with permission.

dreaming is noted to occur during NREM sleep (Aserinsky & Kleitman, 1953; Foulkes, 1962). Over the sleep period (12-18 minutes in rats and about 90 minutes in humans) an ordered cycle is usually maintained from NREM to REM to wake however switching may occur between NREM and REM and brief awaking can interrupt the cycle (Figure 1.0, bottom).

1.1.1. Two-process model of sleep

Sleep propensity is governed by two distinct processes: a circadian regulator (Process C), defining the diurnal rhythm and a homeostatic regulator (Process S), defining the interaction between wake time and sleep time (Borbély, 1982; Daan *et al*., 1984). Homeostatic regulation of sleep refers to the observation that sleep is prolonged and often more profound after long periods of waking. An increase in the amount of slow-wave (delta) EEG during subsequent compensatory NREM sleep opposes sleep fragmentation and hence improves sleep continuity. The nature of homeostatic drive for sleep has been the subject of much consideration, with some researchers suggesting that the build-up of a regulatory "sleep-factor" (possibly adenosine) promotes sleep (Strecker *et al*., 2000). Circadian regulation of sleep originates in the suprachiasmatic nuclei (SCN) and is often referred to as the 'biological clock' (Easton *et al*., 2004). Circadian timing originates from the hierarchy of circadian oscillators in the SCN which receive light information from the retinohypothalmic tract entraining the clock to an almost 24-hour cycle of activity (Reppert & Weaver, 2002). Positive and negative transcriptional feedback loops drive repetitive rhythms in RNA and protein levels of important clock genes e.g. *Clock*, *Bmal*, *Per1* and *Per2*. Peripheral molecular clocks located in the kidney, liver and pancreas are controlled by the central SCN clock in order to align metabolic activities with environmental conditions (Reppert & Weaver, 2002). Over time, the two-process model of sleep has been extended by some to include a third process (Process W). The wake component (W) represents reduced levels of alertness normally observed after waking, also referred to as "sleep inertia" (Folkard & Åkerstedt, 1992). Models of sleep have been used by neurobiologists to development mathematical models to evaluate the impact of shift work and travel schedules (Åkerstedt, 1998; Åkerstedt & Folkard, 1997).

1.1.2 Wake-promoting networks

The neural control of the sleep-wake cycle results from the complex interaction of transmitter systems which arise from anatomically and chemically-defined structures within the brain. Current models of the arousal system are based on seminal studies which demonstrated that the rostral brainstem (i.e. midbrain and pons) contains an "ascending reticular activating system" responsible for producing EEG desynchrony and arousal (Moruzzi & Magoun, 1949). Subsequent studies have revealed that the cell groups at the mesopontine junction responsible for arousal consist of cholinergic and monoaminergic neurons (Levey *et al*., 1987; Rye *et al*., 1987). Cholinergic neurons in the pedunculopontine and laterodorsal tegmental nuclei (PPT and LDT) provide major innervation from the mesopontine junction to the thalamic relay nuclei and reticular nucleus as well as the lateral hypothalamus and basal forebrain (Figure 1.1.) (Hallenger *et al*., 1987; Satoh *et al*., 1986). Cholinergic nuclei are heterogeneous, with neurons exhibiting high rates of firing during wakefulness ("wake-on") and also during REM sleep ("REM-on") (Steriade *et al*., 1990). Monoaminergic cell groups at the mesopontine junction which project to the forebrain include noradrenaline from the locus coeruleus (LC) and serotonin (5-HT) from the dorsal and median raphe nuclei (DR and MnR) (Saper *et al*., 2010). In addition, histaminergic neurons from the tuberomamillary nucleus (TMN) and dopaminergic neurons from the ventral tegmentum area (VTA) and substantia nigra (SN) also project to the forebrain (Saper *et al*., 2010). These monoaminergic cell groups innervate the lateral hypothalamus, basal forebrain and cerebral cortex (Krout *et al*., 2002). In addition they also innervate the thalamus, specifically targeting the intralaminar and reticular nuclei (Krout *et al*., 2002; Vertes, 1991). In general, neurons from these nuclei fire at greater rates during wakefulness, decrease activity during NREM sleep and cease firing during REM sleep (Sakai *et al*., 2011; Takahashi *et al*., 2006, 2010). One major exception is the dopaminergic neurons which tend not to change their firing across the sleep-wake cycle (Miller *et al*., 1983).

Another important arousal system is located in the lateral hypothalamus, just dorsal and rostral to the histaminergic neurons of the TMN (Bernardis & Bellinger, 1996). Neurons in the lateral hypothalamus contain orexin neuropeptides (orexin-A and -B, also known as hypocretin-1 and -2). Orexin neurons send axons to the entire cerebral cortex, in addition to the brainstem and basal forebrain (Nambu *et al*., 1999; Peyron *et al*., 1998a). Importantly

orexin neurons innervate the LC, TMN, DRN as well LDT and thalamus (Peyron *et al*., 1998a). Orexin neurons exhibit a similar firing pattern to the other arousal nuclei, firing at greater frequencies during sleep, slowing during NREM and falling silent during REM sleep (Takahashi *et al*., 2008). Orexin-directed lesions (Gerashchenko *et al*., 2001) and orexin receptor "knock-out" mouse (Chemelli *et al*., 1999) studies have revealed a role for orexin neurons in the sleep condition narcolepsy. The apparent role of orexin in narcolepsy suggests that the role of these neurons might be to sustain wakefulness especially *via* the excitation of the other arousal systems. The basal forebrain provides an additional sub-cortical population of arousal-promoting neurons. Many basal forebrain neurons contain either acetylcholine, gamma-amino-butyric acid (GABA) or glutamate (Manns *et al*., 2001). Many of these basal forebrain neurons are wake-active and thought to produce EEG desynchronisation *via* activation (acetylcholine and glutamate) and inhibition (GABA) of cortical circuits (Henny & Jones, 2008; Jones, 2004). The thalamus plays an important role in gating the transmission between subcortical/brainstem nuclei and the cortex. Thalamocortical transmission is modulated *via* GABAergic neurons in the reticular nucleus which have an inhibitory influence over the thalamic relay nuclei (Steriade, 2005). Arousal nuclei, including serotonergic and histaminergic neurons, innervate the reticular nucleus, which may represent an important mechanism by which arousal nuclei modulate activity within thalamocortical circuits (Manning *et al*., 1996; Rodriguez *et al*., 2011).

1.1.3 NREM sleep-promoting networks

Between 1917 and 1931 the neurologist Dr Constantin von Economo reported that patients suffering from encephalitis lethargica had symptoms which manifested as either profound insomnia, or somnolence (reviewed by Triarhou, 2006). He discovered that patients with lesions in the pre-optic area near the rostral end of the third ventricle presented with insomnia. It was a further half a century before the exact population of sleep-promoting neurons was discovered in the ventrolateral pre-optic nucleus (VLPO) (Sherin *et al*., 1996). VLPO neurons were shown to contain the inhibitory neurotransmitters GABA and galanin, the majority of which fire fastest during NREM and REM sleep (Takahashi *et al*., 2009). Furthermore, it was demonstrated that the VLPO contained a dense core of sleep-active neurons that projected to the TMN and a diffuse shell of neurons that projected to the DRN

and LC (Figure 1.1) (Lu *et al*., 2002; Sherin *et al*., 1998; Steininger *et al*., 2001). A second population of sleep-active, GABAergic neurons has been discovered in the median preoptic nucleus (MnPO) (Gong *et al*., 2000 and 2004). Interestingly, MnPO neurons have been shown to fire in advance of sleep, whereas VLPO neurons only fire during sleep (Szymusiak *et al*., 1998). Given that the MnPO provides a robust input into the VLPO it has been suggested that MnPO may drive the activity of the VLPO (Chou *et al*., 2002). VLPO neurons receive reciprocal inputs from a number of the arousal nuclei including the TMN, DRN and LC, whereas MnPO neurons receive only a sparse input (Saper & Levisohn, 1983; Uschakov *et al*., 2007). *In vitro* recordings have revealed that VLPO neurons are inhibited by acetylcholine, noradrenaline, dopamine and serotonin (Gallopin *et al*., 2000, 2004). This reciprocal inhibition between sleep-active VLPO neurons and wake-active monaminergic neurons has been proposed to form a "flip-flop switch" (Saper *et al*., 2001). According to this model, during sleep VLPO neurons would fire at greater rates and inhibit the monoaminergic nuclei, therefore disinhibiting and reinforcing their own firing. Conversely during wakefulness monoaminergic neurons would fire at higher frequencies and inhibit the VLPO neurons, thus dis-inhibiting their own firing (Figure 1.2).

1.1.4 REM sleep-promoting networks

Just prior to and during REM sleep, neurons in the pons, the lateral geniculate nucleus, and the occipital cortex fire bursts of high-voltage spikes (Lim *et al*., 2007). These ponto-geniculo-occipital (PGO) spikes, or waves, are time locked to bursts of firing in the PPT and LDT nuclei (Sakai & Jouvet, 1980). As discussed above, neurons in the LC, DRN and TMN are virtually silent during REM sleep. This reciprocal relationship hinted that cholinergic neurons from PPT and LDT may interact with the monoaminergic cell groups to regulate the switch between NREM and REM sleep. This suggestion was supported by the demonstration that application of cholinergic compounds (e.g. agonists and cholinesterase inhibitors) to the mesopontine area can produce REM sleep, whereas application of compounds that activate monoaminergic cell groups (e.g. MAO inhibitors and SSRIs) can inhibit REM sleep (Datta, 1997; Gervasoni *et* al., 2002; Luppi *et al*., 2007). A number of lesion studies have questioned the ability of these neurons to switch states between NREM and REM sleep, as destruction of the PPT or LDT had minimal effects on REM sleep (Lu *et al*., 2006). Therefore while these systems appear to modulate REM sleep, they are not likely to be involved in the switching mechanism

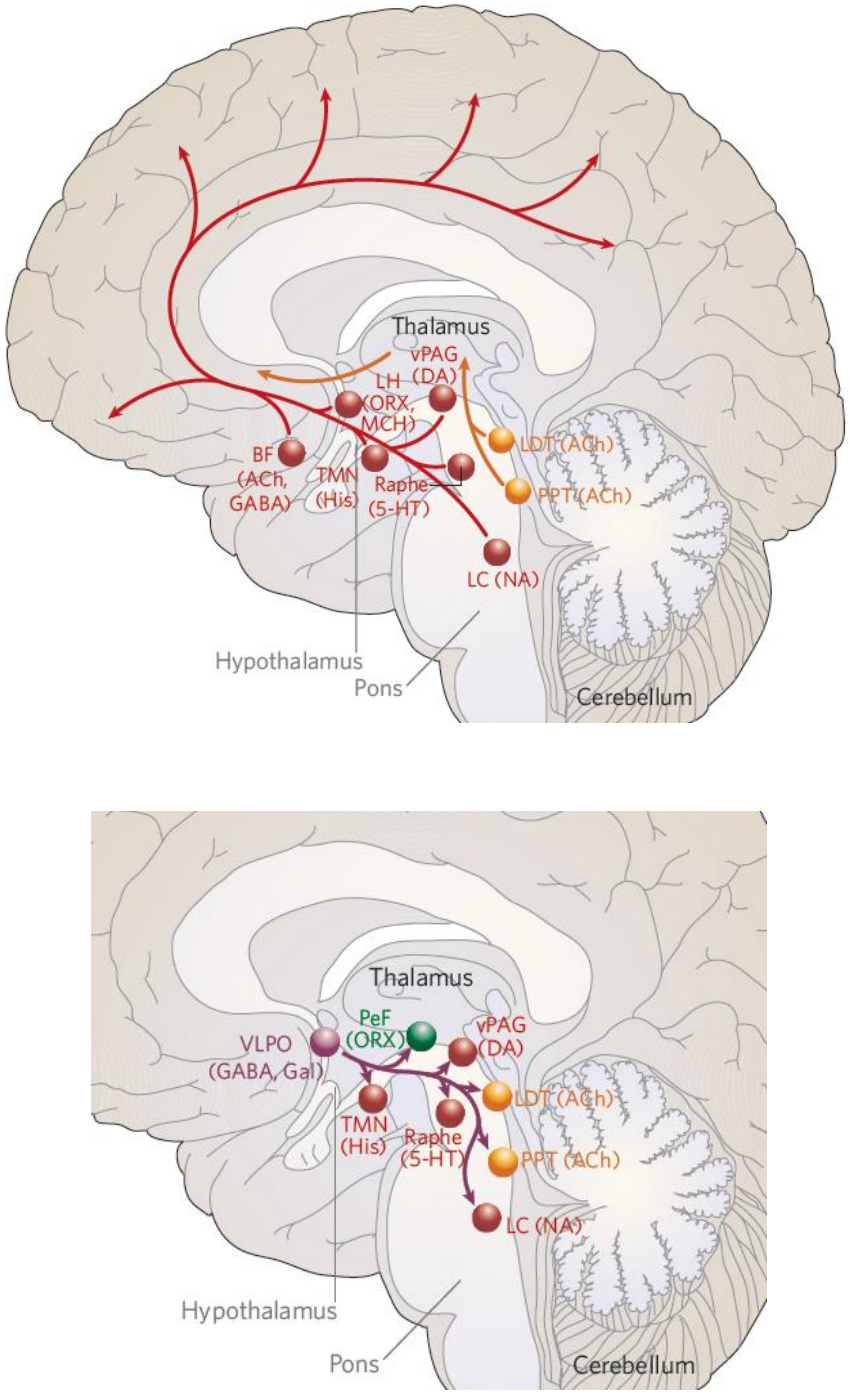

Figure 1.1. Components of the sleep-wake cycle. During wakefulness, cholinergic neurons from the LDT/PPT (yellow) provide the major innervation of the thalamus. A second pathway (red) arising from monoaminergic neurons from the brainstem provides direct input to the hypothalamus, basal forebrain and cortex. The orexin neurons of the LH maintain activity in the ascending arousal system. During sleep, GABAergic and galanergic neurons (purple) from the VLPO and MnPO project to and inhibit the ascending arousal centres. Taken from Saper *et al.*, 2005 with permission.

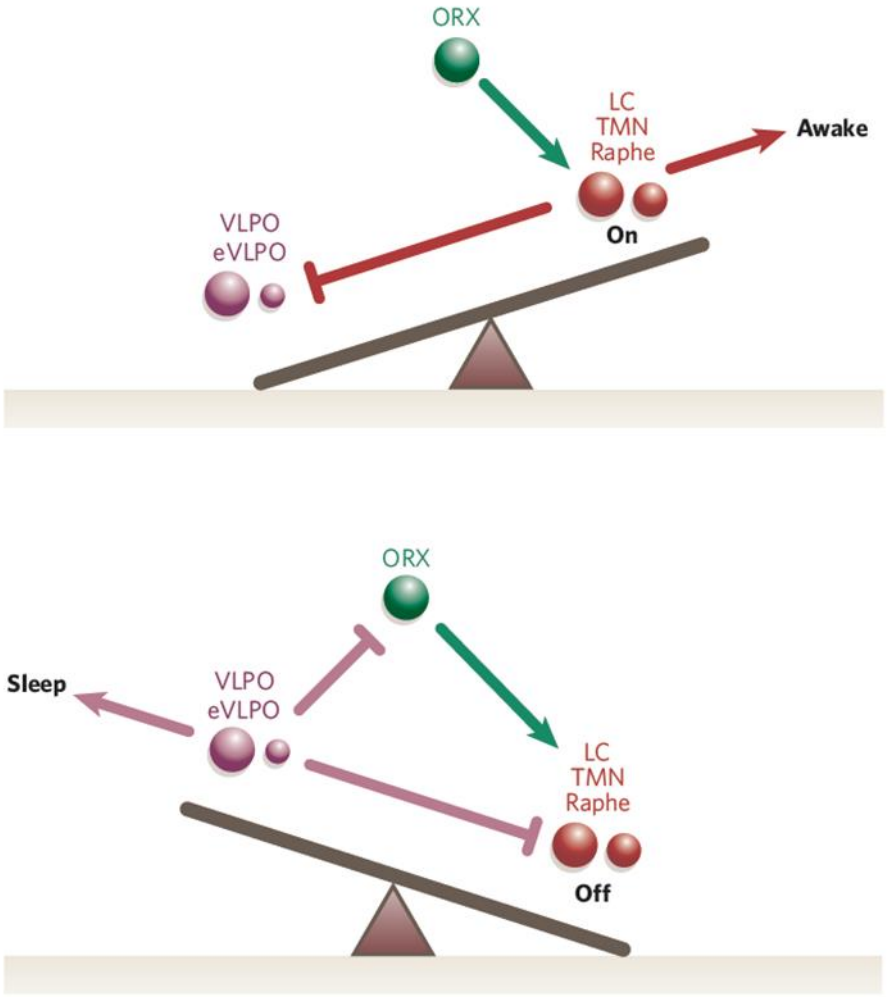

Figure 1.2. The sleep-wake switch. During wakefulness monoaminergic nuclei (red) inhibit GABAergic/galanergic VLPO nuclei (purple), thereby removing the inhibition of monoaminergic cells (LC, TMN and raphe) and cholinergic cells (LDT and PPT). Orexin neurons (green) act primarily to stabilise monoaminergic tone during wakefulness. During sleep VLPO neurons inhibit monoaminergic nuclei, thereby relieving their own inhibition. VLPO neurons also inhibit orexin neurons, further reinforcing monoaminergic inhibition during sleep. This mutual inhibition and excitation between nuclei forms a flip-flop switch, enabling sharp transitions between states, but is relatively unstable. Taken from Saper *et al*., 2005 with permission.

(Saper *et al*., 2010). Fos immunoreactivity studies have been utilised in order to try and discover the identity of the REM-promoting neurons. These studies have highlighted a number of cell groups in the pons that are active during REM sleep, including neurons in the sublaterodorsal nucleus (SLD), the precoeruleus region and medial parabrachial nucleus (Boissard *et al*., 2002; Lu *et al*., 2006). Retrograde tracers have revealed that GABAergic neurons from the ventrolateral periaqueductal grey (vlPAG) and LPT have a mutually inhibitory relationship with GABAergic neurons in the SLD (Lu *et al*., 2006) leading these authors to hypothesise that this mutual inhibition is the basis for NREM-REM sleep switching. Neurons that produce the peptide, melanin-concentrating hormone (MCH) are located in the lateral hypothalamus, in close proximity to orexin neurons (Bittencourt *et al*., 1992). These MCH neurons fire fastest during REM sleep and many neurons also contain GABA, endowing them with the ability to inhibit target neurons (Hassani *et al*., 2009; Jego *et al*., 2013). Given the wide spread projection of MCH neurons in the brain, including to the DRN and LC, it will be important in future studies to investigate the precise role for these neurons in REM sleep.

1.2 Serotonin

Serotonin, or 5-hydroxytryptamine (5-HT), is a biogenic monoamine with diverse effects in the central nervous system (CNS) as well as the periphery (Mohammad-Zadeh *et al*., 2008). It is biosynthetically derived from the essential amino acid tryptophan in a two-step enzymatic process. Tryptophan is first hydroxylated to 5-hydroxytryptophan (5-HTP) by tryptophan hydroxylase (the rate-limiting step) and then 5-HTP is decarboxylated to form 5-HT (Clark *et al*., 1954; Fitzpartick, 1999). Two isoforms of tryptophan hydroxylase have been identified, one which is expressed in the gut (*tph1*) (Walther *et al*., 2003) and one that is expressed exclusively in the brain (*tph2*) (Patel *et al*., 2004). Within the CNS, 5-HT is synthesised and stored in presynaptic terminals (serotonergic neurons, catecholaminergic neurons and the pineal gland). In the periphery, 5-HT storage is limited to enterochromomaffin cells and platelets (Rapport *et al*., 1948; Weiner & Undenfriend, 1957). The concentration of 5-HT in tissues is dependent upon the rate of synthesis and the rate of metabolism. The primary metabolic pathway for serotonin is via metabolism by monoamine oxidase (MAO) to 5-hydroxyindoleacetic acid (McIsaac & Page, 1959). In the CNS, neuronal depolarization causes the release of 5-HT into the synaptic cleft. Once in the synapse, 5-HT can bind to postsynaptic

5-HT receptors or presynaptic 5-HT autoreceptors to exert its actions (Fink & Göthert, 2007; Cerrito & Raiteri, 1979a, 1979b). The selective serotonin transporter (SERT) located on the presynaptic membrane removes 5-HT from the synaptic cleft (Ravna *et al*., 2009). Once inside the neurons, 5-HT is packaged back into synaptic vesicles where it is protected from metabolism. 5-HT remaining in the cytosol is rapidly metabolised by MAO (Jonnakuty & Gragnoli, 2008; Molinoff & Axelrod, 1971).

1.2.1 Serotonin receptors

The diverse effects of 5-HT are mediated via 5-HT receptors. There are currently seven families of 5-HT receptors (designated 5-HT_{1-7}) that are organised into fourteen subtypes, representing one of the most complex families of neurotransmitter receptors. The Receptor Nomenclature Committee of the International Union of Pharmacology (NC-IUPHAR) has proposed a classification scheme of 5-HT receptors based on pharmacological, transductional and structural information (Alexander *et al*., 2011). With the exception of the 5-HT_3 receptor, which is a ligand-gated ion channel, all 5-HT receptors are members of the G-protein coupled receptor (GPCR) superfamily. The NC-IUPHAR classifies serotonin GPCRs into distinct classes with corresponding subtypes: 5-HT_1 (5-$HT_{1A, B, D, e, F}$), 5-HT_2 (5-$HT_{2A, B, C}$), 5-HT_3 (5-$HT_{5a, b}$), 5-HT_4, 5-HT_6 and 5-HT_7 subtypes. This classification includes receptors which have been generated by alternative splicing of single genes (5-HT_4, 5-HT_7) and editing of the receptor RNA (5-$HT_{1B, D}$). Within a given receptor subtype class the overall amino acid sequence homology ranges between 40 and 63%, while the sequence homology between the different families ranges between 25 and 39% (Hoyer *et al*., 2002).

1.2.2 G-protein coupled receptors

GPCRs consist of seven transmembrane-spanning elements with prototypic domains determining agonist binding specificity and activation (Kobilka, 2007). The 5-HT GPCRs are classified as “type A”, rhodopsin-like receptors (Fredriksson *et al*., 2003). GPCRs transduce signals by activating one or more heterotrimeric G proteins which are composed of one α, β and γ subunit. G proteins are divided into four main classes based on the primary sequence

similarity of the Gα subunit: $G\alpha_S$, $G\alpha_i$, $G\alpha_q$ and $G\alpha_{12}$ (Oldham & Hamm, 2008). Each Gα subunit contains a GTPase domain which hydroylses GTP. Guanine nucleotide exchange leads to the dissociation of subunits from the receptor yielding a Gα-GDP monomer and a tightly interacting Gβγ dimer. These receptor-free monomer and dimer elements can modulate the activity of other intracellular proteins until the inactive form of the Gα subunit (Gα-GDP) is regenerated (Oldham & Hamm, 2008). GPCRs were classically thought to function as monomeric units however in recent years dimer/oligomer formation has been reported for many different GPCRs (Gurevich & Gurevich, 2008). The advent of new techniques including immunoprecipitation and resonance energy transfer has enabled researchers to propose that 5-HT_{1A}, 5-HT_{1B}, 5-HT_{1D}, 5-HT_{2C} and 5-HT_4 receptors form functional dimers (Herrick-Davis, 2004; Salim *et al*., 2004). The precise physiological significance of 5-HT receptor dimerisation is still unknown however it is speculated that dimerisation of GPCRs would enable ligand selectivity and/or activation of alternative intracellular pathways (Herrick-Davis, 2013).

A number of theoretical kinetic models have been developed in order to quantify the nonlinear coupling between receptor occupancy and response. In 1965 Monod, Wyman and Changeux proposed a model (referred to as the MWC model) that described the properties of "allosteric systems" (Monod *et al*, 1965). This model proposed that a receptor reversibly adopts two "states" and each state has a different affinity for the "allosteric" ligand. The sigmoidal nature of oxygen binding to haemoglobin and nicotinic cholinergic-mediated Na^+ influx and depolarization represent two processes consistent with this model (Karlin, 1967). The MWC model can be categorized as a "two-state model" where the two states of the receptor are described as: the inactive state (R) and the active state (R*) (Leff, 1995). In the absence of bound ligand the level of basal receptor activity is determined by the equilibrium between R and R* (Figure 1.3). The profile of a ligand can be characterized by its affinity for the receptor and intrinsic activity (efficacy). Agonists display positive intrinsic activity by binding to the receptor and stabilising R*. Partial agonists display varying degrees of affinity and intrinsic activities and produce a submaximal response. Interestingly, receptors can display spontaneous (constitutive) activity independent of ligand activation. Certain ligands can bind to these spontaneously active receptors and appose partial or full agonists by shifting the equilibrium from R* to R. These ligands are termed "inverse agonists" as they preferentially stabilize the receptor in its inactive (R) state and therefore have negative intrinsic activity.

Neutral antagonists do not possess intrinsic activity and therefore oppose the effects of agonists by preventing agonist binding and receptor activation. If receptors do not display spontaneous activity the same inverse agonist could behave as a competitive antagonist. Neutral antagonists lack intrinsic activity and can block actions produced by agonists and inverse agonists (Khilnani & Khilnani, 2011).

1.2.3 GPCRS and inverse agonism

As eluded to above, some receptors can spontaneously interact with G-proteins to initiate GTPase activity in the absence of bound ligands. This constitutive activity can be inhibited *in vitro* by the addition of inverse agonists (with either partial or full activity) whose activity opposes that of agonists. Experimental methods to detect constitutive receptor activity are based on the quantification of ligand affinity at R and R* (with binding assays) on the modulation of GTP binding and hydrolysis. Receptor agonists that activate receptors increase basal effector activity whereas inverse agonists decrease basal GPCR activity. Therefore spontaneous activity of GPCRs can be demonstrated by measuring cAMP levels, GTPase activity or IP_3 production in the presence of inverse agonists. Constitutive GPCR activity was first demonstrated at δ-opioid receptors (Costa & Hertz, 1989) and more recently in benzodiazepine receptors (Braestup *et al*., 1982) and 5-HT receptors (Herrick-Davis *et al*, 2000). It is now well recognized that many conventional GPCR antagonists (including antihistamines) are in fact inverse agonists. Constitutive activity may be present in native or mutated strains and such receptors may be under- or over-active leading to inherited diseases (Khilnani & Khilnani, 2011).

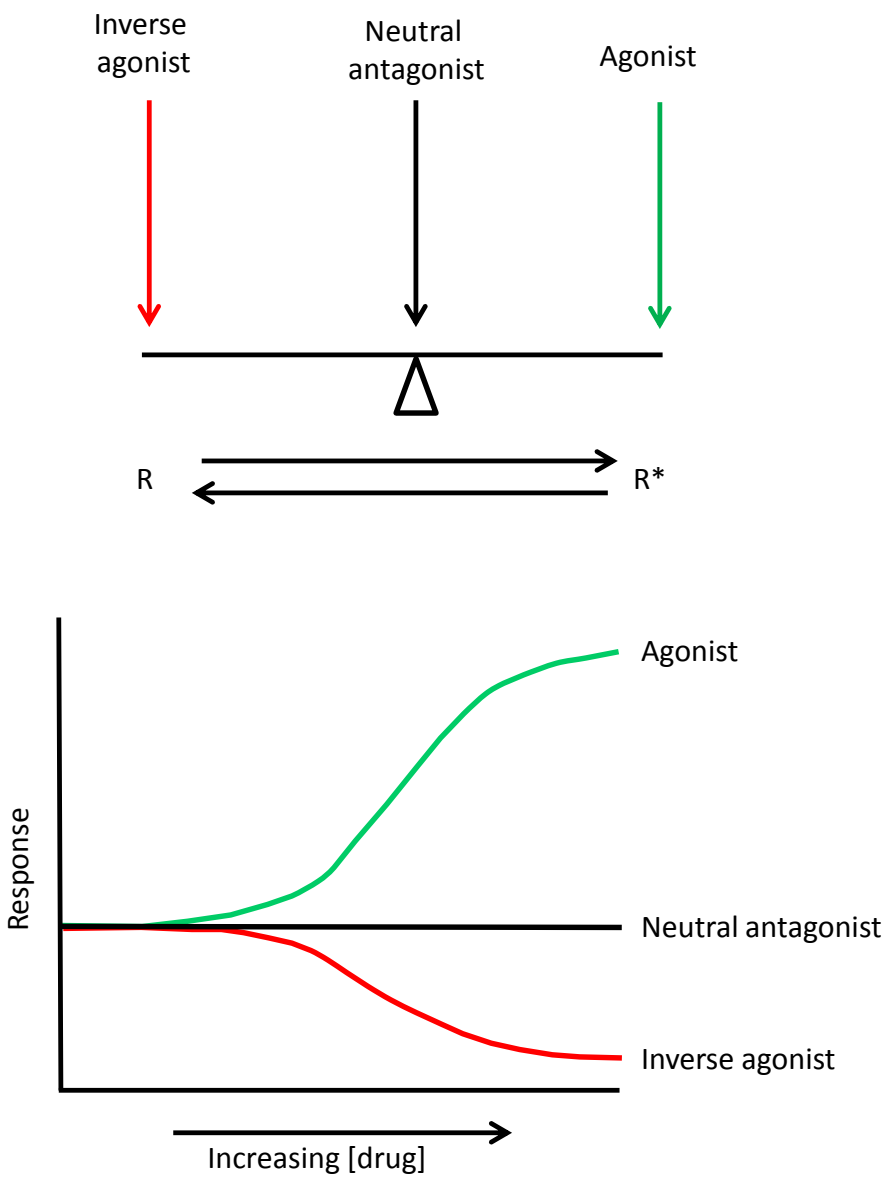

Figure 1.3. Schematic of ligand-receptor binding. Agonists bind to receptors, stabilize R* and display positive intrinsic activity. Neutral antagonists have equal preference for R and R* states, lack intrinsic activity and block the effects of either agonists or inverse agonists. Inverse agonists stabilize R and decrease basal receptor activation.

1.2.4 Signal transduction of 5-HT receptor subtypes

5-HT GPCRs bind to a number of different heterotrimeric G proteins to exert their effects. Receptors of the 5-HT_1 class couple preferentially, although not exclusively, to $G_{i/o}$. Activation of $G_{i/o}$ leads to inhibition of adenylate cyclase and reduced production of cyclic adenosine monophosphate (cAMP) (Hoyer *et al*., 2002). cAMP is an intracellular messenger that interacts with numerous targets including protein kinase A and cyclic nucleotide-gated ion channels (Nichols & Nichols, 2008). 5-HT_{1A} receptors are both located pre- and post-synaptically and are expressed on various neurons throughout the CNS (Aznavour *et al*., 2006; Palchaudhuri & Flugge, 2005). Activation of 5-HT_{1A} receptors in either location leads to neuronal hyperpolarization and reduced firing. Pre-synaptic 5-HT_{1A} autoreceptors in the DRN have been shown to mediate neuronal hyperpolarisation *via* G-protein coupled K^+ channels (Sprouse & Aghajanian, 1987). 5-HT_{1B} receptors are localised on axon terminals (Riad *et al*., 2000) where they can function as presynaptic heteroreceptors on non-serotonergic neurons or presynaptic autoreceptors on serotonin neurons (Sari, 2004). There has only been limited functional evidence of 5-HT_5 receptors in the brain (Goodfellow *et al*., 2012) and it is currently thought that 5-HT_5 receptors, like 5-HT_1, couple negatively to adenylate cyclase. However the development of selective antagonists and knock-out mice should enable a better understanding of these receptors in the future. Receptors of the 5-HT_2 class couple preferentially to $G_{q/11}$. Activation of $G_{q/11}$ leads to an increase in inositol phosphate production and an increase in cytosolic Ca^{2+} levels (Hoyer *et al*., 2002). 5-HT_2 receptors have widespread expression in the brain (McKenna & Saavedra, 1987; Pazos *et al*., 1985). 5-$HT_{2A/2C}$ receptors are the target of many hallucinogen drugs including DOI (Krebs-Thomson *et al*., 1998) while 5-HT_{2B} receptors play an important role during development, especially in the co-ordination of brain and heart formation (Nebigil *et al*., 2001). Receptors of the 5-HT_4, 5-HT_6 and 5-HT_7 classes couple positively to G_s and promote the formation of cAMP (Hoyer *et al*., 2002). In contrast to all of the other 5-HT receptors, the 5-HT_3 is a ligand gated ion channel. The 5-HT_3 receptor belongs to the cysteine-loop transmitter-gated receptor superfamily, which includes the $GABA_A$ receptor, glycine receptor, nicotinic acetylcholine receptor and the Zn^{2+} activated ion channel (Boess & Martin, 1994; Davies *et al*., 2003). 5-HT_3 receptors are located both pre- and post-synaptically throughout the brain where they trigger the depolarization of target cells via the opening of a nonselective cationic channel (Peters *et al*., 2010).

1.3 The dorsal raphe nucleus (DRN)

The distribution of brainstem serotonergic neurons in the rat brain has been elegantly discerned by histochemical fluorescence (Dahlstrom & Fuxe, 1964). The localisation of serotonergic cell bodies and axons was classified into 9 clusters: B1-B9, with the numbers indicating caudal-rostral order of the nuclei. The dorsal raphe nucleus (DRN), comprising of clusters B6 and B7, contains the largest group of serotonin neurons in the brainstem (Descarries *et al*., 1982; Vertes & Crane, 1997). The DR is located in the rostral pontine and caudal midbrain tegmentum and can be divided into several subregions based on cytoarchitectonic grounds, including the rostral, caudal (DRC), dorsal (DRD), ventral (DRV), ventrolateral (DRVL), and interfascicular (DRI) parts (Lowry *et al*., 2008). Serotonergic neurons are located throughout the rostral-caudal axis of the DRN, in all subdivisions of the DRN (Crawford *et al*., 2010). However, they predominate along the midline of the dorsal, rostral, and ventral subdivisions of the DRN (Abrams *et al*., 2004). Developmentally, by day 15 of gestation, serotonergic neurons can be observed throughout all subdivisions of the rat DRN (Jacobs & Azmita, 1992; Lauder & Bloom, 1974).

1.3.1 Morphology and neurochemistry of DRN 5-HT neurons

In the rat DR four cell types are observed: small and round, medium-sized and fusiform/bipolar, large and fusiform, and very large and multipolar (Steinbusch. 1981). These neurons are topographically organised within the different subdivisions of the DR, suggesting the possibility of functional differences of 5-HT neurons across the DR based on their morphology (Abrams *et al*., 2004). In addition to regional differences in the morphology of serotonergic neurons, immunohistochemical studies have demonstrated that topographically organised subpopulations of serotonergic neurons are chemically diverse. Serotonin is the major neurotransmitter in the DR (accounting for 30-70% of neurons, depending on the species) however serotonergic neurons have been shown to co-express different neurotransmitters and neuropeptides. In the rat, 5-HT neurons co-express the vesicular glutamate transporter 3 (VGLUT3) (Fermeau *et al*., 2002; Commons, 2009), the GABA synthesizing enzyme glutamic acid decarboxylase 67 (GAD67) (Shikanai *et al*., 2012), nitric oxide synthase, galanin (Xu & Hökfelt, 1997), and corticotropin-releasing factor (CRF)

(Commons *et al*., 2003). In the mouse, 5-HT neurons display a more restrictive neurochemical diversity, with neurons co-expressing GAD67, VGLUT3 and CRF (Fu *et al*., 2010).

1.3.2 Efferent and afferent projections of the DRN

Efferent outputs from the DR extend throughout the entire brain and provide the major source of 5-HT in the forebrain. Efferent projections of serotonergic neurons from DRN display a topographic organization along the rostral-caudal axis, with neurons located more rostrally projecting to more rostral areas of the brain and neurons located more caudally projecting to more caudal areas (Abrams *et al*., 2004). The DRN projects along three ascending pathways: the dorsal, medial and ventral pathways (Michelson *et al*., 2007). These pathways reach a multitude of targets throughout the brain including the thalamus, hypothalamus, basal forebrain and cortex, all of which play an important role in regulating sleep-wake cycle (Vertes, 1991). In addition four descending projections leave the DRN (Michelson *et al*., 2007), which project to and innervate the locus coeruleus, mesencephalic reticular formation, predunculopontine tegmental nucleus, laterodorsal tegmental nucleus and pontine raphe nucleus (Vertes & Kocsis, 1994). Furthermore, individual serotonergic neurons can give rise collateralized efferents capable of innervating multiple brain regions, enabling the DRN to integrate modulation of distinct but functionally related brain regions (Waselus *et al*., 2011).

Anatomically and neurochemically diverse axons innervate and regulate the neuronal activity of DRN neurons. Of note, anatomical studies have demonstrated projections to the DRN from all of the major arousal systems (Lee *et al*., 2004; 2005a,b). These afferent fibers project to the DRN in a highly topographical order. Retrograde tracing has shown the DRN receives a highly robust histaminergic innervation from the TMN (Lee *et al*., 2005a), orexinergic projection from the lateral hypothalamus (Lee *et al*., 2005b), noradrenergic input from the locus coeruleus (Lee *et al*., 2004) and cholinergic systems (Woolf & Butcher, 1989). Few studies have examined the projections of arousal pathways to specific subdivisions of the DRN. Noradrenergic neurons project to the DRD, DRVL, DRI and DRC (Kim *et al*.,2004) and orexinergic neurons project to the DRD, DRVL and DRC (Lee *et al*., 2005b). In addition, glutamatergic and GABAergic neurons from various brain regions innervate the DRN. The medial prefrontal

cortex (PFC) provides the major glutamatergic input to each subdivision of the DRN with subcortical regions also providing inputs (Lee *et al*., 2003). GABAergic projections to the DRN arise from the lateral hypothalamus, preoptic area (an important sleep center) and also from the surrounding periaqueductal grey (Gervasoni *et al*., 2000). A recent study utilised array tomography immunofluorescence to demonstrate that GABA-containing axons are organised in a "synaptic triad" with glutamatergic axons and serotonergic neurons in the DRN (Soiza-Reilly *et al*., 2013).

1.3.3 Intra-raphe projections

Important neural connections exist between serotonergic neurons in different parts of the raphe complex. The DRN gives rise to a robust projection to the median raphe (MnR) (Vertes & Kocsis, 1994). Functional interactions also exist between neighbouring cell groups in the DRN. Retrograde tracing studies have demonstrated a connection between the DRV and DRVL/VLPAG region (Peyron *et al*., 1998b). Selective lesion of serotonergic neurons in the DRVL/VLPAG region led to an increase in tryptophan hydroxylase (TPH) mRNA expression within the DRV region, suggesting a tonic inhibitory role for DRVL/VLPAG neurons (Ljubic-Thibal *et al*., 1999). Intra-raphe, GABAergic interneurons have been demonstrated to synapse directly with serotonergic neurons (Allers & Sharp, 2003; Fu *et al*., 2010; Gervasoni *et* al., 2000; Jankowski & Sesack, 2004) providing a local inhibitory feedback circuit. There is tentative evidence to suggest glutamatergic interneurons may exist within the DRN (Commons, 2009) however further immunohistochemical work is required to confirm this.

1.3.4 Physiology of serotonergic neurons in the DRN

Early extracellular single-unit recordings from neurons within the DRN of anaesthetized rats revealed a population of neurons exhibiting a slow and regular firing pattern (Aghajanian *et al*., 1968). These slow, rhythmically firing neurons were later confirmed to be serotonergic by intracellular recording combined with Falck-Hillarp histochemical fluorescence (Aghajanian & Vandermaelen, 1982a; Falck *et al*. 1982). Serotonergic neurons in the DRN demonstrate a rhythmic, bi- or tri-phasic, wide action potential (2-4ms) with a pronounced post-spike after-

hyperpolarisation and depressant response to 5-HT (Vandermaelen & Aghajanian, 1983; Williams *et al*., 1988). These pharmacological and electrophysiological characteristics made it possible to identify serotonin neurons *in vitro* and *in vivo,* and over time they became accepted hallmarks of serotonergic neuronal identity.

An early study performed with freely moving cats identified two subtypes of serotonergic neurons based on their state-dependent and independent firing across the sleep-wake cycle (Rasmussen *et al*., 1984). Type I neurons fired at relatively high frequencies during active wake, decreased firing during quiet waking and SWS and virtually ceased firing during paradoxical (REM) sleep. Whereas type II neurons maintained a relatively constant firing rate irrespective of the behavioural state. Type I neurons were distributed throughout the DRN, however type II neurons were shown to be localised to the interfascicular subdivision of the DRN (Rasmussen *et al*., 1984). More recently a study has extended this classification of serotonergic neurons further, describing six different subtypes of neurons (Sakai & Crochet, 2001). Serotonergic neurons were classified into two typical groups (types I-A and I-B) and four atypical groups (types I-C, II-A, II-B and II-C), according to differences in firing patterns during the sleep-wake cycle. Typical neurons (similar to type I described previously) discharged regularly at a high rate during waking, progressively slower rates during SWS, and ceased firing either during SWS with PGO waves and paradoxical sleep (type I-A), or only during paradoxical sleep (type I-B). Typical neurons were evenly distributed in the DRN. Atypical neurons displayed distinct firing pattern, either exhibiting sustained tonic activity during paradoxical sleep (types I-C and II-C), or firing at greater frequencies during SWS, with suppression of firing during both waking and paradoxical sleep (type II-B). Atypical neurons were unevenly distributed in the DRN. This study recorded from a large sample of serotonergic neurons from the DRN and for the first time suggested a high degree of functional heterogeneity of serotonergic neurons within the DRN (Sakai & Crochet, 2001).

Later studies, performed on head-restrained rats (Urbain *et al*., 2006) and mice (Sakai, 2011) have revealed a similar heterogeneity of serotonergic neuronal firing across the sleep-wake cycle. It should be noted that no definitive proof of the serotonergic nature of these neurons was provided in any of these studies, therefore a portion of the neurons may in fact be non-serotonergic. Future recordings from neurons in the DRN therefore require labeling to establish their serotonergic nature. However given these results it is very likely that atypical

serotonergic neurons have been underrepresented in electrophysiological studies because they do not conform to properties that were considered diagnostic of serotonergic neuronal identity *i.e.* highest discharge rate during wakefulness.

1.4 Regulation of serotonergic neurons in the DRN

5-HT neuronal activity in the DRN is controlled by two main mechanisms: autoregulation, arising directly from 5-HT neurons and heteroregulation, arising from local neurons and afferents including; GABAergic (Gervasoni *et al*., 2000), glutamatergic (Lee *et al*., 2003) and noradrenergic inputs (Peyron *et al*., 1996).

1.4.1 Autoregulation of serotonergic neurons in the DRN

5-HT neuronal activity and 5-HT release is controlled by 5-HT_{1A} receptors located on the soma and dendrites of 5-HT neurons (Riad *et al.,* 2000; Sotelo *et al*., 1990). Activation of local 5-HT_{1A} autoreceptors by application of 5-HT_{1A} agonists into the DRN reduces serotonergic cell firing *in vitro* (Aghajanian & Lakoski, 1984) and *in vivo* (Sprouse & Aghajanian, 1987; Fornal *et al*., 1994). This decrease in neuronal firing occurs via 5-HT_{1A} receptors, which are coupled to a G-protein coupled inwardly-rectifiying potassium (GiRK) channel. Therefore, activation of 5-HT_{1A} receptors causes an increase in K^+ conductance that leads to a hyperpolarisation of serotonergic neuronal membranes (Katayama *et al*., 1997; Penington *et al*., 1993). Surprisingly, there is very little evidence to support that 5-HT_{1A} autoreceptors are functionally active under physiological conditions. While some *in vivo* studies have demonstrated that the 5-HT_{1A} antagonist, WAY 100635 produces a disinhibitory effect on the firing of DRN 5-HT neurons (Fornal *et al*., 1996; Hajos *et al*., 2001), others have found little or no effect (Gartside *et al*., 1995; Haddjeri *et al*., 2004). A recent *in vitro* study has provided evidence that WAY 100635 can also act at α_1 adrenoreceptors located in the DRN, suggesting that at high concentrations the drug may mask endogenous 5-HT_{1A} auto-inhibition (Liu *et al*., 2005). The response of 5-HT neurons to application of 5-HT_{1A} agonists has been shown to vary across different subdivision of the DRN (Calizo *et al*., 2011). A recent genetic study has demonstrated that the magnitude of 5-HT neuronal autoinhibition is not related to the sensitivity of 5-HT_{1A}

receptors, suggesting that adaptive changes in receptor sensitivity can occur to compensate for alterations in 5-HT levels (Araragi *et al*., 2013). These data have important clinical implications for the control of the sleep-wake cycle, pathogenesis of mood disorders and in the action of antidepressant drugs.

Autoregulation of 5-HT neurons is also controlled in part by 5-HT_{1B} receptors however reliable evidence for this regulatory role in the DRN is somewhat limited. 5-HT_{1B} receptors have been shown to be located on the axon terminals of 5-HT neurons in the DRN (Boschert *et al*., 1994; Doucet *et al*., 1995; Riad *et al*., 2000) and their activation leads to a decrease in the release of 5-HT (Adell *et al.,* 2001; Morikawa *et al*., 2000). A recent study has revealed that activation 5-HT_{1B} receptors can enhance SERT activity in the DRN of mice (Hagan *et al*., 2012) supporting an autoregulatory role for these receptors. An autoregulatory role for 5-HT_{1D} receptors in the DRN has also been suggested (Stamford *et al*., 2000) however the evidence for this is scarce due to the limited availability of selective ligands. The physiological relevance of multiple 5-HT_1 receptors regulating 5-HT neurons is currently unknown. Given the recent demonstration that not all 5-HT neurons express 5-HT_{1A} receptors (Kiyasova *et al*., 2013), it is possible that 5-HT_{1B} and 5-HT_{1D} receptors could provide heterogeneous regulation of 5-HT neurons in the DRN.

1.4.2 Heteroregulation of serotonergic neurons in the DRN

Neurochemical and morphological studies have revealed that serotonergic neurons in the DRN form synaptic connections with local GABAergic interneurons (Fu *et al*., 2010; Gervasoni et al., 2000; Gocho *et al*., 2013). Immunohistochemical studies have demonstrated that GABAergic interneurons are preferentially distributed in the DRVL subdivision of the DRN (Brown *et al*., 2008; Shikanai *et al*., 2012). These local GABAergic interneurons can negatively regulate the activity of 5-HT neurons and 5-HT release in the DRN. In support of this, $GABA_A$ and $GABA_B$ receptors have been shown to be located on DRN 5-HT neurons (Gao *et al*., 1993; Serrats *et al*., 2003). Release of GABA from local interneurons would therefore cause the inhibition of nearby 5-HT neurons. Electrophysiological studies have revealed that activation of local GABAergic interneurons, via 5-$HT_{2A/2C}$ receptors, causes an increase of inhibitory synaptic events onto 5-HT neurons (Liu *et al*., 2000). Interestingly, some 5-HT neurons have been

shown to co-express GABA (or its synthetic enzyme, GAD), suggesting a possible co-release of 5-HT and GABA from neurons (Belin *et al.,* 1983; Fu *et al*., 2010; Shikanai *et al*., 2012). This would represent a novel mechanism which would regulate 5-HT neuronal firing via autoregulatory feedback inhibition. Complicating matters further, postsynaptic 5-HT_{1A} receptors (Calizo *et al*., 2011) and 5-HT_{1B} receptors (Lemos *et al*., 2006) have been shown to regulate GABAergic interneurons in the DRN. Activation of 5-HT_{1A} or 5-HT_{1B} receptors expressed by GABAergic interneurons would therefore cause the indirect disinhibition of 5-HT neurons in the DRN. The heteroregulation of GABAergic interneurons by 5-HT_{1B} receptors would account for the observation that application of selective 5-HT_{1B} agonists, leads to an increase in 5-HT neuronal firing (Adell *et al*., 2001; Evrard *et al*., 1999).

GABAergic inputs from outside of the DRN have been shown to synapse directly with 5-HT neurons in the DRN (Soiza-Reilly *et al*., 2013; Wang *et al*., 1992). Retrograde tracing combined with immunohistochemistry has revealed that GABAergic afferents into the DRN arise from various brain regions including the VLPO, lateral hypothalamus, VTA and vlPAG (Gervasoni *et al*., 2000). Numerous pharmacological and electrophysiological studies have provided evidence that GABA has an inhibitory influence on serotonergic neurons in the DRN. An early investigation demonstrated that ionotophoretic application of GABA to the DRN of anaesthetised rats reduced the firing of neurons, an effect reversed by the GABA antagonist, picrotoxin (Gallager & Aghajanian, 1976). A later study revealed that application of the selective $GABA_A$ receptor agonist, THIP and $GABA_B$ receptor agonist, baclofen reduced the firing of presumed 5-HT neurons recorded from rat brain slices (Judge *et al*., 2004). The physiological significance of GABA-inhibition in the DRN is highlighted by reports that GABA mediates the reduction of serotonergic neuronal activity during NREM and REM sleep. In rats and cats, local administration of the GABA receptor antagonist, bicuculline into the DRN during NREM sleep increased the discharge of serotonergic neurons to the level observed during wakefulness (Gervasoni *et al*., 2000; Levine & Jacobs, 1992). Furthermore in rats, it was demonstrated that local infusion of bicuculline into the DRN during REM sleep increased the firing of serotonergic neurons to the level observed during wakefulness (Gervasoni *et al*., 2000). In contrast to rats, bicuculline infusion in the DRN of cats did not increase serotonergic neuronal discharge during REM sleep (Levine & Jacobs, 1992). This result was confirmed and extended with the demonstration that during REM sleep cats, serotonergic neuronal activity is reduced by “disfacilitation” of noradrenergic and histaminergic neurons rather than by

GABAergic inhibition (Sakai & Crochet, 2000). It is possible that these conflicting observations reflect species differences.

Glutamatergic inputs to the DRN originate from a number of nearby brainstem sites, several hypothalamic nuclei and the cerebral cortex (Lee *et al*., 2003). It has been demonstrated that the majority of glutamatergic terminals synapse on non-5-HT neurons in the DRN (Commons *et al*., 2005), recently confirmed to be GABAergic neurons (Soiza-Reilly *et al.,* 2013). Glutamate has an excitatory effect on DRN 5-HT neurons which is mediated via both glutamate and AMPA/kainate receptors (Pan *et al*., 1989). Therefore while glutamatergic inputs can directly excite DRN 5-HT neurons, evidence exists to suggest that glutamatergic neurons could restrain 5-HT neurons by feed-forward inhibition via GABAergic neurons.

Early electrophysiological studies revealed that the number of spontaneously active 5-HT neurons was much lower when recording *in vitro* from acute brain slices in comparison to *in vivo* (Vandermaelen & Aghajanian, 1983). This observation suggested that spontaneous firing of 5-HT neurons in the DRN was dependent upon an intact excitatory afferent drive and subsequent studies revealed that noradrenergic input from the LC was the source (Baraban and Aghajanian, 1980; Baraban and Aghajanian, 1981). Pharmacological investigations have revealed that noradrenaline directly excites 5-HT neurons via postsynaptic α_1-adrenoreceptors (Trulson & Crisp, 1984; Vandermaelen & Aghajanian, 1983) and indirectly inhibits 5-HT neurons via presynaptic α_2-adrenoreceptors (Garratt *et al*., 1991). The release of 5-HT in the DRN is similarly regulated by α_1- and α_2-adrenoreceptors (Pudovkina *et al*., 2003). Noradrenergic neurons have a discharge profile similar to 5-HT neurons, firing fastest during wakefulness and slowing during sleep (Takahashi *et al*., 2010). Application of the selective α_1 adrenoreceptor agonist, phenylephrine to the DRN can block the cessation of discharge of 5-HT neurons during REM sleep (Sakai & Crochet, 2000). Taken together these results demonstrate an important physiological role for the noradrenergic innervation of DRN 5-HT neurons during the sleep-wake cycle.

1.5 The role of serotonin in the sleep-wake cycle

The role of serotonin in the sleep-wake cycle has evolved considerably over the last five decades. In the 1960's a series of studies were performed in cats in order to investigate the role of raphe serotonergic neurons in sleep-wake control. Lesion studies revealed that there was a significant correlation between the destruction of the DRN and the decrease of both NREM sleep and cerebral levels of 5-HT (Jouvet, 1968 & 1969). Neuropharmacological studies revealed that the chemical destruction of serotonin by pCPA injection produced a dose-dependent reduction in the amount of sleep (Koella *et al*., 1968). Taken together these studies formed the basis for the "monoaminergic theory of sleep and waking" which postulated that 5-HT neurons in the DRN were responsible for NREM sleep (Jouvet, 1972). However, a serious challenge to the concept of 5-HT as a sleep transmitter came in the 1970's with the development of techniques making it possible to record unit data in spontaneously sleeping cats. It was revealed that the unitary electrical activity of DRN neurons increased during waking then decreased during NREM sleep, becoming silent during REM sleep (McGinty & Harper, 1976). This pattern of DRN neuronal firing was later confirmed in rats (Guzmán-Martin *et al*., 2000). The unit data was supported by microdialysis studies which confirmed that 5-HT release in several brain regions was highest during waking, reduced during NREM sleep and even more reduced during REM sleep in both cats (Portas & McCarley, 1994) and rats (Portas *et al*., 1998). These studies, as well as many others conducted during the 1980's, led to the revision of 5-HT as a wake-promoting neurotransmitter. The appearance of new techniques and new data from the 1980's onwards however did not simplify the role of 5-HT in wake control, rather it revealed the complex nature of 5-HT regulation and release of the sleep-wake cycle.

1.5.1 Effects of 5-HT receptors on the sleep-wake cycle

There have been various strategies aimed at understanding the role of 5-HT receptors in the regulation of the sleep-wake cycle including: genetic (knock-out, KO) studies, intra-raphe delivery of 5-HT receptor ligands and systemic or intracerebroventricular (i.c.v) administration

of 5-HT receptor ligands. To date, investigations aimed at characterising the role of 5-HT receptors on the sleep-wake cycle have been limited to the 5-HT_{1A-1B}, 5-HT_{2A-B-C}, 5-HT_3, 5-HT_6 and 5-HT_7 (Monti *et al*., 2011). It should be noted that methodological differences between studies can produce inconsistencies in results and therefore care should be taken when interpreting the overall result. A brief summary of studies investigate the role of 5-HT_{1A} and 5-HT_{2A-2C} receptors is discussed here.

5-HT_{1A} receptor regulation of REM sleep had been demonstrated previously in a number studies using a pharmacological approach. Microdialysis perfusion of the 5-HT_{1A} agonist, 8-OH DPAT into the DRN was shown to increase REM sleep compared to perfusion with artificial cerebrospinal fluid (aCSF) in both cats (Portas *et al.,* 1996) and rats (Bjorvatn *et al*., 1997), while wake and NREM sleep remained unaffected. In support of these finding, microinjection (i.e. direct infusion) of 8-OH-DPAT in the DRN increased REM sleep in rats, and this effect was inhibited by local infusion of the 5-HT_{1A} antagonist, WAY100635 (Monti & Jantos, 2002). Microinjection of WAY100635 (Monti & Jantos, 2002) or a second antagonist, p-MPPI (Sørensen *et al*., 2001) into the DRN reduced REM sleep. 5-HT_{1A} receptor knock-out mice (i.e. mice that do not express 5-HT_{1A} receptors) have been observed to exhibit greater amounts of REM sleep than wild type (WT) mice, while wakefulness and NREM remain unaffected (Boutrel *et al*., 2002). From this study it was proposed that the increase in behavioural state in 5-HT_{1A} receptor KO mice is due to the absence of postsynaptic 5-HT_{1A} mediated inhibition of LDT/PPT REM-on neurons. In support of this, microinjection of 8-OH-DPAT or a second agonist, flesinoxan into the LDT selectively inhibited REM sleep in the cat (Stanford *et al*., 1994) and rat (Monti & Jantos, 2003). These data are therefore consistent with the hypothesis that 5-HT_{1A} receptors in the LDT/PPT have an inhibitory role in REM sleep generation (McCarley *et al*., 1995). Systemic application of 5-HT_{1A} ligands has been reported to have quite different effects to local application. Therefore, systemic application of 8-OH-DPAT consistently increases waking while decreasing NREM and REM sleep in animals (Bjorvatn *et* al., 1997; Monti & Jantos, 1992; Monti & Jantos, 1994). There was however some evidence to suggest that different doses of 8-OH-DPAT have opposite effects on behavioural state i.e. at lower doses, 8-OH-DPAT decreases waking (Monti & Jantos, 1992). It is not currently known what causes the observed increase in wake following systemic administration of 5-HT_{1A} agonists, however, it is proposed that it may be due to inhibition of the sleep-promoting GABAergic neurons in the VLPO (Monti, 2010).

5-HT_{2A} and 5-HT_{2C} KO mice both show a significant increase of wakefulness and a reduction in NREM sleep while REM sleep remains unchanged (Frank *et al*., 2002; Popa *et al*., 2005). Interestingly, opposite effects have been demonstrated by pharmacological manipulation of 5-HT_2 receptors. Therefore, systemic administration of non-selective 5-$HT_{2A/2C}$ agonists or a selective 5-HT_{2C} agonist has been demonstrated to increase wakefulness and decrease sleep (Monti, 2010). The reason for this discrepancy is currently unclear however it has been suggested that the greater amount of wakefulness in 5-HT_{2C} (and 5-HT_{2A}) KO mice could be due to the increase of catecholaminergic neurotransmission involving the noradrenergic and dopaminergic systems (Frank *et al*., 2002). 5-HT_{2A} and 5-HT_{2C} receptors are expressed on GABAergic interneurons which participate in the control of noradrenergic and dopaminergic neurons (Fink *et al*., 2007). Hence, the reduction of GABA release at these sites in 5-HT_{2A} and 5-HT_{2C} KO mice could be indirectly responsible for the increased levels of noradrenaline and dopamine (Monti, 2010). Infusion of the non-selective 5-$HT_{2A/2C}$ agonist, DOI into the DRN induced a significant reduction of REM sleep (Monti *et al*., 2006a). This reduction of REM sleep was prevented by pre-treatment with selective 5-HT_{2A} and 5-HT_{2C} antagonists (pruvanserin and EMD 281014, respectively). Systemic or intra-raphe administration of DOI consistently inhibited the firing of serotonergic neurons, an effect shown to be mediated via GABAergic interneurons (Liu *et al*., 2000). Therefore the observed DOI effect on REM sleep does not appear to be mediated directly via serotonergic neurons but rather by indirect activation of GABAergic interneurons. Similarly, in the LDT, 5-$HT_{2A/2C}$ receptor expression is absent from cholinergic neurons but is present in GABAergic interneurons (Fay & Kubin, 2001). In keeping with this, DOI has an indirect inhibitory effect on cholinergic neurons in the LDT which results in decreased REM sleep episodes (Amici *et al*., 2004). Systemic administration of 5-HT_2 antagonists has been consistently shown to increase NREM sleep in animals (Monti & Jantos, 2006a, b; Monti *et al*., 2011; Morairty *et al*., 2008). Given the robust increase in NREM sleep of animals, numerous studies have been conducted in humans in order to investigate the therapeutic potential of 5-HT_2 receptor antagonists as sleep aids. When given to healthy subjects, the non-selective 5-HT_2 receptor antagonists, ritanserin and ketanserin have been shown to increase stage 3 and 4, and stage 2 of NREM sleep, respectively (Idzikowski *et al*., 1986; Sharpley *et al*., 1994). In addition, the 5-HT_2 inverse agonist, nelotanserin has been shown to increase NREM sleep and increase the duration of sleep bouts (Al-Shamma *et al*., 2010). The precise mechanisms for this reliable increase in NREM sleep (observed in animals and humans) is currently unclear although it is reasonable to postulate that inhibition of cell groups involved in wake-promotion, either indirectly or directly, is likely.

1.6 Orexins (hypocretins)

The neuropeptides orexin-A and orexin-B (hypocretin-1 and hypocretin-2) were concurrently and independently discovered as endogenous ligands in the brain (de Lecea *et al*., 1998; Sakurai *et al*., 1998). Orexin-A and orexin-B are comprised of 33 and 28 amino acids, respectively, with a 46% amino acid sequence homology. Both neuropeptides are produced from a common precursor polypeptide, prepro-orexin (prepro-hypocretin) which is expressed in the lateral hypothalamus and perifornical nucleus (Peyron *et al*., 1998a). Importantly, orexin-containing neurons project throughout the brain with particularly dense innervation of the ascending arousal system, including the LC, TMN and DRN (Nambu *et al*., 1999; Peyron *et al*., 1998a). Two orexin receptors have been discovered; orexin-type 1 receptor and orexin-type 2 receptor (OX_1R and OX_2R). Orexin-A has equal affinity at both receptors whereas orexin-B has a 10-fold greater affinity at the OX_2R (Sakurai *et al*., 1998). In situ hybridization has revealed that orexin receptors are distributed throughout the brain, each having a distinct, yet overlapping pattern (Marcus *et al*., 2001). Several studies have also demonstrated that in some brain regions, including the DRN, mRNA for both receptors can be co-localised (Eriksson *et al*., 2001; Brown *et al*., 2002). OX_1 and OX_2 receptors belong to the GPCR superfamily. Activation of orexin receptors by orexin-A or orexin-B predominantly produces a depolarisation in the postsynaptic cell leading to an increase in cell firing, hence orexins are universally considered to be excitatory neuropeptides (Brown *et al*., 2001; Eriksson *et al*., 2001a, b). Studies have demonstrated that orexins produce their excitatory actions via G_q signaling although OX_2Rs can also couple to G_s and G_i proteins (Hoang *et al*., 2003; Karteris *et al*., 2005). As described above, orexin neurons play an important role in promoting wakefulness via regulation of other ascending arousal pathways including the serotonergic neurons of the DRN.

1.6.1 Regulation of DRN 5-HT neurons by orexins

Immunohistochemical studies have demonstrated the orexin neurons innervate the DRN (Date *et al*., 1999; Nambu *et* al, 1999; Peyron *et al*., 1998a). A subsequent investigation using electron microscopy revealed that axon terminals of orexin neurons make synaptic connections with the dendrites and cell bodies of DRN neurons (Wang *et al*, 2003). A double-labeling study later determined that orexin terminals were in fact synapsing with serotonergic

DRN neurons (Wang *et al*., 2005). Retrograde labeling has revealed that serotonergic neurons from the DRN also provide a reciprocal innervation of orexin neurons in the lateral hypothalamus (Yoshida *et al*., 2006). In situ hybridisation studies have shown that OX_1 and OX_2 receptors are located in the DRN (Marcus *et al*., 2001; Trivedi *et al*., 1998). In the DRN, electron microscopy combined with staining has revealed that OX_1Rs are expressed on both serotonergic neurons and non-serotonergic neurons in the DRN (Wang *et al*., 2005). The location of OX_2Rs was not explored in this study therefore it remains to be elucidated whether OX_2Rs are located on non-serotonergic neurons. Electrophysiological studies have revealed that application of orexin-A to DRN slices from the rat produced an excitation of 5-HT neuronal firing and a depolarization of the membrane voltage (Brown *et al*., 2001). A subsequent study compared the effects of orexin-A and orexin-B and given the affinity difference of the two ligands, suggested that the orexin-induced depolarisation was predominantly mediated by the OX_2R (Brown *et al*., 2002). Furthermore in this study, current-voltage responses of serotonergic neurons to application of orexin-A were consistent with the involvement of a non-selective cationic channel. The authors hypothesised that the channel could be the canonical form of the transient receptor potential (TRP). In a parallel study, orexin-A and orexin-B also increased the firing of 5-HT neurons in the DRN (Liu *et al*., 2002). Interestingly, at higher concentrations the neuropeptides also increased discharge frequency of local GABAergic interneurons suggesting a possible feed-forward inhibition in the DRN. Complicating matters further, electrophysiological recordings have demonstrated that orexin-B can depress glutamatergic input onto serotonergic neurons (Haj-Dahmane & Shen, 2005). Further investigation by these authors revealed that the depression of glutamatergic signaling was mediated via retrograde endocannabinoid release. Infusion of orexin-A and orexin-B into the DRN of freely moving rats has been shown to increase 5-HT release (Tao *et al*, 2006). Thus far no *in vivo* studies have been performed to elucidate the physiological role of orexin-mediated regulation of GABA and glutamate neurons in the DRN.

1.7 Histamine

Histamine is an important monoamine with diverse functions in the body. In the brain, histamine is synthesised from the L-histidine through oxidative decarboxylation by histidine-decarboxylase (HDC) (Fleming *et al*., 2004). The rate of histamine synthesis is determined by

the bioavailability of L-histidine, which can be transported into neurons by L-amino acid transporters (Haas *et al*., 2003). Histamine synthesis can be inhibited by exogenous application of α-fluromethylhistamine, an irreversible inhibitor of the HDC enzyme (Kollonitsch *et al*., 1978). In neurons, histamine is carried into vesicles by the vesicular monoamine transporter (VMAT-2) and is released upon the arrival of action potentials (Merickel & Edwards, 1995). No high-affinity uptake system for histamine has been reported. Instead, inactivation of histamine in the extracellular space is achieved by methylation to tele-methylhistamine by neuronal histamine N-methyltransferase (HNMT) (Barnes & Hough, 2002). Histamine-producing neurons are located exclusively in the TMN of the posterior hypothalamus (Ericson *et al*., 1987). The terminal areas of histaminergic projections from the TMN are widespread throughout the entire brain. The cerebral cortex, substantia nigra, amygdala and striatum receive dense histaminergic innervation while the hippocampus and thalamus receive more moderate staining (Lee *et* al., 2008; Panula *et al*., 1989). Reciprocal innervations between histaminergic TMN neurons and other aminergic cell groups including the DRN and LC have been reported (Lee *et al*., 2005a). GABAergic and galanergic neurons from the sleep-promoting VLPO have also shown to input onto the cell bodies and proximal dendrites of histaminergic TMN neurons (Sherin *et al*., 1998).

1.7.1 Histamine receptors

There are currently known to be four histamine receptors (H_1-H_4) all of which belong to the rhodopsin-like family of GPCRs (Alexander *et al*., 2011). H_1-H_3 receptors are expressed robustly in the brain whereas the H_4 receptor occurs mainly in the periphery (De Esch *et al*., 2005). In invertebrates histamine has been shown to activate ionotropic receptors (Hardie, 1989) and more recently two genes for histamine-gated ion channels have been discovered (Gisselmann *et al*., 2002). The molecular structure of a similar histamine-gated ion channel in vertebrates has remained elusive however histamine has been shown to directly open recombinant heteromultimeric $GABA_A$ receptors (Bianchi *et al*., 2011; Saras *et al*., 2008).

H_1Rs are expressed throughout the brain including the brainstem, hypothalamus, thalamus, cortex and hippocampus (Martinez-Mir *et al*., 1990; Palacios *et al*., 1981). Binding studies utilizing [^{3}H]mepyramine suggest that a significant portion of H_1Rs are associated with non-

neuronal elements e.g. glia and blood vessels. Activation of H_1Rs normally leads to neuronal excitation on postsynaptic cells in all of these areas (Brown *et al*., 2002; McCormick & Williamson, 1991; Selbach *et al*., 1997). Classical (first generation) antihistamines acts at H_1 receptors and have well-known sedative properties (Reiner & Kamondi, 1994; Unno *et al*., 2012) although it should be noted that part of the sedation may have been due to non-specific anticholinergic activity. More recent (second generation) antihistmamines e.g. cetirizine and loratadine have less profound sedative properties in part due to more specific H_1R binding and in part due although their reduced ability to cross the blood brain barrier. The signal transduction of H_1Rs occurs via $G\alpha_{q/11}$ coupling (Haas *et al*., 2008). Activation of PLC leads to the formation of diacylglycerol (DAG) and inositol triphosphate (IP_3). IP_3 releases Ca^{2+} from intracellular stores leading to the activation of a number of Ca^{2+}-dependent process throughout the brain including: activation of Na^+/Ca^{2+} exchange in supraoptic neurons (Smith & Armstrong, 1996), opening of K^+ channels resulting in hyperpolarisation of pyramidal cells in the hippocampus (Selbach *et al*., 1997) and cGMP formation in cultured mouse neuroblastoma cells (Richelson, 1978). DAG activation of PLC can cause excitation in the thalamus and hippocampus via closure of K^+ channels (Brown & Haas, 1999; McCormack & Williamson, 1991). Furthermore, activation of H_1Rs on serotonergic neurons of the DRN leads to the activation of a mixed cationic conductance believed to belong to the transient receptor potential family (TRPC) (Brown *et al*., 2002; Sergeeva *et al*., 2003).

H_2Rs are also expressed throughout the brain and can be co-localised with H_1Rs many brain regions e.g. DRN (Barbara *et al*., 2002), hippocampus (Garbarg & Schwartz, 1988) and cerebral cortex (McCormack & Williamson, 1989). A synergistic interaction of H_1 and H_2 receptors has been suggested after the observation of amplified histamine-induced stimulation of cAMP in hippocampal cells (Garbarg & Schwartz, 1988). The H_2R is coupled to $G\alpha_s$ and its signal transduction includes stimulation of adenylate cyclase and increase in intracellular cAMP which activates protein kinase A and the transcription factor CREB (Baudry *et al*., 1975; Haas *et al*., 2008). H_3Rs re coupled to $G_{i/o}$ proteins and high voltage activated Ca^{2+} channels and are negatively coupled to cAMP. H_3Rs function as autoreceptors on the soma, dendrites and axons of TMN neurons (Arrang *et al*., 1987; Pollard *et al*., 1993) causing inhibition of cell firing and histamine release (Stevens *et al*, 2001). In addition, H_3Rs function as presynaptic heteroreceptors, to control the release of a variety of other transmitters including acetylcholine (Blandina *et al*., 1996) and noradrenaline (Schlicker *et al*., 1999). Distribution of

H_3Rs is widespread throughout the brain, with expression normally present in areas known to receive histaminergic innervation (Chazot *et al*.,2001; Pillot *et al*., 2002). Transient expression of H_1 receptors in SV40 cells (Bakker *et al*., 2000) and H_2 receptors in CHO cells (Smit *et al*., 1996) has revealed that these receptors are constitutively active i*n vitro*. To date, only the H_3 receptor has been shown to be constitutively active *in vivo* (Morisset *et al*., 2000).

1.7.2 Regulation of 5-HT DRN neurons by histamine

Retorgrade studies have demonstrated that histaminergic neurons from the TMN innervate the entire rostro-caudal extent of the DRN (Lee *et al*., 2005a). Binding studies with [^{3}H] mepyramine and [^{3}H]-tiotidine have revealed that H_1 and H_2 receptors are located in the DRN (Bárbara *et al*., 2002). Furthermore, high levels of H_3 receptor mRNA have been localised in the DRN (Drutel *et al*., 2001; Pillot *et al*, 2002). Early electrophysiological studies suggested that histamine reduces the firing of 5-HT neurons in the DRN via the H_2 receptor (Lakoski & Aghajanian, 1983; Lakoski *et al*., 1984). Subsequent electrophysiological studies have shown that application of histamine to slices containing the DRN results in an increase in the firing of serotonergic neurons (Bárbara *et al*., 2002; Brown *et al*., 2002). The histamine-induced increase in 5-HT neuronal firing was shown to be mediated via the H_1 receptor and not the H_2 receptor (Bárbara *et al*., 2002). Furthermore, the histamine induced excitation of 5-HT neurons appears to be mediated via non-selective cationic conductance, identical to that described from orexin receptors in the DRN (Brown *et al*., 2002). In support of this, occlusion experiments in the DRN have revealed that histamine, orexin and noradrenaline converge on a common ionic mechanism to increase the firing the serotonergic neurons (Brown *et al*., 2002).

1.8 Aims

This thesis aims to develop the understanding of how serotonergic neurons in the DRN are regulated by transmitters systems involved the sleep-wake cycle. In order to investigate this broad study aim the project was divided into three main sections.

1. How are mouse DRN serotonergic neurons regulated by 5-HT_2 receptors, orexin receptors and adrenoreceptors *in vitro*? It was hypothesised that activation of 5-HT_2 receptors in the nucleus would produce inhibition of 5-HT neurons while activation of orexin and adrenoreceptors would produce excitation. Extraceullar and patch clamp electrophysiology was utilised and combined with pharmacological investigation of serotonin neurons in mouse brain slices.

2. How are DRN serotonergic neurons regulated by histamine receptors *in vitro*? It was hypothesised that activation of H_1 and H_2 receptors would cause an excitation of 5-HT neurons while activation of H_3receptors would cause an inhibition. Similar to the previous aim patch clamp electrophysiology was utilised in order to investigate the histaminergic regulation of 5-HT neurons in mouse brain slices.

3. How are DRN serotonergic neurons regulated by histamine receptors *in vivo*? It was hypothesised that blockade of histamine receptors in the DRN would lead to reduced level of firing of 5-HT neurons and more widely a profound sedation of the whole animal. Extraceullar recordings, and separately, EEG recordings were performed in rats in order to investigate the pharmacological inhibition of H_1Rs.

Chapter 2:

Materials and Methods

2.1 Animal supply, housing and breeding

All animal procedures were carried out in accordance with UK home office guidelines laid out in the U.K Government Animals (Scientific Procedures) Act 1986. Furthermore all procedures were performed in accordance with the University of Dundee and Eli Lilly code of practise for use of experimental animals. Every effort was taken to reduce animals use and suffering.

In vitro slice experiments were carried out on neonatal (P16-P30), wild-type (WT), C57/BL6 mice of either sex which were obtained from an in-house colony maintained within the Medical School Resource Unit at the University of Dundee. Animals were kept under controlled conditions with a 12 hour light: 12 hour dark cycle, constant temperature (21 ± 2°C) and humidity (55%) and provided with food and water *ad libitum.* Animals were killed by cervical dislocation in accordance with Schedule 1 of the Animals (Scientific Procedures) Act 1986 (Maguire *et al*., 2013). *In vivo* experiments were carried out on adult (250-370g), male, Wistar rats which were obtained from Charles River laboratories (Wilmington, MA, USA) and housed within the animal research facility at Eli Lilly. Animals were kept under controlled conditions with a 12 hour light: 12 hour dark cycle, constant temperature (21 ± 2°C) and humidity (55%) and provided with food and water *ad libitum.* After completion of *in vivo* experiments rats were terminally anaesthetised (Rasmussen *et al*., 2004).

2.2 Electrophysiological recording from brain slices

Understanding the relationship between the electrical activity of individual neurons and the behaviour they mediate is major goal in the field of neuroscience. In neurons, the generation of action potentials reflects the combination of intrinsic membrane properties and extrinsic inputs from neurotransmitters. The *in vitro* brain slice preparation offers a direct approach to investigate the changes in electrical characteristics that govern neuronal behaviour. Numerous studies have demonstrated comparable electrical activity between brain slices and the intact animal thereby solidifying the importance of the brain slice preparation in neurophysiology research. Extracellular single-unit recordings and whole-cell voltage-clamp recordings have been combined here in order to study the electrophysiology of neurons within the DRN.

Extracellular recordings are performed in order to obtain information about the electrical activity of single neurons (single-unit recordings). Extracellular recordings are useful for studying the firing properties of neurons and have the advantage of producing very stable and long-lasting experiments. However single-unit recordings can only provide limited electrophysiological information about individual neurons. In order to better understand the intrinsic cellular properties that govern the electrical behaviour of neurons more advance techniques are required. Whole-cell patch-clamp recordings allow high resolution recordings to be made from individual neurons and permit a more detailed understanding of their cellular properties. In particular, voltage-clamp recordings allow the study of ionic conductance across cellular membranes.

2.3 Slice preparation

Following cervical dislocation and decapitation the brain was rapidly removed and placed in ice cold (0-4°C) oxygenated (95% O_2, 5%CO_2) artificial cerebrospinal fluid (aCSF) containing (in mM): 126 NaCl, 26 $NaHCO_3$, 10 $MgSO_4$, 10 Glucose, 2.5 KCl, 1.25 NaH_2PO_4, 0.5 $CaCl_2$, (pH 7.4, 309-312mOsm). A small section of the frontal lobe was removed to form a flat base and to allow coronal sections to be taken in the caudal to rostral direction. The brain was dried on filter paper and then mounted on the metal base of a vibratome plate using cyanoacrylate (Super) glue. It was then submerged in oxygenated, ice-cold aCSF in the slicing chamber. Coronal slices were cut (thickness 300-350µM) using a Vibratome series 1000 (Intracel; Royston, Hertfordshire, UK) and then transferred to a holding chamber containing circulating, oxygenated aCSF at room temperature. Slices were placed on a suspended nylon mesh platform, allowed to recover for 1 hour and used for experimentation between 1 and 8 hours after slicing. Generally 3-4 good quality slices containing the DRN were obtained per animal.

2.4 Reagents and drugs: *in vitro* electrophysiology

All chemicals are listed in Table 1.1 with the corresponding site of action, concentration used, vehicle solution and the company from which they were obtained. Briefly, stock solutions of drugs were dissolved in destilled/de-ionised water or DMSO and final dilutions (x1000) were

made in extracellular recording solution, ECS (see section 2.5). DMSO was used to dissolve water-insoluble drugs and was always made as a concentrated stock to ensure the maximum DMSO concentration never exceeded 0.1%. This concentration had no effect upon ionic currents (data not shown). All drugs and salts were purchased from VWR (West Sussex, UK), Tocris (Bristol, UK), Sigma Aldrich (Dorset, UK), Abcam (Cambridge, UK) or were a kind donation from Eli Lilly (Surrey, UK). The osmolarity of solutions were measured using a Roebling Osmometer (Camlab, Cambridge, UK).

For extracellular single-unit recordings drug application and solution perfusion was achieved by a pump fed perfusion system with a flow rate of 1-2 ml/min. All solutions reached slices within 3mins and were run to waste. Solutions were preheated before entering the recording chamber (block heater; Jencons, UK) and heated in-line (G23, University College London). This heating procedure was implemented to prevent the formation of bubbles which could perturb the recording. A heating element located in the lower chamber body ensured the temperate was maintained at 35 ± 0.5°C (PTC03; Digitimer, UK). For whole-cell patch-clamp recordings solution delivery was achieved by a gravity-fed perfusion system with a flow rate of 3-4 ml/min. Solutions reached slices within 3 minutes and were recycled with a peristaltic pump (Gilson, UK). A metal probe was placed within the chamber in close proximity to the slice and the temperature was maintained at 35 ± 0.5 °C by a temperature controller (School of Pharmacy, University of London). In certain experiments drugs were focally applied to neurons via a drug-filled pipette which was placed in close proximity to the neuron (within 1000µm). The glass pipette was made from the same capillary tubing as the patching electrode but had a lower resistance of 1-2 MΩ. The pipette was placed in an MP Series microinjection electrode holder and positioned close to the neurone using an MX10 micromanipulator (Stratton Technologies, Bedfordshire, UK). Ejection of the drug from the pipette was achieved using a pneumatic system operated by a Picosprtizer II unit (Intracel, Hertfordshire, UK). The pressure and duration of the drug delivery was adjusted according to the position of the pipette in relation to the cell. The drug was normally diluted by a factor between 10 and 30 when it reached the neuron (estimated by comparison with bath applications of known concentrations of the drug). Focal drug application could be delivered manually or via an automated system using an external stimulator (Grass S88 Stimulator, West Warwick, USA). The frequency and duration of drug application was kept constant throughout each experiment.

Table 1.1. List of chemicals used for *in vitro* electrophysiology experiments. Full chemical names are detailed in the abbreviation list. Note the DMSO concentration did not exceed 0.1% v/v when diluted in ECS (1000 fold dilution).

Chemical name	Receptor/mode of action	Concentration used	Vehicle solution	Company
5-HT	Serotonin (5-HT) agonist	1-30µM	Distilled water	Sigma
DOI	5-HT_2 agonist	10µM	Distilled water	Lilly
MDL 100907	5-HT_{2A} antagonist	30nM	Distilled water	Lilly
SB 242084	5-HT_{2C} antagonist	30nM	DMSO	Tocris
Histamine	Histamine (H) agonist	10µM	Distilled water	Sigma
Mepyramine	H_1 inverse agonist	100nM - 1µM	Distilled water	Sigma
Dimethendene	H_1 inverse agonist	100nM	Distilled water	Lilly
Histabudifen	H_1 antagonist	20µM	DMSO	Lilly
Oxatomide	H_1 antagonist	30-100nM	DMSO	Lilly
Ranitidine	H_2 antagonist	10µM	Distilled water	Sigma
Thioperamide	H_3 antagonist	1-10µM	Distilled water	Abcam
Orexin	Orexin (OX) agonist	100nM	Distilled water	Sigma
Almorexant	OX_1/OX_2 antagonist	1µM	DMSO	Lilly
NBQX	AMPA antagonist	10mM	DMSO	Tocris
TTX	Voltage-gated Na^+ channel blocker	0.5µM	Distilled water	Tocris
QX-314	Leak Na^+ channel blocker	5mM	Distilled water	Sigma
ATP	Substrate for ATP-dependent systems	2mM	Distilled water	Sigma
GTP	Activates signal transduction pathways	0.5mM	Distilled water	Sigma
GDP-βS	Non-hydrolysable GDP analogue	1mM	Distilled water	Sigma

Salts were purchased from VWR and dissolved in distilled water in order to make aCSF, ECS and ICS solutions.

2.5 Extracellular single-unit recordings

Slices (350μM thick) were transferred to an interface recording chamber (BSC1 chamber; Digitimer, UK) where they were perfused with oxygenated extracellular recording solution (ECS) containing (in mM): 126 NaCl, 26 $NaHCO_3$, 10 glucose, 2.95 KCl, 2 $MgCl_2$, 2 $CaCl_2$ and 1.25 NaH_2PO4 (306-309mOsm). The ECS was delivered at a rate of 1-2 ml/min and maintained at 35°C. The DRN was visualised with a dissecting microscope (Olympus SZ30, UK) equipped with a x10 objective lens. Glass microelectrodes were prepared from glass capillary tubing (0.95mm I.D., 1.55mm E.D., Garner Glass Co., Claremont, CA) using a PP830 electrode puller (Narashige, Japan) to have a resistance of 1-3MΩ when filled with 2M NaCl. Filled electrodes were positioned above the DRN using a micromanipulator (Warner Instruments, CT, USA) and then slowly advanced through the slice. Signals were recorded with a DP-301 differential amplifier (Warner Instruments, CT, USA) and fed to a PC via a 1401 computer analogue to digital converter interface (CED, UK) at a sampling rate of 100 Hz. Signals were filtered (500Hz-3kHz) and when required, 50/60kHz noise was removed using a Humbug noise eliminator (AutoMate Scientific, USA). Data were collected using Spike2 software (version 5, CED, UK). The frequency of cell firing was monitored on line using a simple threshold crossing.

2.5.1 Identification of putative 5-HT neurons in the DRN

Putative 5-HT neurons were identified on the basis of their location: along the midline of the DRN (Abrams *et al*., 2004) and basal electrophysiological characteristics: regular spikes, 2-4ms duration with a slow frequency of 0.3-4.5Hz (Aghajanian & Vandermaelen, 1982b, Allers & Sharp, 2003). In coronal sections the DRN was positioned ventral to the aqueduct, dorsal to the medial longitudinal fasciculus and superior cerebellar peduncle decussation and contained within the periaqueductal grey (Fig 2.1). Spontaneous (basal) firing can be recorded from DRN 5-HT neurons however due to the removal of noradrenergic inputs to the nucleus during the slicing process many neurons do not display their characteristic basal firing. The α_1-adrenoreceptor agonist, phenylephrine (10μM) can be bath applied to the slice in order to increase the likelihood of 5-HT neuronal firing. In approximately 50% of neurons 10μM phenylephrine was used to drive firing. The addition of phenylephrine is highlighted in the relevant section.

2.5.2 Data analysis

All data were analysed offline using Spike 2 software (Version 5, CED, UK). Events which were captured on-line were carefully checked and any noise was removed. This edited channel was then used to calculate the firing frequency and inter-event-interval (IEI). The spike width was calculated by averaging spikes over a 100s period from the raw trace. The basal firing rate (control) was determined in a 300s period at the start of each recording and expressed as an average frequency (Hz). Each response to drug was determined in a 300s period during the maximum change in the baseline and expressed as an average frequency (Fig 2.2). The drug response was then calculated as the percentage change relative to control (i.e. control = 100%, drug effect = % of control). The Coefficient of Variation (CV) was calculated (standard deviation divided by the mean inter-spike interval) for control and drug periods in order to measure spike train regularity. The reversibility of all drugs used was tested (data not shown).

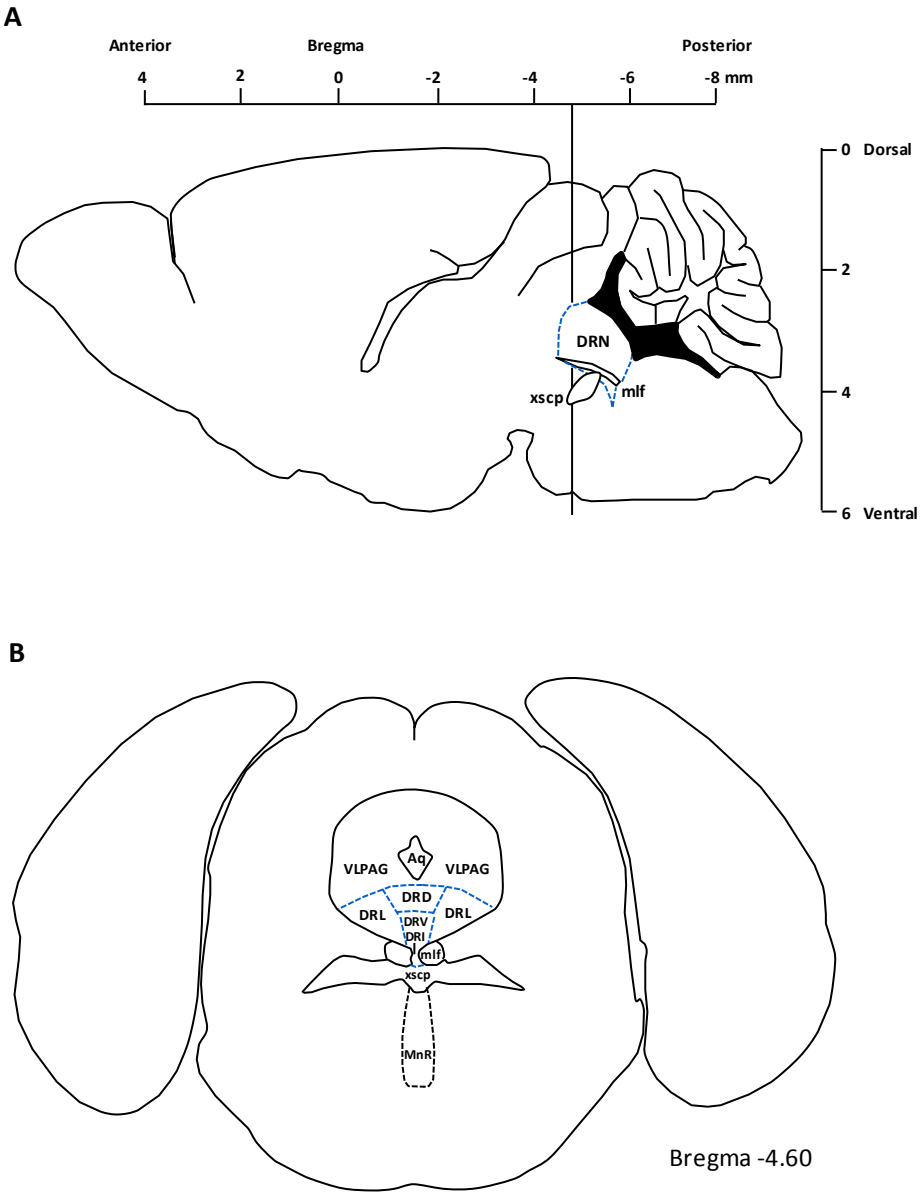

Fig 2.1. Schematic illustration of the mouse brain on a sagittal and coronal plane illustrating the location of the DRN within the brainstem and the DRN subdivisions respectively. (A) Mid sagittal section of the mouse brain showing the DRN within the brainstem. The vertical line represents the level of coronal sectioning. (B) Coronal section of the brain (4.6mm posterior to bregma) with the DRN subdivisions outlined. The DRN lies ventral to the Aq and dorsal to the xscp. Abbreviations: Aq, aqueduct, DRD, dorsal raphe nucleus, dorsal part, DRV, dorsal raphe nucleus, ventral part, DRL, dorsal raphe nucleus, lateral part, DRI, dorsal raphe nucleus, interfascicular part, VLPAG, ventrolateral periaqueductal gray, mlf, medial longitudinal fasciculus, xscp, decussion of the superior cerebellar peduncle, MnR, median raphe nucleus (adapted from the Franklin & Paxinos mouse brain atlas, 2007).

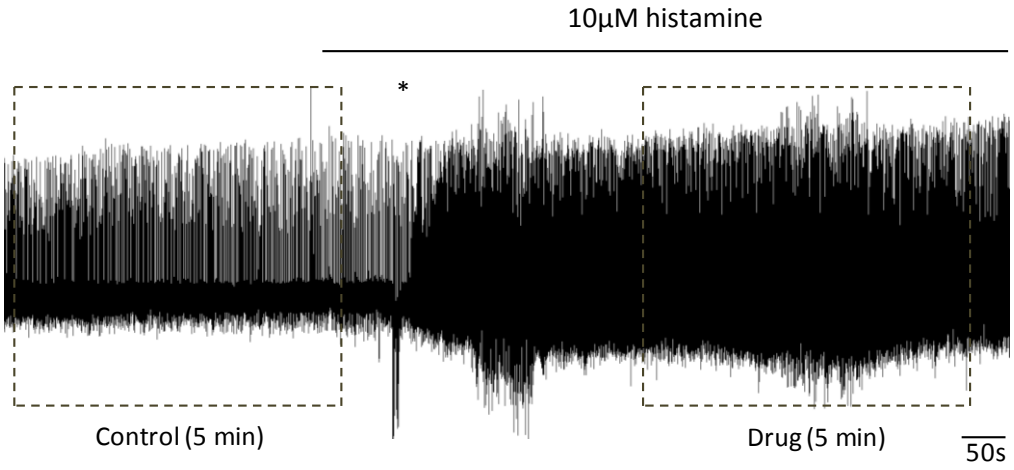

Fig 2.2. Putative 5-HT neurones of the DRN fire spontaneously. Representative extracellular recording trace (20min) from a spontaneously firing DR, 5-HT neuron**.** Action potentials (spikes) appear as sharp deflections from the baseline. Drug application is denoted by the horizontal line above the trace and is shown to start as soon as the drug solution begins to perfuse. The drug solution takes approximately 2mins to reach the slice (*). The average firing frequency for control is calculated from 5mins before drug application and the average firing frequency for drug is calculated from 5mins during its peak effect (dashed boxes). The reversibility of drug was also tested (data not shown).

2.6 Patch-clamp electrophysiological recordings

Slices (300µM thick) were transferred to submerged recording chamber and perfused with oxygenated ECS (as above). The ECS was delivered at a rate of 3-4 ml/min and maintained at 35°C. Neurons within the DRN were visually identified using a black and white camera (Hitachi, CCD KP-MIE/K-510, USA) connected to an upright microscope (Zeiss Axioskop 2 FS, Zeiss, Welwyn Garden City, U.K.) equipped with Achromat x10 and x40 water-immersion optics. A further x1.6 magnification was achieved using an Optivar. Microscope images were displayed on a black and white video monitor (PVM-14SE, Sony, Korea). Recordings were obtained using an Axopatch 200B amplifier (Molecular Devices Ltd, CA, USA) connected to a CV-4 head stage. A set voltage command (-4mV, 30ms duration, every 0.1s) was supplied by an external, computer-based protocol stimulator (generated by WinEDR in the seal test mode) in order to monitor the formation of the whole-cell configuration and adjust whole-cell capacitance and series resistance values. All recordings and cell parameter adjustments were performed using a filter setting of 5kHz and a 8-pole low pass Bessel filter. The filter bandwidth was reduced to 2kHz for recording whole-cell currents.

The recording electrode was positioned onto the selected neuron by using a PCS-5000 piezoelectric micromanipulator (EXFO-Burleigh, Ontario, Canada). The electrode was advanced into the bath at which point corrections were made for offsets due to the liquid-junction potential (potential difference formed due to differences in the ionic concentration and mobilities between in the ECS and intracellular solution). Upon reaching the surface of the neuron the positive pressure was released and gentle negative pressure was supplied in order to form a tight (giga-ohm) seal with the cell membrane. A giga-ohm seal was confirmed by a stable, minimal holding current, near 0pA, at a holding potential of -60mV. Transient currents due to pipette capacitance were cancelled. Brief, sharp negative pressure was then applied to rupture the cell membrane and provide electrical access to the cell (whole-cell mode). The appearance of transient currents of opposite polarity confirmed the correct establishment of the whole-cell configuration (Fig 2.3). These transient currents emerged and decayed with the rising and falling edges of the step command and represented the charging and discharging of the membrane capacitance. The fast component of the transient current was minimised using whole cell capacitance and series resistance compensation in order to prevent saturation of

output from the head stage. A period of 3-5 minutes was allowed to elapse immediately after the whole-cell configuration was established in order to allow the dialysis of solutions between the electrode and cytosol. The access resistance was monitored throughout each experiment; the series resistance was 5-20 MΩ with up to 70% compensation (20µs lag). Cells were discarded if the series resistance exceeded 20 MΩ or changed significantly (20% tolerance) during the course of the recording.

2.6.1 Whole-cell voltage-clamp recordings

In the whole-cell voltage-clamp configuration currents were recorded at 35°C in ECS (as above) at a V_{HOLD} of -60mV. Glycine receptors were blocked by the addition of 0.5µM strychnine to the ECS (as described previously by McGuire *et al*., 2013). Recording electrodes were prepared from glass capillary tubing to have a resistance of 3-6 MΩ when filled with intracellular solution (ICS). Electrodes were filled with CsCl- or KGluconate-based intracellular solutions. CsCl based intracellular contained (in mM): 140 CsCl, 10 HEPES, 10 EGTA, 2 $MgCl_2$, 1 $CaCl_2$, 2 Mg-ATP and 5 QX-314 (pH 7.2 - 7.3, 314-319mOsm). This intracellular solution provides an equal intra- and extra-cellular chloride concentration thereby enabling the detection of GABAergic synaptic events (reversal potential ~ 0mV). The CsCl and QX-314 in the ICS blocked K^+ conductances and leak Na+ currents respectively. KGluconate based intracellular contained (in mM): 130 K-gluconate, 10 HEPES, 0.2 EGTA, 2 KCl, 2 NaCl, 2 Mg-ATP, 0.5 GTP-Na, 10 phosphocreatine-tris (pH 7.2 - 7.3, 285-295mOsm). This low chloride intracellular solution represents a near physiological ionic state allowing the detection of glutamatergic synaptic events (reversal potential ~0mV). Where stated, GTP was substituted for 1mM GDP-βS in the intracellular solution in order to inhibit G protein receptor signalling and 0.5µM TTX was included in the ECS in order to block Na^+-dependent action potentials. Different ICS was used due to the observation that histamine-induced currents were difficult to record with CsCl ICS (possibly due to the blockage of K^+ channels) therefore all recordings performed in Chapter 4 utilised KGluconate ICS.

2.6.2 Cell-attached voltage-clamp recordings

Cell-attached voltage-clamp recordings were made using the same equipment set up as described above, at 35°C in ECS. Electrodes were filled with ECS. Action currents were recorded from putative 5-HT neurons by lowering the electrode onto the cell, while applying positive pressure. Once contact was made with the cell gentle suction was applied to form a loose seal (< giga-ohm) with the membrane. Action currents were recorded at a voltage clamp that maintained a 0pA leak current (Perkins, 2006). The patch seal was regularly checked throughout the recording to ensure the seal was maintained and the cell did not enter whole-cell configuration.

2.6.3 Whole-cell current-clamp recordings

Whole cell current clamp recordings were made at 30°C. The whole-cell configuration was achieved as described previously for whole-cell voltage-clamp experiments. Whole-cell capacitance and series resistance were estimated in the voltage-clamp mode and then recordings were switched to current clamp mode and bridge balance adjusted (using the series resistance control) to correct any voltage drop error. To monitor access resistance, recordings were regularly switched back to voltage clamp mode. Patch electrodes were filled with KGluconate solution (described above) and the osmolarity of the intracellular solution was increased to 310-320mOsm 1^{-1} with D-mannitol. The liquid junction potential was not corrected for.

2.6.4 Identification of putative 5-HT neurons

Putative 5-HT neurons were identified on the basis of their location and morphology. Neurons were densely populated along the midline and more sparsely populated in the lateral wings of the DRN. The neurons were larger when compared to local GABAergic neurons and displayed a varied morphology including round, fusiform, bipolar and multipolar neurons. Extensive immunohistochemistry carried out within the laboratory in partnership with an external collaborator has confirmed that these characteristics are hallmarks of 5-HT neurons (McGuire

et al., 2013).

2.6.5 Data analysis

Recordings were digitised using an analogue to digital converter (NI-DAQ mx; National Instruments, UK) at a 10 kHz sample rate onto a personal computer using the Strathclyde Electrophysiology Software (Electrophysiology Data Recorder (WinEDR) and Whole Cell Analysis Program (WinWCP); courtesy of Dr J. Dempster, University of Strathclyde, UK).

IPSC

Individual inhibitory postsynaptic potentials (IPSCs) were detected using an amplitude threshold algorithm (amplitude greater than -4pA, duration longer than 3ms) in WinEDR. Captured events were visually inspected for validity and were rejected if they contained multiple events, an unstable pre- or post-event baseline, or spurious noise. Individual IPSCs were analysed in WinWCP with respect to their peak amplitude, rise time, T_{50} (time to decay to 50%), T_{90} (time to decay to 90%) while a weighted decay time constant, τ_w (Fig 2.4.A) was determined for the averaged signal (see below). Events with a rise time >1ms were removed in order to minimise the contribution of unquantifiable electrical filtering from dendritic IPSPs. Accepted events (a minimum of 40) were subsequently averaged by alignment with the mid-point of the rising phase and fitted with either a mono- ($Y(t)=Ae^{(-t/\tau)}$) or bi-exponential ($Y(t)=A_1e^{(-t/\tau1)} + A_2e^{(-t/\tau2)}$) decay function where Y(t) is the current amplitude at any given time t, A is the current amplitude at time zero and τ is the decay time constant (Fig 2.4.B). An F test was then used to determine whether the decay was best described by a mono- or bi-exponential fit (indicated by a decrease in the standard deviation of the residuals). As the majority of IPSCs were best described by a bi-exponential decay, a weighted decay constant (τ_w) was also calculated to describe the relevant contribution of each decay component according to the equation $\tau_w = \tau_1P_1+\tau_2P_2$, where τ_1 and τ_2 are the decay time constants of the first and second exponential functions and P_1 and P_2 are the proportions of the current described by the respective components.

The frequency of IPSCs were analysed using WinEDR. Individual events were detected on the basis of their rate of rise (≤ 40 pA/ms). Recordings were then visually inspected to ensure all events were included and any detected spurious noise was removed. A 2 minute period was sufficient to calculate the frequency of events, grouped into six bins of 20 s. A mean frequency and inter-event interval was calculated from the average of the 6 bins.

Tonic and drug evoked currents

Drug-induced currents indicative of changes in channel activity were quantified by calculating the difference between the holding current before and after drug application to the bath. The holding current and the root mean square (RMS i.e. standard deviation) were sampled every 102.4ms over a 1min period for each experimental condition. At a sampling rate of 10kHz, 1024 baseline points for each 102.4ms provided one data point. Epochs containing synaptic events, or an unstable baseline were excluded from the analysis. In order to ensure that any drug-induced change of the holding current was a genuine effect and not due to a temporal 'drift', two 1min sections of the holding current during control were analysed (C1 and C2). Similarly, a 1min section was analysed following drug application, after the drug effect had reached plateau (D). Both the control sections (C1 and C2) and D were sampled at comparable temporal intervals to control for any temporal drift that may have occurred during the control section and following the drug application (Fig 2.5). The mean D.C. values for C1 and C2 were pooled and the standard deviation calculated. An effect of drug was considered genuine if the absolute value of change in the holding current following drug application (i.e. D – C2) was greater than twice the standard deviation association with the control section measurements.

Cell firing

In cell-attached voltage-clamp experiments investigating the effect of bath application of drug on action current frequency, events were automatically detected using WinEDR on the basis of their rate of rise (~ 40-120 pA/ms). The entire record was visually inspected to ensure that no action currents had been missed by the automated detection and to remove spurious noise that met the detection criteria. The IEIs were measured in control conditions and following bath application of drug onto the neurone and compared (Fig.2.6).

Focal drug application

The change in holding current following focal (spritz) drug application was calculated using WinEDR. Focal drug responses had a slow onset and prolonged decay back to baseline (typically lasting 20-40s). Therefore the picrospritz channel was used to detect each focal application event and a 60s window was extracted to be analysed. The holding current and the RMS were sampled every 102.4ms over a 5s period for control and 2.5s period for the maximum drug effect (Fig. 2.7). As above, at a sampling rate of 10kHz, 1024 baseline points for each 102.4ms provided one data point. Epochs containing synaptic events, or an unstable baseline were excluded from the analysis. An averaged value for the change in holding current and RMS was obtained from 5 drug events during control (i.e. ECS perfusion) and during drug application (i.e. addition to the ECS).

Input-output

To estimate the impact of the histaminergic conductance upon the excitability of DR neurones, input-output curves estimating the number of action potentials (APs) fired in response to current injection were constructed. Input-output curves were calculated in current clamp mode by running a stimulus protocol that injected current pulses that increased sequentially from -40pA to +120pA in 20pA steps with a 400ms duration and a 15s delay between pulses. Each stimulus was repeated three times in the absence and presence of drug. Current injections were detected in WinEDR on the basis of their rate of rise and traces were inspected manually to remove spurious noise that falsely met the detection criteria. Action potentials were then manually detected within the pulse and the frequency calculated.

Input resistance

The input resistance was recorded in voltage-clamp mode by injecting a set voltage pulse (-4 mV amplitude, 30 ms duration, 0.1 s interval). Two 10 s control periods (C1 and C2) were analysed to measure the current induced as a result of the voltage step with the input resistance being calculated from Ohm's law (R = V/I). Similar to above, the control periods were compared to check for any temporal drift that may have occurred and then compared against the corresponding drug period (D – C2). The voltage pulses were detected using

WinEDR on the basis of their rate of rise. They were inspected to remove spurious noise that met the detection criteria and subsequently exported to WinWCP where the associated current changes were measured. Recordings were discarded and not analysed if following voltage injection a steady plateau was not reached.

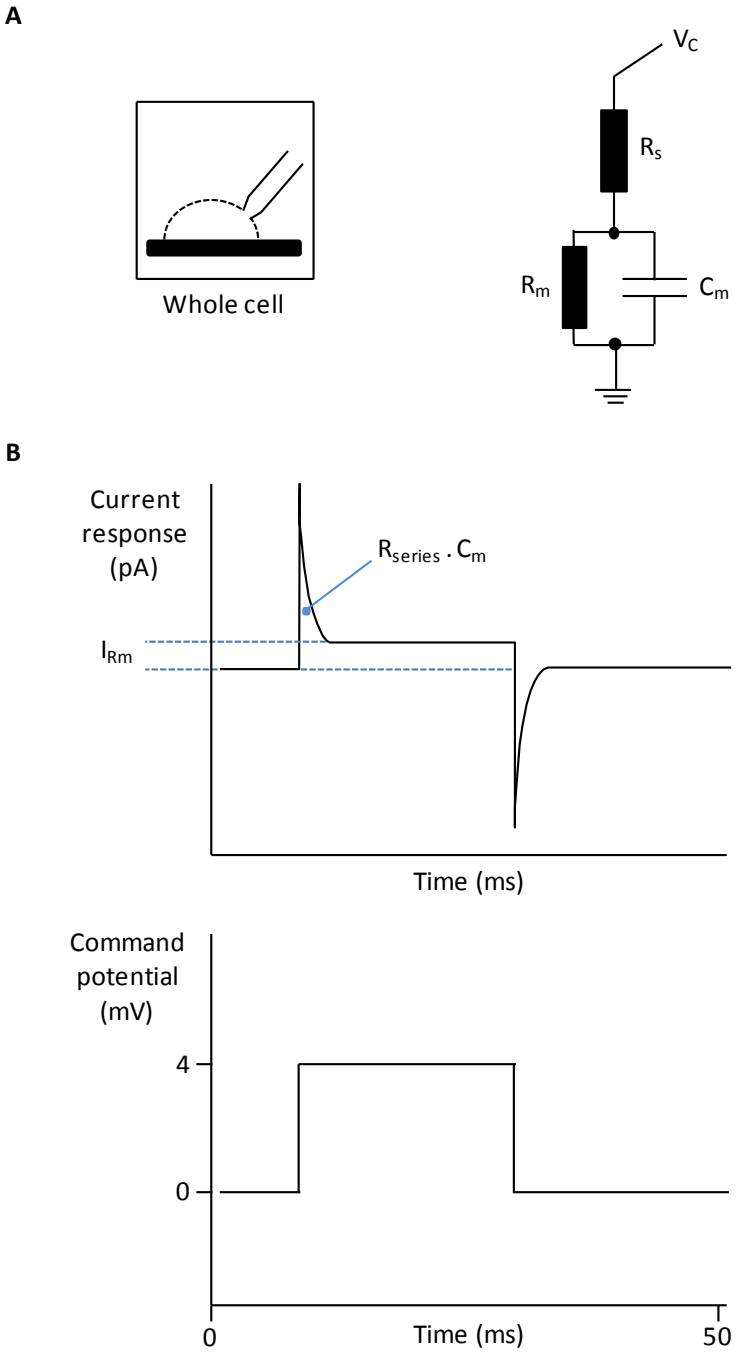

Fig 2.3. Whole-cell recording configuration with corresponding RC circuit and current-voltage traces. (A) Left: A schematic representation of whole-cell recording configuration with the electrode patched on to a small area of the cell membrane. Right: The corresponding RC circuit showing the series resistance, R_s ($R_{pipette}$ + R_{access}) caused by the introduction of the pipette to the cell membrane which has resistance R_m and capacitance C_m. (B) A typical whole-cell current response to a set command voltage, V_c. Note that the current response is made up of a transient response formed by R_s and C_m and a steady-state component determined by R_m (adapted from Patch Clamping by Areles Molleman, 2003).

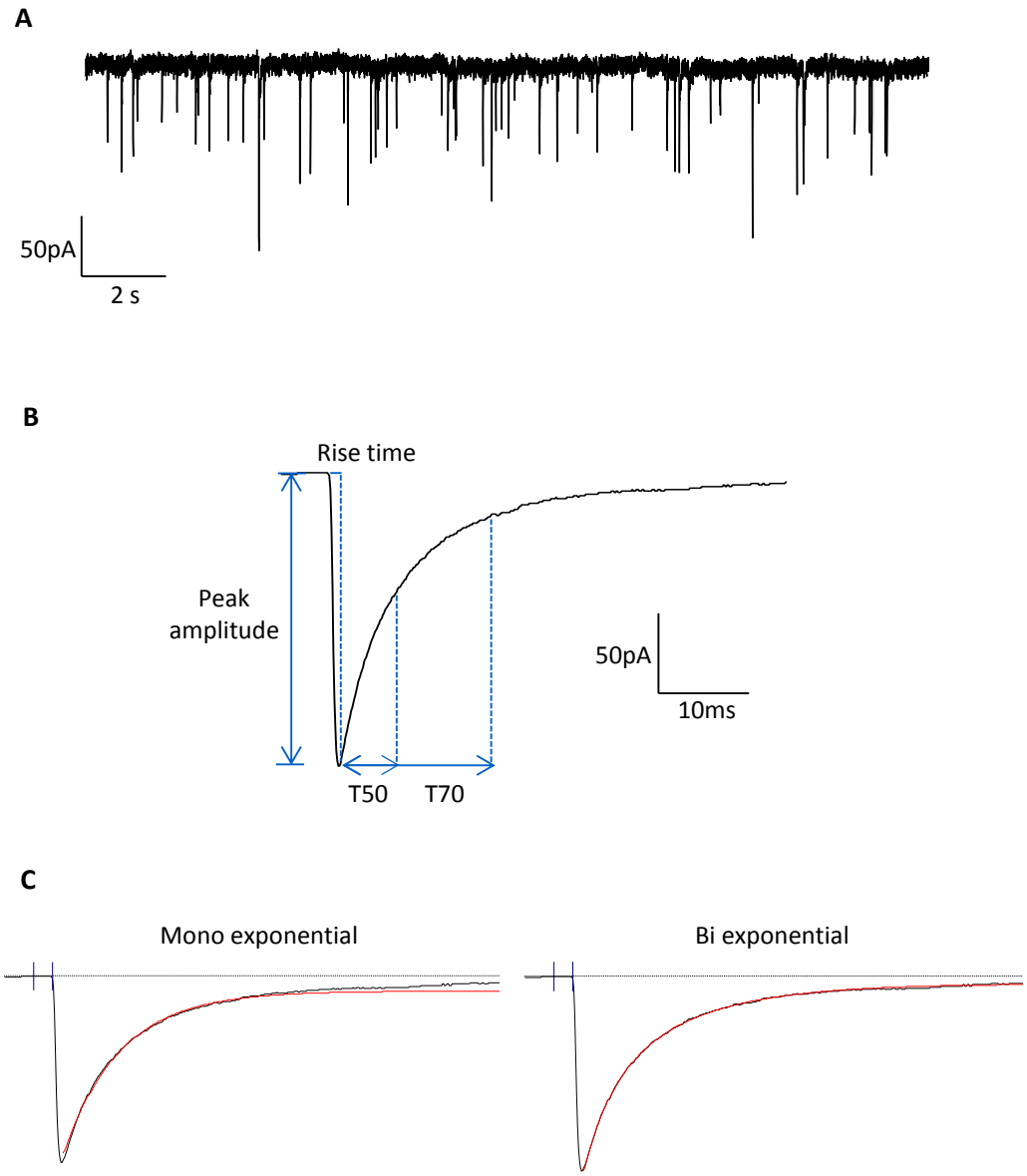

Figure 2.4. Representative whole-cell recording and associated analysis of IPSC from a DR 5-HT neuron. (A) A representative whole-cell recording trace (15s) of IPSCs from a putative 5-HT neuron in the DRN voltage-clamped at -60 mV. (B) The peak amplitude, rise time, T50 and T90 were calculated in WinWCP (C) Ensemble averaged IPSC with a superimposed mono- (left) or bi- exponential (right) fit (blue). Note that the bi exponential decay provide a better fit The frequency was calculated from the raw trace using WinEDR . See section X.Y for details of IPSC analysis, assessment of the best fit and frequency analysis).

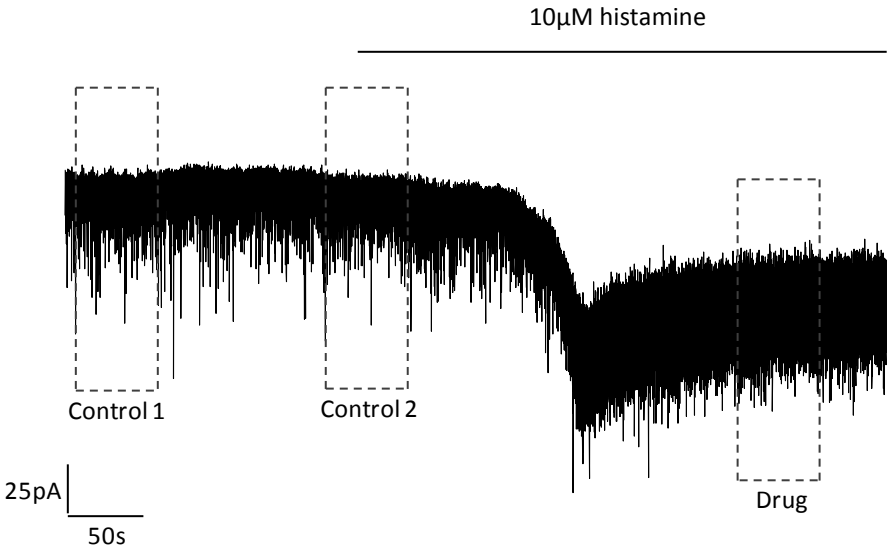

Figure 2.5 Analysis of drug-evoked currents. A representative whole-cell recording from a presumed 5-HT voltage clamped at -60 mV before and after the bath application of Drug X. The holding current and RMS were calculated over two separate one minute periods during control (dashed boxes. control 1 and control 2). The holding current and RMS was calculated over one minute period during the maximal drug effect (dashed box, drug).

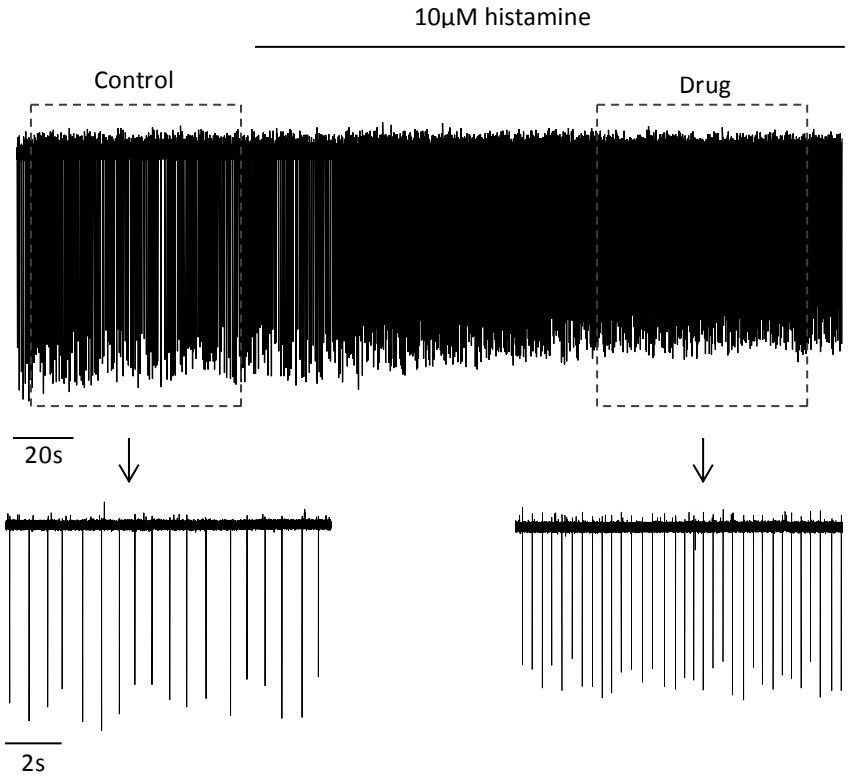

Figure 2.6 Analysis of cell-attached cell firing. A representative cell-attached recording from a presumed 5-HT neuron maintained at 0pA. The firing frequency and inter-event interval was calculated over 60s for control (dashed box) and drug (dashed box).

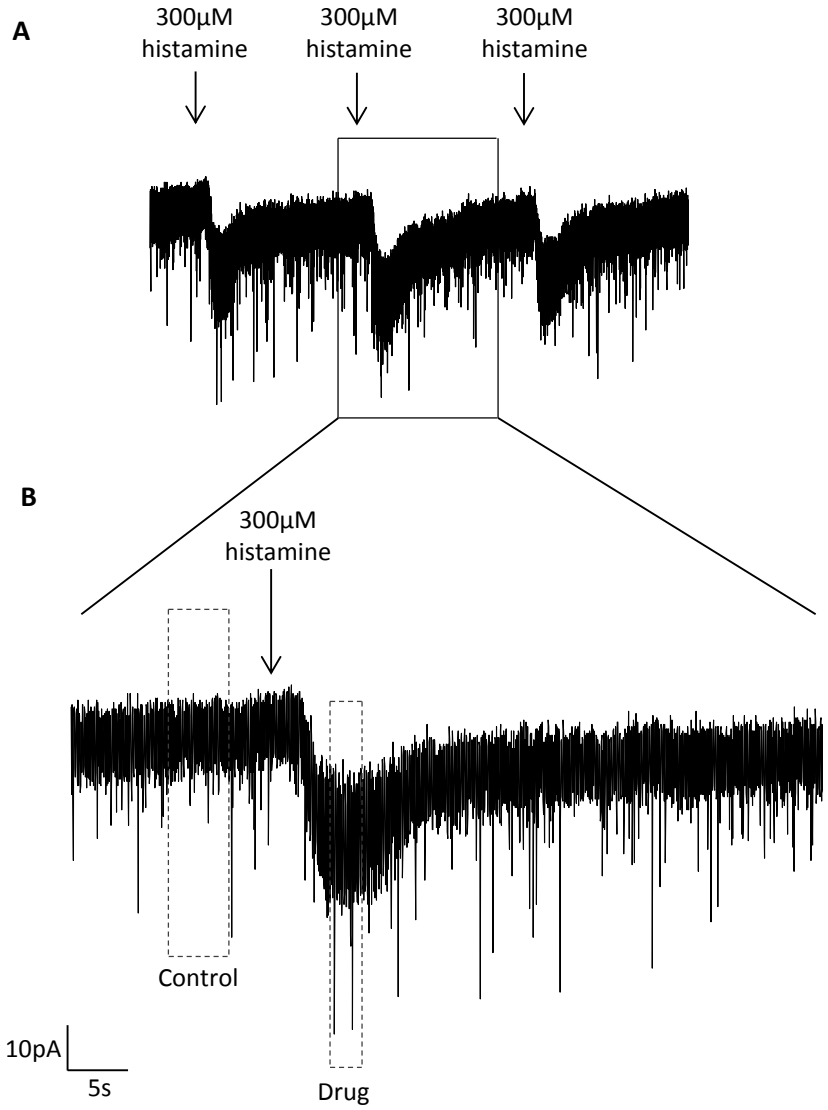

Figure 2.7 Analysis of focal drug application. (A) A representative whole-cell voltage-clamp (V_H = -60mV) recording illustrating the holding current during focal (spritz) application of drug. (B) Expanded view of a single drug response. The holding current and RMS are calculated over a 5s period immediately prior to the drug application (dashed box, control). The holding current and RMS are then calculated during 2.5s of the maximal drug effect (dashed box, drug).

2.7 *In vivo* single-unit recordings

Adult, male Wistar rats (280-370g) were anesthetised with 25% urethane administered via intraperotineal (i.p.) injection. An initial injection of 5ml/kg urethane was given followed by additional injections of 0.3ml (given at 20 minute intervals) until no foot and eye reflexes could be detected. The animal was then transferred to a heat pad and maintained at 37°C via a rectal probe attached to a homeothermic control unit (Harvard Apparatus, UK). The head was shaved and the animal was placed into a stereotaxic frame, secured by ear and teeth bars (KOPF Instruments, CA, USA). The tail vein was cannulated (24GA, 0.75"; Angiocath, UK) and secured in place with surgical tape to allow delivery of drugs. A midline incision was made over the skull and the subcutaneous tissues were cleared. The skull was visualised with a Zeiss microscope (OPMI pico) equipped with x1.6 magnification and adjusted to sit in the flat position (Fig.2.8). A 5mm^2 hole was drilled 7.3mm posterior to Bregma and the exposed dura matter was cut. A miniature stainless steel screw was driven into the skull above the cerebellum and served as a ground electrode. A carbon fibre electrode with 0.4-1.2MΩ impedance (Carbostar-1; Kation Scientific, MN, USA) was position 7.5mm posterior from Bregma and 1.5mm lateral from the midline and set at an angle of 15° (Fig.2.9). The electrode was advanced to a depth of 5-6mm below the brain surface using a micromanipulator (IVM; Scientifica, UK). Signals were recorded with a NL104A pre-amplifier connected to a NL100AK headstage (Neurolog System, Digitimer, UK). Signals were filtered (500Hz-5kHz) and 50/60kHz noise was removed using a Humbug noise eliminator (AutoMate Scientific, USA). Signals were fed to a PC via a micro1401 analogue to digital converter interface (CED, UK) at a sampling rate of 32,000Hz. Data were collected using Spike2 software (version 5, CED, UK). The frequency of cell firing was monitored on line using a simple threshold crossing. Signals were only considered to be from serotonergic neurons if they displayed strict electrophysiological criteria: regular firing, 2-4ms spike duration with a slow frequency of 0.3-4.5Hz (Aghajanian & Vandermaelen, 1982b, Allers & Sharp, 2003).

2.7.1 Data analysis

All data were analysed offline using Spike 2 software (Version 5, CED, UK). Events which were

captured on-line were carefully checked and any noise was removed. This edited channel was then used to calculate the firing frequency and inter-event-interval (IEI). The spike width was calculated by averaging 100 spikes from the raw trace. The basal firing rate was determine in a 10 minute period at the start of each recording and expressed as average frequency (Hz). All cells were then challenged with a vehicle treatment and a 10 minute section of recording was compared with the basal firing to assess if there was any effect. Each response to drug was determine in a 10 minute period during the maximum change in the baseline and expressed as an average frequency. The drug response was then calculated as the percentage change relative to vehicle (i.e. vehicle = 100%, drug effect = % of vehicle). The Coefficient of Variation (CV) was calculated (standard deviation divided by the mean inter-spike interval) for control and drug periods in order to measure spike train regularity

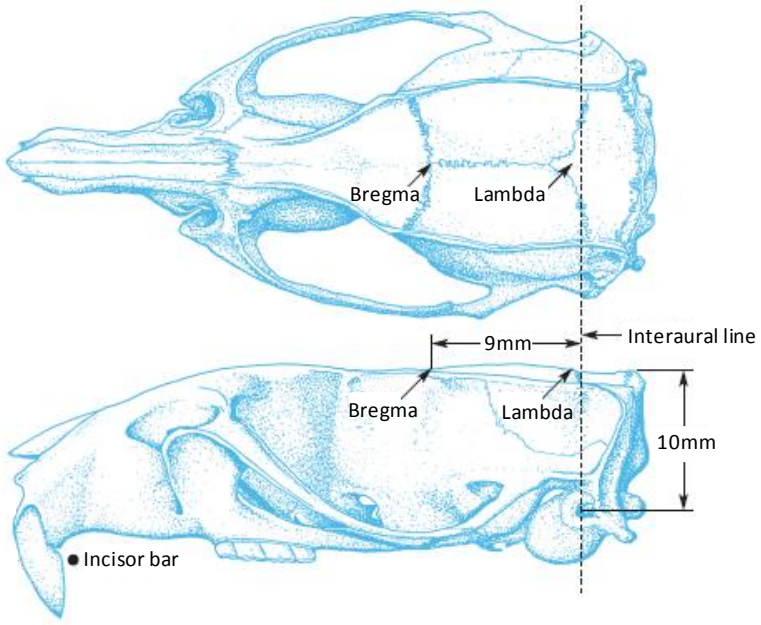

Figure 2.8. Rat skull diagram. Dorsal and lateral views of the skull of a 290g Wistar rat. The positions of bregma, lambda and the plane of the interaural line are shown. Lambda is 0.3mm anterior to the coronal plain passing through the interaural line (adapted from Paxinos & Watson rat brain atlas 2005).

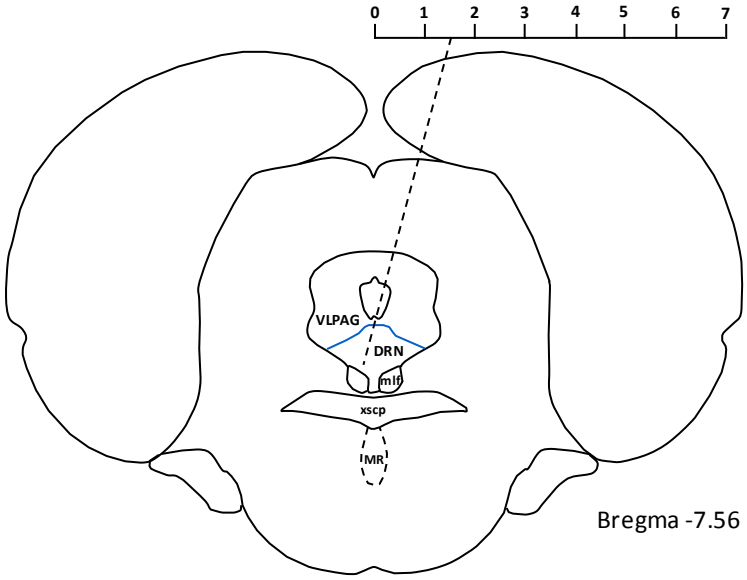

Figure 2.9. Schematic of the rat brain on the coronal plain illustrating the DRN. Coronal section of the rat brain (-7.56mm from bregma). Electrode placement 1.5mm mediolateral at 15° produces the electrode tract illustrated. VLPAG, ventrolateral periaqueductal gray, mlf, medial longitudinal fasciculus, xscp, decussion of the superior cerebellar peduncle, MR, median raphe nucleus (adapted from Paxinos & Watson rat brain atlas 2005).

2.8 *In vivo* sleep studies

2.8.1 Animal preparation

Adult, male Wistar rats (250-300g) were anesthetized (2% isoflurane in 100% oxygen) and surgically prepared with a cranial implant that permitted chronic electro-encephalogram (EEG) and electromyogram (EMG) recording. Body temperature and locomotor activity were monitored via a miniature transmitter (Minimitter PDT4000G, Philips Respironics, Bend, OR) surgically placed in the abdomen during the same anesthetic event in which the cranial portion was implanted. The cranial implant consisted of stainless steel screws (2 frontal [+3.5 AP from bregma, ±2.0 ML] and 2 occipital [-6.5 AP, ±5.2 ML]) for EEG recording (Fig.2.10). Two Teflon-coated stainless steel wires were positioned under the nuchal trapezoid muscles for electromyography (EMG) recording. All leads were crimped to a miniature connector (Omnetics, Minneapolis, MN, USA) and gas sterilized with ethylene oxide prior to surgery. The implant assembly was affixed to the skull by the combination of the EEG recording screws, cyanoacrylate applied between the hermetically sealed implant connector and skull, and dental acrylic. An analgesic (buprenorphine 0.05 mg/kg) was administered subcutaneously pre-operatively, at the end of the surgery day, and the morning of the first post-operative day. To provide additional pain relief, meloxicam 0.15 mg/kg was administered orally twice daily for 6 days post-surgery. The antibiotic cefalexin 20 mg/kg was administered orally 24 hours prior to and immediately before surgery, and twice daily for 7 days after surgery. At least 3 weeks were allowed for recovery.

2.8.2 Recording environment

Each rat was housed individually within a specially modified Ancare™ microisolator cage (Ancare, Bellmore, NY, USA) having a custom polycarbonate filter-top riser and an ultra-low-torque slip-ring commutator (Hypnion Inc., Lexington, MA, USA). A custom engineered flexible tether connected at one end to the commutator and at the other end to the animal's cranial implant. Each cage was located within separate, ventilated compartments of a stainless steel leep-wake recording chamber, and had an infrared light source and digital video camera to

allow a minimum of twice daily remote visual monitoring. Food and water were available *ad libitum*, and the ambient temperature was 23±1°C. A 24-hr light-dark cycle using fluorescent light was maintained and monitored throughout the study. Light intensity averaged 35-40 lux at mid-level inside the cage. Relative humidity averaged 50%. Animals were undisturbed for 48 hours before and after each treatment.

2.8.3 Data collection

Sleep and wakefulness were determined using SCORE-2000™ (hereinafter called SCORE) a validated microcomputer-based sleep-wake and physiological monitoring system (Al-Shamma *et* a., 2010). The system monitored amplified EEG (X10,000, bandpass 1-30 Hz [Grass Corp., Quincy, MA, USA]; initial digitization rate 400 Hz), integrated EMG (bandpass 10-100 Hz, RMS integration), and telemetered body temperature and non-specific locomotor activity, and drinking activity. Arousal states were classified on-line as NREM sleep, REM sleep, wake, or theta-dominated wake every 10 seconds using EEG period and amplitude feature extraction and ranked membership algorithms. Individually taught EEG-arousal-state templates and EMG criteria differentiated states of arousal. A fast Fourier transform (FFT) was used to calculate the spectral power of EEG in each epoch in 0.1 Hz bins. Time series of EEG power in each of 4 bands (delta 0.1-3.9 Hz, theta 4.0-8.9 Hz, alpha 9.0-11.9 Hz, beta 12.0-20.0 Hz) was calculated for all EEG-defined NREM epochs devoid of artifact. Locomotor, drink-related, and food-related activities were automatically recorded as counts per minute, and body temperature was recorded each minute. Locomotor activity was detected in both horizontal and vertical planes by a customized telemetry receiver (ER4000, Minimitter Inc., Bend, OR, USA) beneath the cage. Drink-related and food-related activities were detected by beam break sensors closely situated around recessed access portals to the lixit and the food bin, respectively.

Telemetry measures (locomotor activity and body temperature) were not part of the SCORE arousal-state determination algorithm; thus, sleep-scoring and telemetry data were concurrent but independent measures. In addition to frequent on-line inspection of the EEG and EMG signals, quality control of the data was assured by expert analysts using a suite of programs (ScoreView™, Lilly proprietary software, described below) that allowed data quality

of all variables to be flexibly scrutinized at the level of (1) individual visual examination of raw EEG and EMG signals, (2) individual hourly mean time-series, and (3) group mean time series, using a combination of graphical and statistical assessments. An integrated relational database was updated with data quality control decisions for each individual treatment, and this database controlled all subsequent use of these data.

2.8.4 Data processing

Files of digitized EEG/ EMG data were subject to offline processing. ScoreView™ quality control software allowed EEG-arousal-state templates and EMG criteria to be individually taught and optimized offline, using the pre-treatment baseline portion of a file. It also concurrently provided detailed flexible EEG/EMG visualizations, overviews including locomotor activity and body temperature, FFT, statistics and artifact information for the file being reviewed. Templates were optimized after the first week an animal was online, with occasional further minor optimizations in subsequent weeks. If a template was optimized, the data file was re-scored using the new template. Only the pre-treatment baseline portion of the file was used for scoring optimization. Based on these individual animal data evaluations, preliminary quality control judgments were recorded in the database. ScoreView™ then permitted time series overlay plots of all individuals in a treatment group, allowing visualization of individual 'outliers' in any time series for any variable. Outliers were subject to additional scrutiny facilitated by ScoreView™ to determine whether the underlying data contained unacceptable artifacts. Final quality control judgments were then entered into the database and controlled all subsequent use of the data. A team of experts (≥3 years of experience) conducting these analyses were not blind to the treatment, but they were independent of the persons producing the data and of the project scientists using the data.

2.8.5 Study design and analysis

Mepyramine (1mg/kg) was studied 5 hours after lights on (CT-5, Fig. 2.11). Dosing during lights on was necessary as the tail vein was not visible during lights off (even under red light). The

compound was characterised in a parallel group study design. Drug treatments were pseudo-randomised. The total amount of REM sleep, NREM sleep, and total sleep were calculated in the 7 hours following dosing (CT-5 to CT-12). The longest sleep bout in the 7 hours following dosing was also calculated. In each of the 7 hours following dosing the average sleep bout length was calculated, and then the average of these 7-hour averages was calculated. Corresponding calculations were made 24 hours earlier as baseline variables. The latency to the first 30 continuous seconds of any sleep (3 consecutive epochs), first 60 continuous seconds of any sleep (6 consecutive epochs), and first 20 continuous seconds of REM sleep (2 consecutive epochs) was calculated. No baseline variables were calculated for latency variables. Total locomotor activity counts were calculated for the 12 hour lights off period (CT-12 to CT-24). This was divided by the total amount of wake time in that period to derive a measure defined as locomotor intensity. Total sleep time is also reported. Baseline measures were calculated for all 3 variables (locomotor activity counts, wake time, and locomotor intensity).

2.9 Reagents and drugs: *in vivo* studies

All chemicals are listed in Table 1.2 with the corresponding site of action, dose used, vehicle solution and the company from which they were obtained. Briefly solutions were dissolved in 0.9% NaCl saline, HBCD, or 0.25% MC. All drugs were purchased from Sigma Aldrich (Dorset, UK), National Vetenary Supplies (NVC, Stoke-on-Trent, UK) or obtained from Eli Lilly (IN, USA). Where required, all drug formulations occurred immediately before each treatment, the only exception was for urethane which was made up each week. Each compound was added to its corresponding vehicle and where required was mixed using a sterile ground glass mortar and closely fitting pestle (i.e. tissue homogeniser) until finely suspended. Solutions were agitated immediately before being drawn into a syringe. For sleep studies, to administer the treatment each rat was removed from its cage for approximately 60-90s to be weighed and treated.

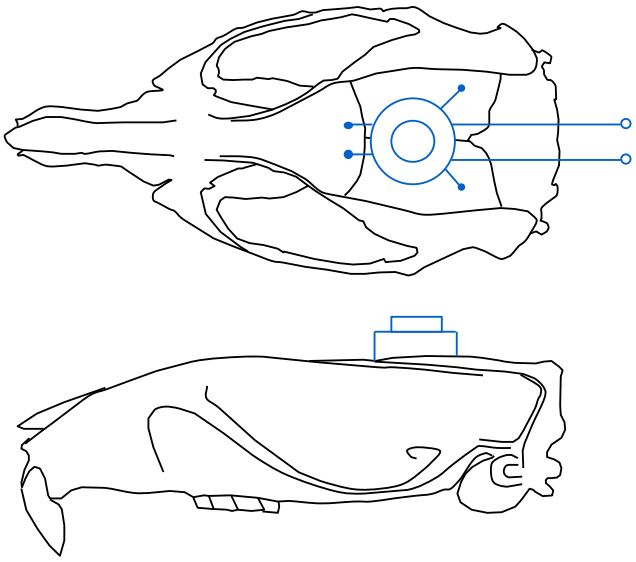

Figure 2.10. Rat skull with cranial implant. Dorsal and lateral views of the skull of a 290g Wistar rat with a cranial implant (blue). Four stainless steel screws (2 frontal and 2 occipital) allowed EEG recording and two stainless steel wires positioned under the nuchal trapezoid muscles allowed EMG recording.

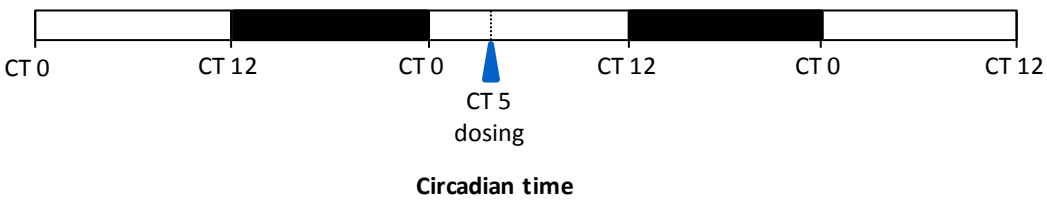

Figure 2.11. 60 hour circadian time scale. Animals were given an i.v. Injection of drug at circadian time 5 (CT-5). Sleep-wake variables (wake, NREM, REM) and locomotor activity were monitored for 60 hours in total (29 hours pre-dosing and 31 hours post-dosing).

Table 1.2 List of chemicals used for *in* vivo experiments. Full chemical names are detailed in the abbreviation list.

Chemical name	Receptor/mode of action	Dose/% used	Vehicle solution	Route	Company
Urethane	Anaesthetic	25% solution	Distilled water	Intraperitoneal	Sigma
Isoflurane	Anaesthetic	2% solution	100% oxygen	Inhalation	NVC
Buprenorphine	Anaelgesic	0.05mg/kg	Ready made	Subcutaneous	NVS
Meloxicam	Anaelgesic	0.15mg/kg	Ready made	Oral	NVS
Cefalexin	Antibiotic	20mg/kg	Distilled water	Oral	NVS
Mepyramine	H_1 inverse agonist	1-10mg/kg	0.9% NaCl saline	Intravenous	Lilly

2.10 Statistical analysis

Data are presented as the arithmetic mean ± standard error of the mean (SEM) and values of n refer to the number of independent cells tested in each group. The statistics software IBM SPSS (version 21) was used to carry out all of the statistical tests reported. Where appropriate a Student's t-test (paired or unpaired), ANOVA (with or without repeated measures design), ANCOVA or General Estimating Equation with clustering (GEE) test was carried out. Note, GEE is an extension of ANOVA which enables clustering of data sets when required e.g. data obtained from multiple slices from a single brain can be clustered together in order to assign each slice as an n of 1 (rather than assigning a brain to an n of 1). Post hoc tests were also carried out where appropriate. Details of the relevant statistical tests used to determine the effect of each drug are described within the relevant results section.

Chapter 3:

Regulation of dorsal raphe neurons *in vitro*

3.1 Introduction

The DRN contains one of the largest groups of serotonergic neurons in the brain and is the principle source of serotonergic innervation of the forebrain. Early *in vivo* electrophysiological studies demonstrated that DRN serotonergic neurons displayed remarkably consistent pharmacological and electrophysiological characteristics. These cells were shown to exhibit slow (0.3-4Hz), regular, spontaneous activity, to fire broad action potentials (3-4ms duration) followed by a prominent after-hyperpolarisation, and to be inhibited by 5-HT (Aghajanian and Vandermaelen, 1982a, 1982b). Moreover *in vitro* recordings made from 5-HT neurons in the DRN demonstrated that the electrophysiological characteristics of these neurons were indistinguishable from 5-HT neurons recorded *in vivo* (Mosko & Jacobs, 1976; Vandermaelen & Aghajanian, 1983). These criteria became accepted hallmarks of serotonergic neurons and were viewed as necessary and sufficient for neuronal identity. This has permitted the distinction between 5-HT and non-5HT neurons (e.g. GABA and glutamate) within the DRN and has enabled the study of how 5-HT neurons could be regulated. Importantly it has been demonstrated that serotonergic neurons are not only under regulatory control by local, inter-raphe mechanisms but also by afferent inputs from neurotransmitters systems located throughout the brain. Noradrenergic neurons from the locus coeruleus are thought to provide an important tonic input to 5-HT neurons within the DRN which maintains the firing level of these neurons (Baraban and Aghajanian, 1980; Baraban and Aghajanian, 1981). In addition orexin neurons from the posterior hypothalamus have been shown to excite 5-HT neurons within the DRN and this has been implicated in regulating these neurons during wakefulness (Brown *et al*., 2001). This chapter has focussed on investigated how the electrophysiological output from DRN 5-HT neurons can be regulated by specific neurotransmitters and peptides including: 5-HT, phenylephrine and orexin.

3.2 Electrophysiological and pharmacological characterisation of DRN neurons

3.2.1 Electrophysiological characterisation of spontaneously firing 5-HT neurons

Using the extracellular recording configuration 25 spontaneously firing neurons were recorded from the midline of the DRN. Twenty two of these neurons (87.5%) satisfied all of the criteria

required to classify them as putative 5-HT neurons. A representative action potential (spike) from a putative 5-HT neuron can be seen in Figure 3.1. Overall these neurons fired bi-phasic (positive-negative), broad action potentials (3.56 ± 0.87ms, Fig 3.1.A1) in a highly regular pattern, as evident by the low CV value (0.29 ± 0.04, Fig 3.1.A2) and with low frequency (2.05 ± 0.32Hz, Fig 3.1.A3). A small subset of neurons recorded (12.5%) also displayed bi-phasic, broad action potentials (3.52 ± 0.84ms) with a highly regular firing pattern (0.14 ± 0.3) however these neurons fired at a much higher frequency (7.84 ± 0.55Hz, Fig 3.1B). Although it is historically thought that "fast firing" neurons (frequency >4.5Hz) located along the midline of the DRN are non-5-HT there is evidence to suggest that a portion may in fact be 5-HT neurons (Allers and Sharp, 2003). As there was no possibility of confirming the neurochemical identity of these cells all subsequent extracellular experiments were performed on "slower firing", putative 5-HT neurons.

Note that these experiments were performed on tissue derived from mice P16-27 of either sex. At this age mice are sexually immature but contain a fully developed raphe serotonin system (Deng et al., 2007). In addition data were collected from more than one brain slice per animal. In order to investigate whether age and/or gender may have had a significant effect on the electrophysiological criteria of putative 5-HT (spike duration, CV or firing frequency) Generalised Estimating Equation (GEE) analyses were performed. In the GEE test age and gender were included as factors and brain slices were included as a subject variable. There was no significant effect ($p > 0.05$) of age or gender on the spike duration, CV or firing frequency therefore data was pooled from both genders and all ages.

3.2.2 Electrophysiological characteristics of 5-HT neurons are regulated by phenylephrine

It is well documented that 5-HT neurons within the DRN receive tonic excitatory input from noradrenergic neurons of the locus coeruleus (Pan et al., 1994, Sakai and Crochet, 2000). During the brain slicing process these noradrenergic afferents are severed causing a reduction or complete cessation of firing from 5-HT neurons in the DRN. The α_1-adrenoreceptor agonist phenylephrine can be used to restore 5-HT neuronal firing to levels similar to those seen *in vivo* (Smith and Gallager, 1989, Vandermaelen and Aghajanian, 1983). Here we used phenylephrine to restore the role of the noradrenergic input into the DRN.

Using the extracellular recording configuration a total of 43 putative 5-HT neurons were recorded in the presence of phenylephrine (10μM). When the electrophysiological characteristics of 5-HT neurons are compared in the absence and presence of phenylephrine it can be seen that neurons recorded in the presence of phenylephrine fire at a significantly faster frequency (2.77 ± 0.13Hz, Fig 3.2A) and in a more regular firing pattern (CV = 0.16 ± 0.02, Fig 3.2B). Note that these two populations of neurons are unpaired. A table summarising all of the neurons recorded under these conditions can be seen in Fig 3.2C. A qualitative observation noted during these experiments was that, as one may expect, it was easier to locate firing neurons in the slice when phenylephrine was present.

As these experiments were carried out on tissue derived from mice P16-27 of either sex GEE analyses were carried in order to check whether age and gender may have an effect on the spike duration, CV or firing frequency of phenylephrine-driven 5-HT neurons. In the GEE test age and gender were included as factors and brain slices were included as a subject variable. In addition phenylephrine was also added as a factor to determine if it had a significant effect on any of the measurements. There was no significant effect ($p > 0.05$) of age or gender on the spike duration, CV or firing frequency therefore data were pooled from both genders and all ages. When GEE analysis was run with drug (PE) as a factor it can be seen that phenylephrine has a significant effect on the CV ($p < 0.05$) and firing frequency ($p < 0.05$) but no significant effect on the spike width ($p > 0.05$).

3.2.3 Pharmacological characterisation of 5-HT neurons with 5-HT

In addition to the electrophysiological characterisation described above putative 5-HT neurons recorded in the DRN have been pharmacologically characterised as being inhibited by 5-HT (Vandermaelen and Aghajanian, 1983). This 5-HT-induced inhibition has been shown to occur via the 5-HT_{1A} autoreceptor located on the soma and dendrites of 5-HT neurons (Judge and Gartside, 2006, Sprouse and Aghajanian, 1986). Here we investigated the effect of 5-HT on neurons within the DRN.

Utilising the extracellular recording configuration a total of 39 putative 5-HT neurons were tested with varying concentrations of 5-HT (1, 3, 10 and 30µM). All of these neurons were recorded in the presence of 10µM phenylephrine. Thirty seven neurons were inhibited by 5-HT in a concentration-dependent manner with an IC_{50} = 7.2µM (Fig 3.3.A). One neuron was excited by 5-HT (3 and 10µM; $p < 0.05$, paired Student's t-test) and one neuron did not respond (10 and 30µM; $p > 0.05$, paired Student's t-test). Application of 10µM 5-HT to neurons revealed a wide range of inhibition from 12-100% (Fig 3.3.B). A representative recording of the firing frequency in the absence and presence of 10µM 5-HT can be seen in Figure 3.3.C. The inhibitory effect of all concentrations 5-HT were reversible (data not shown).

GEE analyses were carried out to assess whether 5-HT had a significant effect on cell firing. Age, gender and 5-HT concentration were included as factors and brain slices were included as a subject variable. Analysis carried out on the absolute values revealed that 3, 10 and 30µM had a significant effect of the firing frequency ($p < 0.01$) whereas analysis carried out on the normalised data revealed that all concentrations of 5-HT had a significant effect on firing ($p < 0.05$).

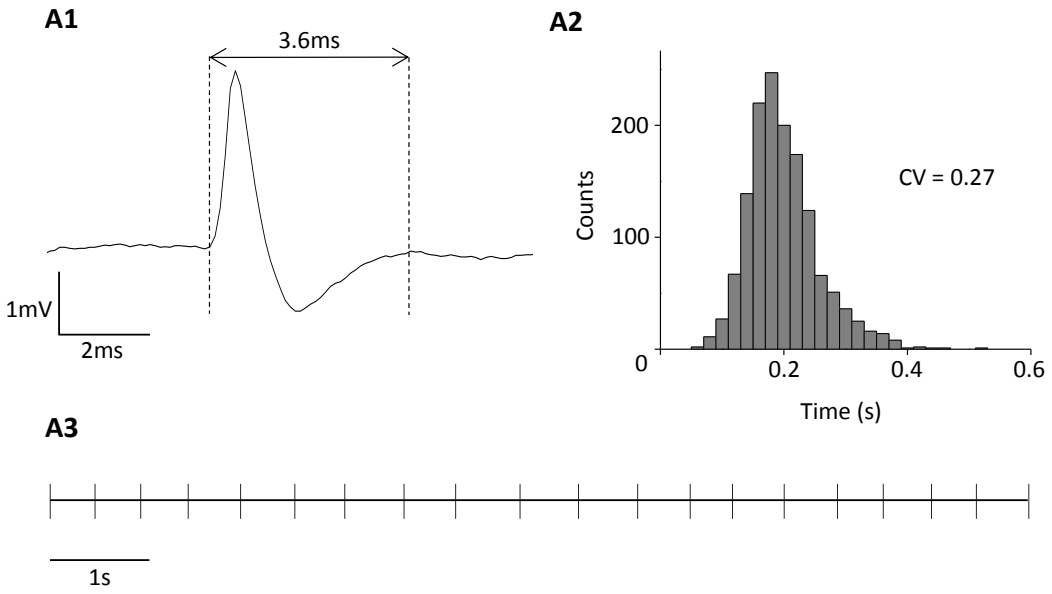

B

Type of neuron	n	Spike width (ms)	CV	Frequency (Hz)
"Slow firing neurons"	22	3.62 ± 0.25 (1.2-5.0)	0.29 ± 0.04 (0.08-0.88)	2.05 ± 0.32 (0.32-4.50)
"Fast firing neurons"	3	3.52 ± 0.84 (2-5.0)	0.14 ± 0.3 (0.1-0.19)	7.84 ± 0.55 (7.23-8.94)

Figure 3.1. Extracellular characterisation of 5-HT neurons in the DRN. (A1) A representative biphasic, broad-width action potential (spike) recorded from the midline of the DRN. (A2) A representative interevent-interval histogram (in 25ms bins) indicating a very regular firing pattern (CV = 0.27). (A3) A representative 10 second section of the spike train. (B) A table summarising the electrophysiological properties analysed to establish 5-HT neuronal identity. Values are displayed as the average ± SEM. Values in parentheses represent the range of values.

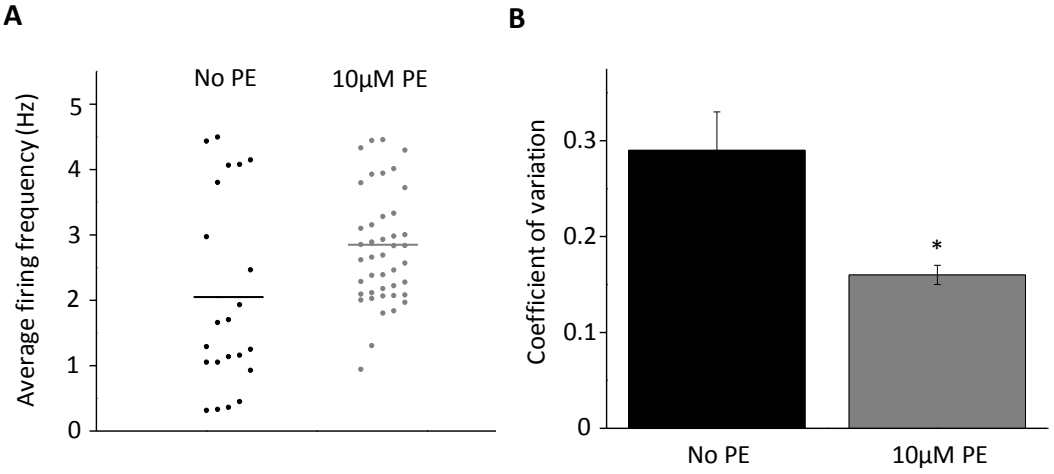

C

	n	Spike width (ms)	CV	Frequency (Hz)
No phenylephrine	22	3.62 ± 0.25 (1.2-5.0)	0.29 ± 0.04 (0.08-0.88)	2.05 ± 0.32 (0.32-4.50)
10µM phenylephrine	43	3.76 ± 0.15 (2.0-5.0)	0.16 ± 0.02* (0.04-0.45)	2.77 ± 0.13* (0.94-4.46)

Figure 3.2. A comparison of 5-HT neuronal characteristics in the presence and absence of phenylephrine. (A) A scatter plot of the average firing frequency of putative 5-HT neurons in the absence and presence of the α_1-adrenoreceptor agonist phenylephrine, PE (10µM). The horizontal line denotes the average value. (B) A bar graph depicting the average coefficient of variation (CV) associated with recordings performed either in the presence or in the absence phenylephrine (PE). (C) A table summarising the electrophysiological characteristics of 5-HT neurons in the presence and absence of phenylephrine. Values are displayed as the average ± SEM. Values in parentheses represent the range of values. Note that 5-HT neurons recorded in the presence of 10µM phenylephrine fire at a significantly faster frequency and in a more regular pattern i.e. lower CV. *$p < 0.05$, GEE analysis.

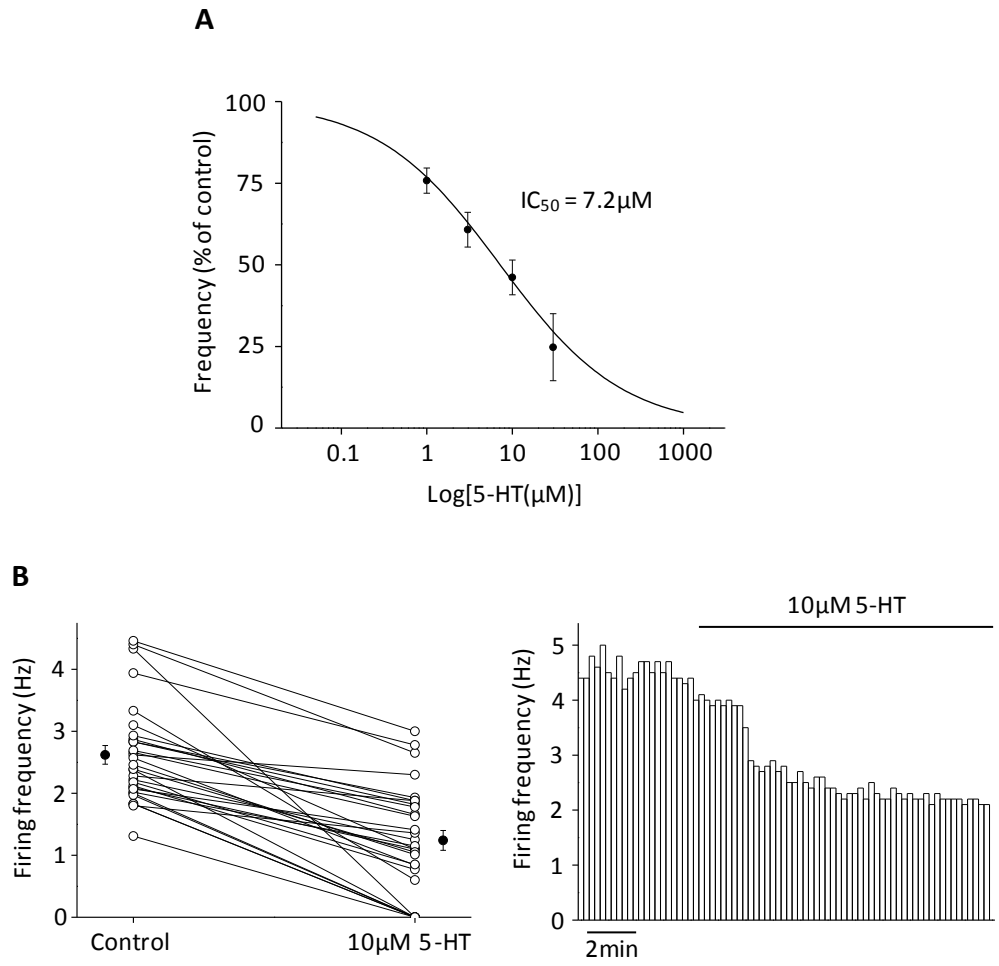

Figure 3.3. 5-HT inhibits in a concentration-dependent manner the firing of putative 5-HT DRN neurons. (A) A plot illustrating the 5-HT concentration-dependent inhibition of DRN neuronal firing. Firing frequency of putative 5-HT DR neurones (expressed as % of control) is plotted on the Y axis as a function of increasing concentration of 5-HT on the x axis (log scale). The corresponding IC_{50} value is given to the right of the curve and was obtained from non-linear regression analysis. Note that 5-HT causes concentration-dependent inhibition of firing with an IC_{50} equal to 7.2 ± 0.1 µM. (B) Left: Firing frequency of individual putative 5-HT neurons (open circles) in the absence (control) and presence of 5-HT (10µM). The average firing frequency in control and in the presence of 5-HT is shown by the closed circles (mean ± SE). Right: A representative recording of the firing frequency (20s bins) from a phenylephrine-driven 5-HT neuron in the presence of 10µM 5-HT.

3.3 Regulation of 5-HT neuronal firing by 5-HT$_2$ receptors

It has been well established that somatodendritic 5-HT$_{1A}$ autoreceptors located on 5-HT neurons provide an important local feedback regulation within the DRN (Aghajanian and Lakoski, 1984, Williams et al., 1988). In addition to 5-HT$_{1A}$ receptor regulation, mounting evidence has emerged implicating postsynaptic 5-HT$_2$ receptors in the 5-HT-mediated feedback regulation of DRN activity (Boothman et al., 2003, Garratt et al., 1991, Kidd et al., 1991, Wright et al., 1990). Immunohistochemistry (Boothman and Sharp, 2005) and in situ hybridisation studies (Serrats et al., 2005) have shown that 5-HT$_2$ receptors are located on local GABAergic neurons which synapse onto 5-HT neurons. In support of these findings, an electrophysiological investigation in rat brain slices demonstrated the bath application of 5-HT or DOI (a mixed 5-HT$_{2A/2C}$ agonist) increased the frequency of GABA-mediated synaptic currents in 5-HT cells (Liu et al., 2000). Here I utilised extracellular and whole-cell voltage-clamp recordings to assess the role of 5-HT$_2$Rs in the regulation of mouse DRN neuronal activity by 5-HT and explored a putative contribution by GABAergic neurons.

3.3.1 Selective 5-HT$_2$ receptor antagonists do not alter 5-HT-induced inhibition

All recordings described below were performed in the presence of phenylephrine. Utilising the extracellular single-unit recording configuration neurons were initially challenged with 5-HT (10µM) to establish the neuron sensitivity to 5-HTR activation. After complete washout either a selective 5-HT$_{2A}$ receptor (MDL 100907, 30nM) or a selective 5-HT$_{2C}$ (SB 242084, 30nM) antagonist was applied. 5-HT (10µM) was subsequently applied in the presence of each antagonist and the ensuing response compared with that initially established in the absence of the antagonist. (Fig.3.2.1). 5-HT application produced a reduction of firing in both treatment groups (Fig3.4). Application of either antagonist MDL 100907 (Fig.3.4A) or SB 242084 (Fig.3.4B) in the absence of 5-HT did not affect the firing of neurons (see Fig.3.2.1A and Fig.3.2.1B for MDL 100907 and SB 242084 respectively). Furthermore neither antagonist was able to alter the 5-HT response.

A one-way repeated measures ANOVA (with drug treatment as the within-subjects factor) performed on the normalised data revealed a significant main effect of drug application on the

percentage of control firing ($F(4,8) = 8.091$; $p < 0.01$). In order to see if 5-HT application was significantly different from MDL + 5-HT application pairwise comparisons were performed using Bonferronni correction. No significant difference was revealed. This statistical analysis was repeated for cells which received SB 242084 treatment. A one-way repeated measures ANOVA performed on the normalised data revealed a significant main effect of drug application ($F(4, 8) = 17.734$; $p < 0.01$). Pairwise comparisons using Bonferronni correction were performed. No significant different was revealed between 5-HT application and SB + 5-HT application.

3.3.2 Direct activation of 5-HT_2 receptors caused inhibition of 5-HT neuronal firing

To investigate the role of 5-HT_2 receptors in the DRN further we applied the mixed 5-$HT_{2A/2C}$ agonist, DOI to slices treated with phenylephrine (10μM). Using the extracellular single-unit recording technique, 5 putative 5-HT neurons were tested with 10μM DOI (Fig.3.5). A representative recording from a putative 5-HT neuron is illustrated in Fig3.5A. Application of DOI caused the firing frequency of the cell to decrease rapidly until it reached a stable plateau. When the control firing frequency is compared with the firing frequency in the presence of DOI we can see clearly that in each cell tested that DOI induces a significant inhibition (Fig3.2.5B1). When expressed as a percentage of control it can be seen that DOI caused a significant inhibition (53.2%, $p < 0.05$, paired Student's t-test) of cell firing across all 5 cells tested (Fig3.2.5B2).

3.3.3 DOI prolongs the decay kinetics of DRN IPSCs

Electrophysiological studies have demonstrated that 5-$HT_{2A/2C}$ receptors are located on GABAergic neurons which synapse onto 5-HT DRN neurons (Liu *et al*., 2000). In order to better understand the DOI-induced inhibition of 5-HT neurons we investigated the properties of sIPSCs and mIPSCs recorded in the absence and presence of DOI. Using the whole-cell voltage-clamp configuration and conditions described in the material and methods (section 2.6) sIPSCs and mIPSCs were recorded from DRN 5-HTneurons voltage-clamped at -60mV, in the presence

of 2mM kynurenic acid and 0.5µM strychnine. Under these conditions IPSCs are evident as inward currents (i.e. downward deflections from the baseline (Figure.3.6).

A summary of the properties of sIPSCs and mIPSCs (Fig3.7A) reveal that the peak amplitude, rise time and frequency are not significantly affected by DOI (10µM). The T70 value of sIPSCs is longer in the presence of DOI ($p < 0.05$, paired Student's t-test). The T70 value of mIPSCs is also longer in the presence of DOI ($p < 0.05$, paired Student's t-test). In support the decay time constant τ of mIPSCs was also significantly longer in the presence of DOI ($p < 0.05$, paired Student's t-test). An averaged $GABA_A$ receptor mediated sIPSC (Fig.3.7B left) and mIPSC (Fig.3.7B right) in the absence and presence of 10µM DOI illustrates the prolongation of the decay kinetics.

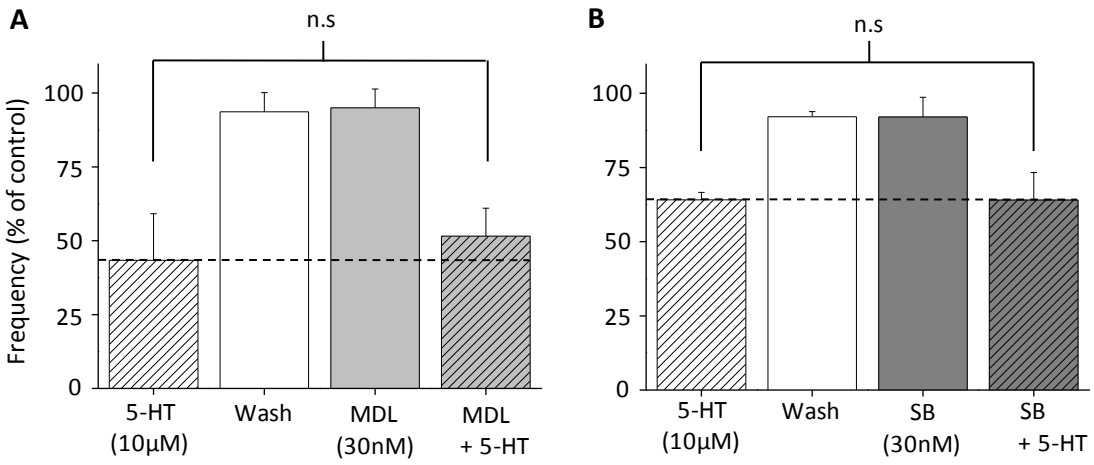

Figure 3.4. Selective antagonists of 5-HT$_2$ receptors have no effect on 5-HT-induced inhibition of DRN neuronal firing. (A) 5-HT (10µM) caused an inhibition of cell firing. After washout the 5-HT$_{2A}$ antagonist, MDL 100907 (30nM) was applied the cells were re-tested with 5-HT (n = 3). (B) 5-HT (10µM) caused an inhibition of cell firing. After washout the 5-HT$_{2C}$ antagonist, SB 24204 (30nM) was applied the cells were re-tested with 5-HT (n = 3). Neither antagonist caused a change in the firing of neurons and neither antagonist was able to alter the 5-HT response ($p > 0.05$, One-way repeated measures ANOVA with Bonferonni analysis).

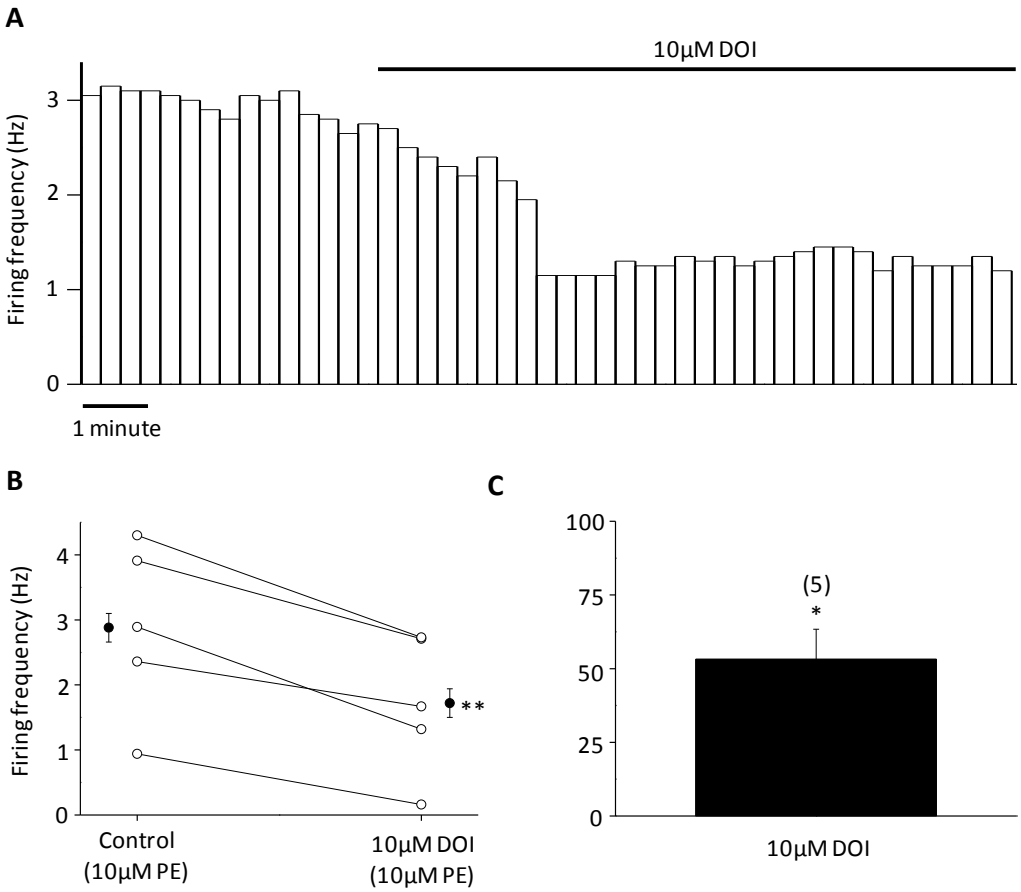

Figure 3.5. The 5-HT$_2$ receptor agonist DOI inhibits the firing of putative 5-HT neurons. (A) A representative recording of the firing frequency (20s bins) from a phenylephrine-driven 5-HT neuron in the presence of 10μM DOI. (B) Firing frequency of individual putative 5-HT neurons (open circles) in the presence of 5-HT (10μM) before (control) and after the application of DOI (10μM). The average firing frequency in control and in the presence of DOI is shown by the closed circles (mean ± SE). (C) Bar graph showing the average effect of DOI when applied to phenylephrine-driven 5-HT neurons. Effect is displayed as a mean percentage of the control firing frequency ± SEM. Values in parenthesis denote the number of DOI applications. *$p < 0.05$ and ** $p < 0.01$ paired Student's t-test.

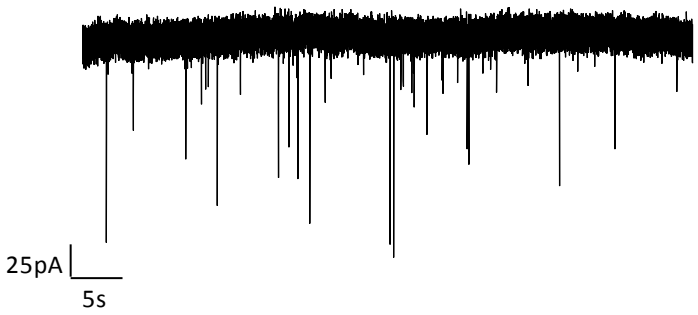

Figure 3.6. GABA receptor synaptic events recorded from a putative 5-HT neuron in the DRN. A representative whole-cell voltage-clamp (-60mV) recording (60s) of a neuron in the presence of 2mM kynurenic acid and 0.5µM strychnine. GABA receptor synaptic events are evident as downward deflection from the baseline.

A

	GABA receptor mediated currents			
	No TTX (sIPSCs) n = 5		With TTX (mIPSCs) n = 5	
	Control	DOI (10µM)	Control	DOI (10µM)
Peak amplitude (pA)	-131 ± 47	-90 ± 5	-82 ± 9	-78 ± 10
Rise time (ms)	0.6 ± 0	0.6 ± 0	0.6 ± 0.1	0.6 ± 0.1
T70 (ms)	9.6 ± 0.7	11.8 ± 0.9 *	10.8 ± 1.5	12.6 ± 1.1 *
τ (ms)	8.1 ± 0.7	9.2 ± 0.8	8.3 ± 1.0	9.8 ± 0.7 *
Frequency (Hz)	2 ± 0.8	1.9 ± 0.9	1.8 ± 0.5	1.4 ± 0.3

B

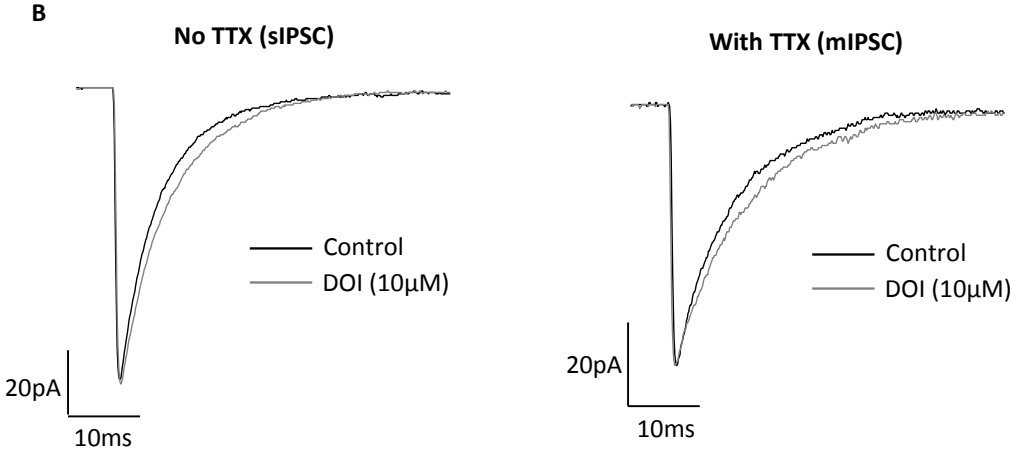

Figure.3.7. GABA receptor synaptic events recorded from putative 5-HT neurons in the DRN. (A) Table comparing the properties of sIPSCs and mIPSCs in the presence and absence of DOI (10µM). * $p < 0.05$ and ** $p < 0.01$ paired Student's t-test. (B) A representative trace of an averaged $GABA_A$ receptor mediated sIPSC (left) or mIPSC (right) recorded in the absence (black) and presence (grey) of DOI.

3.4 Regulation of 5-HT neuronal firing by orexin

Orexin-containing neurons (orexin-A and orexin-B) from the lateral hypothalamus densely innervate 5-HT neurons in the DRN (Peyron *et al*., 1998a; Lee *et al*., 2005b). Orexin-A and orexin-B elicit their effects through two G-protein coupled receptors OX_1 and OX_2 both of which are present in the DRN (Marcus *et al*., 2001). *In vivo* extracellular recordings demonstrate that orexin excites putative 5-HT neurons in the DRN (Takahashi *et al*., 2005) and *in vitro* studies indicate this excitation is mediated via a non-selective cationic conductance (Brown *et al*., 2002; Liu *et al*., 2002; Kohlmeier *et al*., 2008). Here I utilised extracellular and whole-cell voltage-clamp recordings to investigate the role of $OX_{1/2}$Rs in the regulation of mouse DRN neuronal activity.

3.4.1 Orexin-A excites putative 5-HT neurons in the DRN

Using the extracellular single-unit recording technique, 7 putative 5-HT neurons were tested with 100nM orexin-A (Fig.3.8). A representative recording from a putative 5-HT neuron is illustrated in Fig.3.8.A. Application of orexin caused the firing frequency of the cell to increase rapidly until it reached a stable plateau. When the control firing frequency is compared with the firing frequency in the presence of orexin we can noticeably see that in each cell tested orexin induces significant excitation (Fig.3.8.B). When expressed as a percentage of control (normalised data) it can be seen that orexin causes a significant excitation (393 ± 57%, $p < 0.01$, paired Student's t-test) of cell firing across all 7 cells tested.

3.4.2 Orexin-A induces a large inward current in putative 5-HT neurons in the DRN

In order to further investigate the role of orexin-A in the DRN I utilised the whole-cell voltage-clamp recording technique. Experiments were performed at a holding potential of -60mV with a KGluconate intracellular solution (see section 2.6). In 12/12 neurons (100%) orexin-A produced an inward current (-25 ± 4pA, $p < 0.001$ paired Student's test) and an increase in the RMS (2 ± 0.4pA, $p < 0.01$ paired Student's t-test). In seven neurons, the dual $OX_{1/2}$R antagonist almorexant was bath applied after the orexin-induced current had reached a stable plateau. A representative voltage-clamp recording is illustrated in Fig.3.9.A. It can be seen that bath

application of 100nM orexin-A produces an inward current which is reversed by the subsequent application of 1μM almorexant. When the average change in holding current (-24 ± 4pA, Fig.3.9.B left) and RMS (+23 ± 4pA, Fig.3.9.B right) are graphed we can see that almorexant completely reverses the effect of orexin. A one-way repeated-measures ANOVA was conducted to compare the effect of drug treatments on the holding current and RMS. There was a significant main effect of drug treatment on holding current ($F(1.17, 7.092) = 5.504$; $p < 0.05$) and RMS ($F(1.645,10.087) = 9.720$; $p < 0.01$) therefore post hoc t-test were performed. Post hoc, paired t-tests indicated that orexin application was significantly different from control for holding current ($p < 0.01$) and RMS ($p < 0.05$) values whereas almorexant was not significantly different ($p > 0.05$) for either. This confirms that almorexant is able to fully reverse the effects of orexin-A.

3.4.3 Almorexant application does not reveal a tonic orexin conductance in the DRN

Given the large effect of orexin-A on putative 5-HT neurons in the DRN I wanted investigate whether a tonic orexin conductance may be present in these neurons. In order to assess this possibility I performed whole-cell voltage-clamp recordings and bath applied 1μM almorexant followed by 100nM orexin. A representative voltage-clamp (V_H = -60mV) recording can be seen in Fig.3.10.A. The holding current was not attenuated by the application of almorexant and furthermore remained unaffected by the additional application of orexin. When the average change in holding current (Fig.3.10.B left) and RMS (Fig.3.10.B right) are graphed it can be seen that almorexant and orexin do not have an effect on either measurement (n = 5). A one-way repeated measures ANOVA confirmed that this drug treatment did not produce a significant effect on holding current ($F(1.548,6.192) = 3.704$; $p = 0.93$) or RMS ($F(1.338,5.350) = 2.631$; $p = 0.162$).

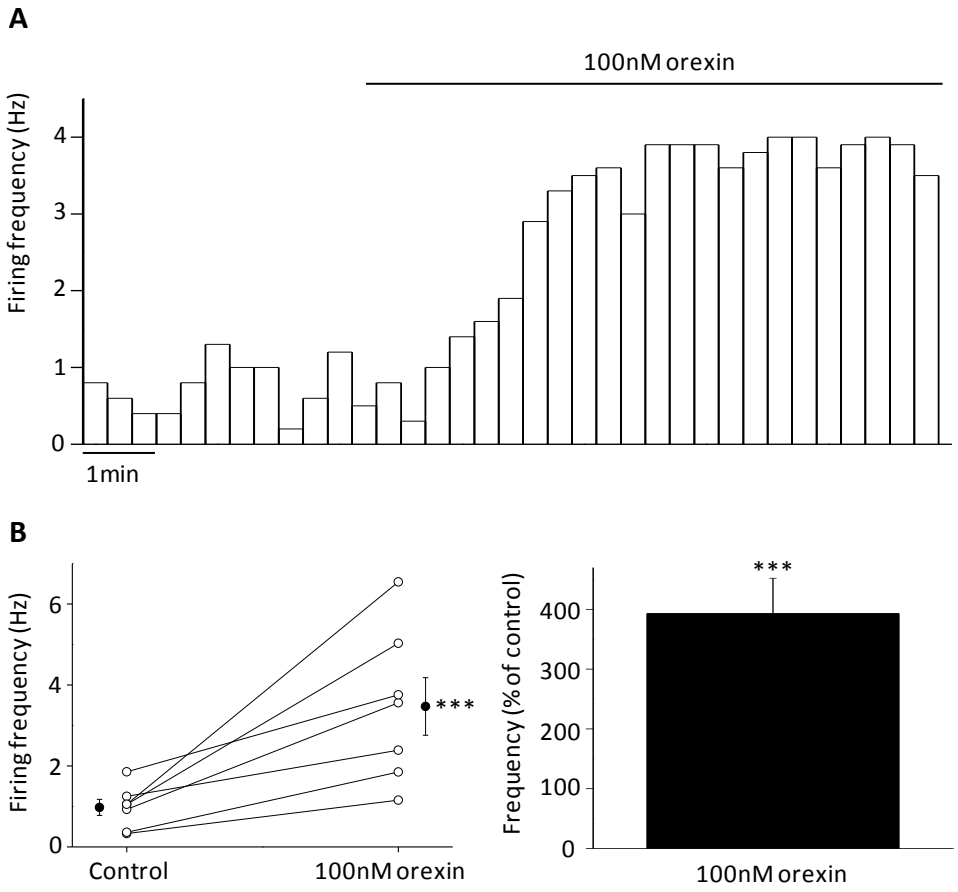

Figure 3.8. Orexin increases the firing of putative 5-HT neurons. (A) A representative extracellular singe-unit recording of the firing frequency (20s bins) from a spontaneously firing neuron in the presence of 100nM orexin. (B) Left: firing frequency of individual neurons (open circles) before (control) and after the application of orexin (100nM). The average firing frequency in control and in the presence of histamine is shown by the closed circles (mean ± SEM). Right: Bar graph showing the average effect of histamine when applied to spontaneously firing 5-HT neurons (n = 7). Effect is displayed as the mean percentage of control firing frequency ± SEM. *** $p < 0.01$, paired Student's t-test.

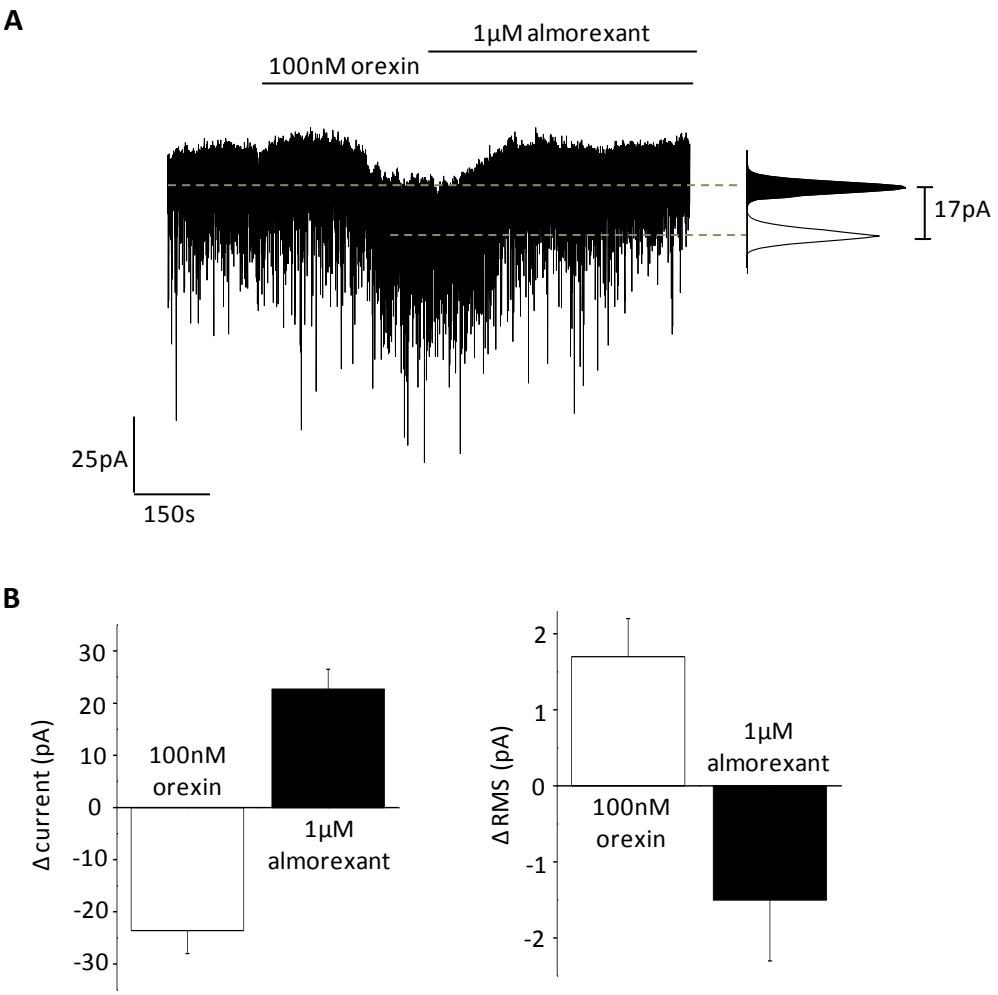

Figure 3.9. Orexin induces an inward current which is reversed by the $OX_{1/2}R$ antagonist, almorexant. (A) A representative recording (V_H = -60mV) from a putative 5-HT neuron illustrating the inward current induced by the bath application of 100nM orexin and the subsequent reversal by almorexant. The corresponding all-points histograms are given to the right. (B) A bar graph summarising the changes in holding current (left) and RMS (right) evoked by the bath application of orexin and almorexant (n = 7). Error bars indicate SEM.

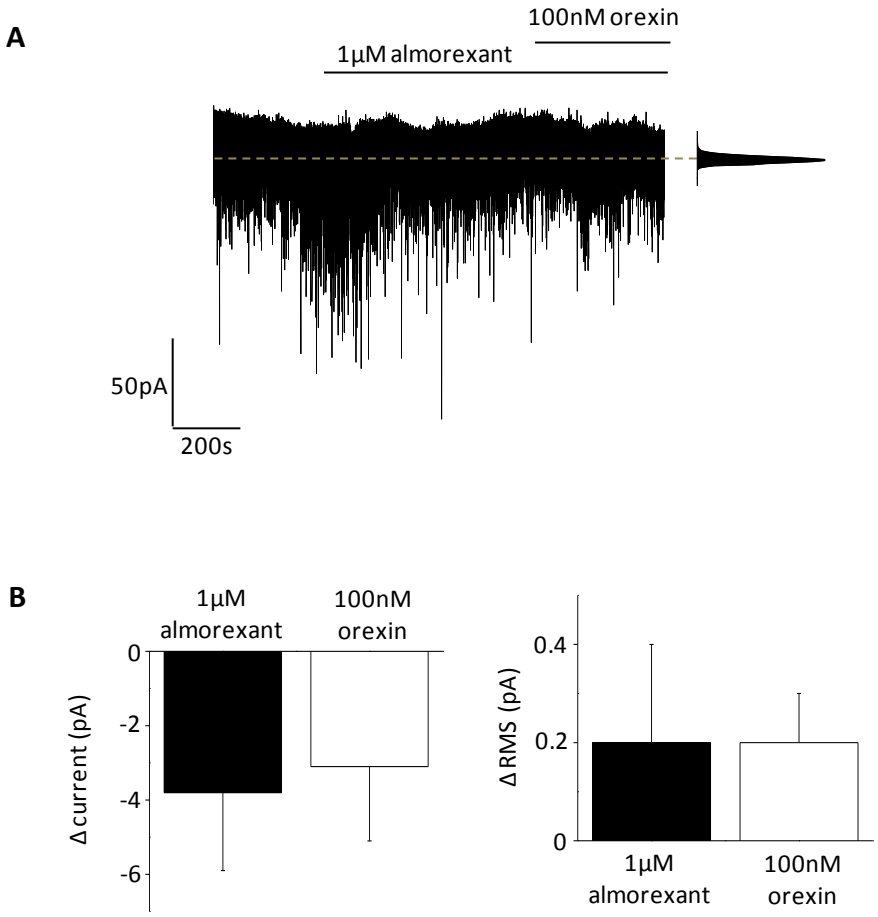

Figure 3.10. Almorexant blocks the effect orexin and fails to demonstrate an endogenous orexin tone. (A) A representative recording (V_H = -60mV) from a putative 5-HT neuron illustrating that the bath application of 1µM almorexant does not reveal an endogenous orexin tonic current but does block the subsequent application of 100nM orexin. (B) A bar graph summarising the changes in holding current (left) and RMS (right) evoked by the bath application of almorexant and orexin (n = 6). Error bars indicate SEM.

3.5 Discussion

3.5.1 Electrophysiological characterisation of putative 5-HT neurons in the DRN

Extracellular single-unit recordings performed from putative 5-HT neurons in the DRN revealed that these neurons fired slow (2.1 ± 0.3Hz), rhythmic, bi-phasic action potentials (3.6 ± 0.3ms). These electrophysiological data are consistent with previous studies performed *in vitro* in mice (Trulson & Crisp, 1986) and rats (Mosko & Jacobs, 1976; Aghajanian & Vandermaelen, 1982b; Vandermaelen & Aghajanian, 1983). Extracellular recordings also revealed that putative 5-HT neurons in the DRN are spontaneously active *in vitro*. The observation of spontaneous firing in the DRN is somewhat inconsistent *in* vitro with some studies reporting high levels (Macri *et al*., 2006), low levels (Vandermaelen & Aghajanian, 1983; Kirby *et al*., 2003) or no spontaneous firing at all (Beck *et al*., 2004). The intrinsic pacemaker property of 5-HT neurons (characterised by a pronounce AHP, followed by a gradual interspike depolarisation) is known to be produced by a calcium-activated potassium current (Aghajanian, 1985; Crunelli *et al.,* 1983; Burlhis & Aghajanian, 1987). It is therefore possible that the discrepancy between spontaneously active and silent neurons across these studies is due to differences in the extracellular Ca^{2+} concentration. The level of extracellular Ca^{2+} in the slice is dependent upon the slicing and recording conditions i.e. the level of Ca^{2+}, presence of Ca^{2+} chelators and pH and will hence vary between studies. A small proportion of fast-firing neurons (7.8 ± 0.6Hz) were also observed in this study. These neurons fired rhythmic, bi-phasic action potentials (3.5 ± 0.8ms) very similar to those which fired at a slower rate. Historically these neurons were classified as non-serotonergic (most likely GABAergic) however recent electrophysiological studies conducted in combination with immunohistochemistry have revealed that a portion of these faster firing neurons are in fact serotonergic (Allers & Sharp, 2003). Similar to the results present here, these fast firing 5-HT neurons had electrophysiological characteristics almost identical to slower firing 5-HT neurons (rhythmic, broad, bi-phasic action potentials). Given that this population of fast firing 5-HT neurons has been excluded from extensive study it will be important in the future to understand exactly what role these neurons have within the DRN.

In vivo DRN serotonergic neurons are spontaneously active however, as noted above, the

number of neurons showing spontaneous activity is markedly reduced when recording *in vitro*. This suggests that the spontaneous activity of the DRN 5-HT neurons is dependent on intact afferent drive, most likely originating from noradrenergic neurons of the locus coeruleus (Baraban & Aghajanian, 1980; Baraban & Aghajanian, 1981; Vandermaelen & Aghajanian, 1983). When the spontaneous firing properties of DRN 5-HT neurons were compared with the firing properties during phenylephrine application it was observed that the firing frequency was significantly higher in the phenylephrine-driven 5-HT neurons (2.1Hz verses 2.8Hz). In addition the number of active neurons per slice was much higher in the presence of phenylephrine. It therefore appears that 5-HT DRN neurons possess intrinsic pacemaker potentials, however, for most of these neurons the expression of these spontaneous potentials is dependent upon the presence of excitatory inputs. These inputs can be provided by noradrenergic synaptic input as occurs *in vivo*, or by the exogenous application of phenylephrine, as was done in the present study. Given the results from this study were provided from two separate groups of neurons it would be interesting to test the direct effect of adding phenylephrine to spontaneously firing neurons to assess what proportion of neurons would respond and to what degree. Furthermore it would be interesting to observe the effect of applying an α_1 adrenoreceptor antagonist to spontaneously firing neurons *in vitro*.

Pharmacological characterisation of DRN 5-HT neurons with bath applied 5-HT revealed that the majority of neurons (37/39) were inhibited by 5-HT in a concentration-dependent manner. This 5-HT-induced inhibition of firing is consistent with previous studies which applied 5-HT to rat brain slices (Vandermaelen & Aghajanian, 1983; Judge & Gartside, 2006). In addition a small minority of neurons were not inhibited by 5-HT, instead one neuron failed to respond to 5-HT and one was excited. This heterogeneous response to 5-HT has been reported previously in DRN 5-HT neurons recorded from rat brain slices although a slightly higher proportion of neurons were excited by 5-HT than was observed here (Judge & Gartside, 2006). Although not investigated directly here, previous studies have revealed that 5-HT produces its inhibitory effect by activating 5-HT_{1A} autoreceptors located on the soma and dendrites of 5-HT neurons (Aghajanian & Lakoski, 1984; Sotelo *et al*., 1990). Subsequent work has revealed differing 5-HT_{1A} receptor sensitivity across different subfields of the DRN (Calizo *et al*., 2011). This heterogeneous 5-HT_{1A} receptor sensitivity could account for the wide range of 5-HT-induced inhibition observed here. It should be noted however that GABAergic interneurons in the DRN are also known to express 5-HT_{1A} autoreceptors (Bonnavion *et al*., 2010). Studies which have

combined electrophysiological recordings with immunohistochemistry have revealed that some GABAergic neurons are indistinguishable from 5-HT neurons based on their firing properties alone (Beck *et al*., 2004; Calizo *et al*., 2011). It is therefore plausible that some neurons recorded in this study could be GABAergic. The likelihood of misidentification of neurons was reduced in this study by making recordings from the midline of the DRN, where the neurons are predominantly serotonergic (Beck *et al*., 2004; Brown et al., 2008; Calizo *et al*., 2011). A recent study has also reported on the existence of a subpopulation of DRN 5-HT neurons which do not express 5-HT_{1A} receptors (Kiyasova *et al*., 2013). This could account for the lack of 5-HT effect seen in one neuron. These studies, taken together, suggest that different functional subclasses of 5-HT neurons exist within the DRN and in light of this, great care should be taken when interpreting any results which have not been supported by immunohistochemical work.

3.5.2 Regulation of putative 5-HT neurons by 5-HT_2 receptors

Exogenous application of the 5-HT_{2A} receptor antagonist, MDL 100907 and the 5-HT_{2C} receptor antagonist, SB 242084 failed to attenuate the firing of DRN 5-HT neurons. This suggests that there is no 5-HT_{2A} or 5-HT_{2C} tonic conductance in 5-HT DRN neurons recorded in acute mouse brain slices. This observation is consistent with a previous study which performed whole-cell recordings from 5-HT neurons in rat brain slices (Liu *et al*., 2000). These authors failed to demonstrate any effect of MDL 100907 and SB 242084 when these antagonists we applied in the absence of agonist. In the results presented here, pre-application of each antagonist failed to attenuate the 5-HT-induced inhibition. This is at odds with the study conducted on rat brain slices where they demonstrated that each antagonist was able to significantly reduce the 5-HT response. The authors did note that applying both antagonists (in either order) produced a larger attenuation of the 5-HT response. It is therefore possible that combining both antagonists here could have produced an attenuation of the 5-HT response. However it is also possible that the limited number of neurons recorded here (n = 3 for each antagonist treatment) were not under regulatory control by 5-HT_2 receptors.

Application of the mixed 5-$HT_{2A/2c}$ agonist, DOI produced a significant inhibition of firing in 5-HT DRN neurons. The DOI-induced inhibition reported here is consistent with previous studies performed in anaesthetised rats. Intra-raphe (Garratt *et al*., 1991) or systemic administration

(Boothman *et al*., 2003; Wright *et al*., 1990) of DOI produced a marked reduction in the firing of DRN 5-HT neurons. While not investigated here, a previous study demonstrated that the DOI-induced inhibition of DRN 5-HT neurons could be blocked by pre-treatment with ritanserin (5-HT_2 receptor antagonist) or MDL 100907 (Boothman *et al*., 2003). It would therefore be pertinent in future studies to investigate which receptors were responsible for the DOI-induced inhibition demonstrated in acute mouse brain slices. To date no study has revealed whether 5-HT_{2A} and 5-HT_{2C} receptors are located on the same neuron or different neurons.

Whole-cell voltage-clamp recordings from DRN 5-HT neurons revealed that bath application of DOI prolonged the decay kinetics of GABAergic sIPSCs and mIPSCs but failed to attenuate the frequency or amplitude of these synaptic events. The DOI-induced prolongation of decay kinetics could indicate that DOI is directly modulating the $GABA_A$ receptor, causing the channel to remain open for a significantly longer time. To date, there are no other reports of DOI modulating the $GABA_A$ receptor directly. A previous study conducted in rat brain slices observed that application of DOI caused an increase in the amplitude and frequency of GABAergic IPSCs, an effect which was blocked by application of TTX, bicuculline and selective 5-HT_2 receptor antagonists (Liu *et al*., 2000). These results indicate that DOI is activating pre-synaptic 5-HT_2 receptors located on GABAergic neurons to produce its effect. This pre-synaptic action of DOI at 5-HT_2 receptors located on GABAergic neurons has been demonstrated elsewhere in the brain including the hippocampus (Shen & Andrade, 1998) and midbrain periaqueductal grey (Jeong *et al*., 2013). Another explanation for effect of DOI observed here could be that DOI activated 5-HT_2 receptors leading to increased intracellular second messenger systems which in turn modulated $GABA_A$ receptors. Alternatively, DOI could have attenuated GABA reuptake from the synapse. Neither of these effects has been demonstrated previously. While it is possible that the DOI effects observed here are real there are a number of considerations which much be discussed. Firstly these results are preliminary; the number of experiments reported here was low (n =5), to be confident in the observed effects more experiments would need to be performed. Secondly recovery from DOI was not investigated; this could be explored by post-application of a 5-HT_2 antagonist or by washout of DOI. Lastly all of the experiments reported here were performed from the same vial of DOI powder, it is possible that there was contamination and hence using a new batch of drug would be important. One final point to note is that while the data reported here were not consistent with that reported previously, none of these authors investigated whether DOI altered the

decay kinetics of the GABAergic IPSCs (personal communication). It therefore remains to be seen whether DOI acts at both 5-HT_2 receptors and $GABA_A$ receptors.

3.5.3 Regulation of putative 5-HT neurons by orexin

Extracellular single-unit recordings revealed that the bath application of orexin-A to DRN 5-HT neurons produced a significant increase in the firing frequency of all neurons tested. This is comparable to a previous study which applied orexin-A to 5-HT neurons in rat brain slices (Brown *et al*., 2002). These authors demonstrated that orexin-A had an excitatory effect on DRN 5-HT neurons and that this orexin-induced excitation could be occluded by pre-application of phenylephrine. Whole-cell voltage-clamp recordings revealed that orexin-A produced a large, noisy inward current in DRN 5-HT neurons which could be blocked by the application of the mixed OX_1/OX_2 receptor antagonist, almorexant. This demonstration of a large, noisy inward current induced by orexin is in keeping with previous studies in mice (Kohlmeirer *et al*., 2008) and rats (Brown *et al*., 2002). These previous studies also demonstrated that application of orexin-A caused a significant depolarisation of DRN 5-HT neurons and was most likely due to the involvement of a non-selective cationic channel, possibly the canonical form of the transient receptor potential channel (TRPC). The authors suggested the TRPC was responsible based on the following observations: orexin-induced currents reversed in a Ca^{2+}-free medium at -23mV consistent with a mixed cation channel (Brown *et al*., 2002), TRPC I-VII from classic, non-selective cation channels, TRPC mediate cation currents activated by G_q receptors (Kohlmeirer *et al*., 2008) and the expression of TRPCs was confirmed in the DRN 5-HT neurons that also co-express orexin receptors (Sergeeva *et al*., 2003). To date, there are no pharmacological agents that can selectively inhibit the different TRPCs therefore their role mediated orexin effects in the DRN remains to be unequivocally shown. Interestingly, the excitatory effect of orexin in the DRN has been previously shown to translate into increased 5-HT release *in vivo* (Tao *et al*., 2006) and infusion of orexin-A into the DRN of freely moving rats was shown to cause a dose-dependent increase in 5-HT release.

Application of almorexant to 5-HT neurons under voltage-clamp conditions failed to alter the holding current of any neuron tested. The pre-application of almorexant was able to prevent the orexin-induced inward current. This preliminary data suggests that there is no orexin tone

present in DRN 5-HT neurons *in vitro*. No study has explored what effect intra-raphe administration of almorexant would have on 5-HT neurons. One would expect almorexant to have a depressant effect on DRN 5-HT neuronal firing *in vivo*. The magnitude of the effect would most likely depend on the circadian time point at which almorexant was administered as both orexin and serotonin neurons are known to fire faster during wakefulness and slower during sleep (Takahashi *et al*., 2008; Sakai, 2011). Dual orexin antagonists are currently being explored as novel sleep therapeutics. Pre-clinical data and clinical trials have demonstrated that dual orexin antagonists are able to increase NREM and REM sleep in animals and humans, without producing next day sedation or withdrawal. Almorexant has been shown to affect sleep-architecture in a dose-dependent manner, increasing both NREM and REM sleep, with higher doses decreasing the latency to REM sleep (Hoever *et al*., 2012a, b). Suvorexant has been shown to improve sleep efficiency and sleep latency in primary insomniacs (Herring *et al*., 2012). Merck is currently seeking FDA approval for the authorisation of suvorexant as a sleep aid. Given the profound effect of orexin on 5-HT neurons it is more than likely these drugs produce part of their observed effect by reducing the output of DRN 5-HT neurons.

Chapter 4:

Histaminergic regulation of dorsal raphe neurons *in vitro*

4.1 Introduction

It is currently thought that our state of wakefulness results from the concerted action of multiple transmitter systems found within the brain. Electrophysiological, neuropharmacogical and genetic approaches have revealed that serotonin neurons within the DRN function to promote wakefulness. While considerable progress has been made in elucidating the mechanisms by which serotonin neurons are regulated locally within the DRN much less is known about how other wake promoting neurons in the brain regulate serotonin neurons. The sleep-promoting effect of classical antihistamines which target the H_1 receptor subtype (Hindmarch and Shamsi 1999) and the demonstration that these receptor subtypes are found in the DRN (Barbara *et* al., 2002), suggest a potential important role for DRN H_1 receptors in the regulation of the sleep-wake cycle. This chapter focusses on the characterization of histamine actions upon serotonin neurons within the DRN.

4.2 Histamine increases the firing rate of putative 5-HT neurons

Using the extracellular single-unit recording technique, putative 5-HT neurons were tested with 10 µM histamine (Figure 4.1). A representative recording from a putative 5-HT neuron is illustrated in Fig 4.1.A. Bath application of histamine to the slice caused a large increase in the firing frequency of the cell. After a stable plateau was reached histamine was washed out and the firing frequency returned to control (pre-histamine) levels. When the control firing frequency is compared with the firing frequency in the presence of histamine we can see clearly that in every cell tested histamine causes a significant excitation (Fig 4.1.B). When expressed as a percentage of control it can be seen that histamine causes a significant excitation (340 ± 104%, $p < 0.05$, paired Student's t-test) of cell firing (Fig 4.1C). Using the cell-attached voltage-clamp technique, putative 5-HT neurons were tested with 10 µM histamine (Figure 4.2). A representative recording from a putative 5-HT neuron is illustrated in Fig 4.2A. Similar to the single-unit recordings, bath application of histamine to the slice caused an increase in the firing frequency of the cell. When the control firing frequency is compared to firing frequency in the presence of histamine we again see that in every cell tested histamine caused a significant excitation (Fig. 4.2.B). When expressed as a percentage of

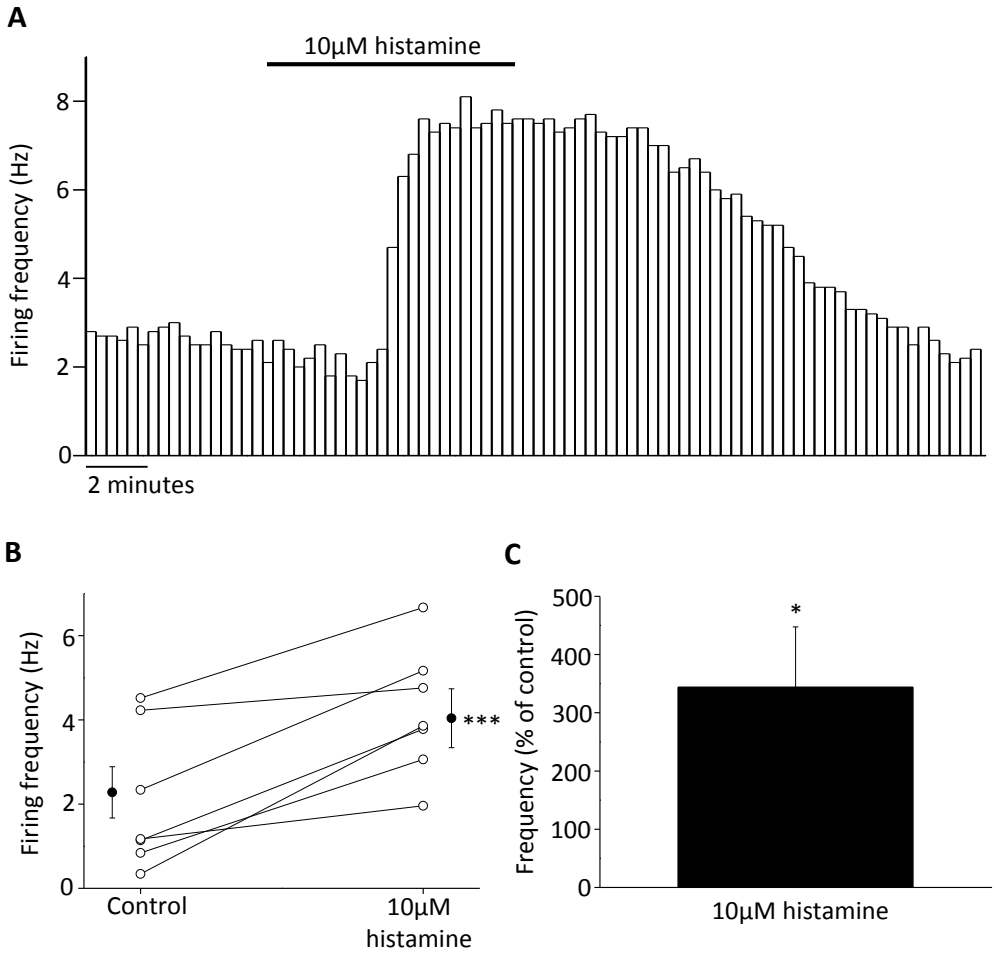

Figure 4.1. Histamine increases the firing of putative 5-HT neurons I. (A) A representative extracellular single-unit recording of the firing frequency (20s bins) from a spontaneously firing neuron in the presence of 10µM histamine. (B) Firing frequency of individual putative 5-HT neurons (open circles) before (control) and after the application of histamine (10µM). The average firing frequency in control and in the presence of histamine is shown by the closed circles (mean ± SEM). (C) Bar graph showing the average effect of histamine when applied to spontaneously firing 5-HT neurons (n = 7). Effect is displayed as the mean percentage of control firing frequency ± SEM. * $p < 0.05$, *** $p < 0.001$, paired Student's t-test.

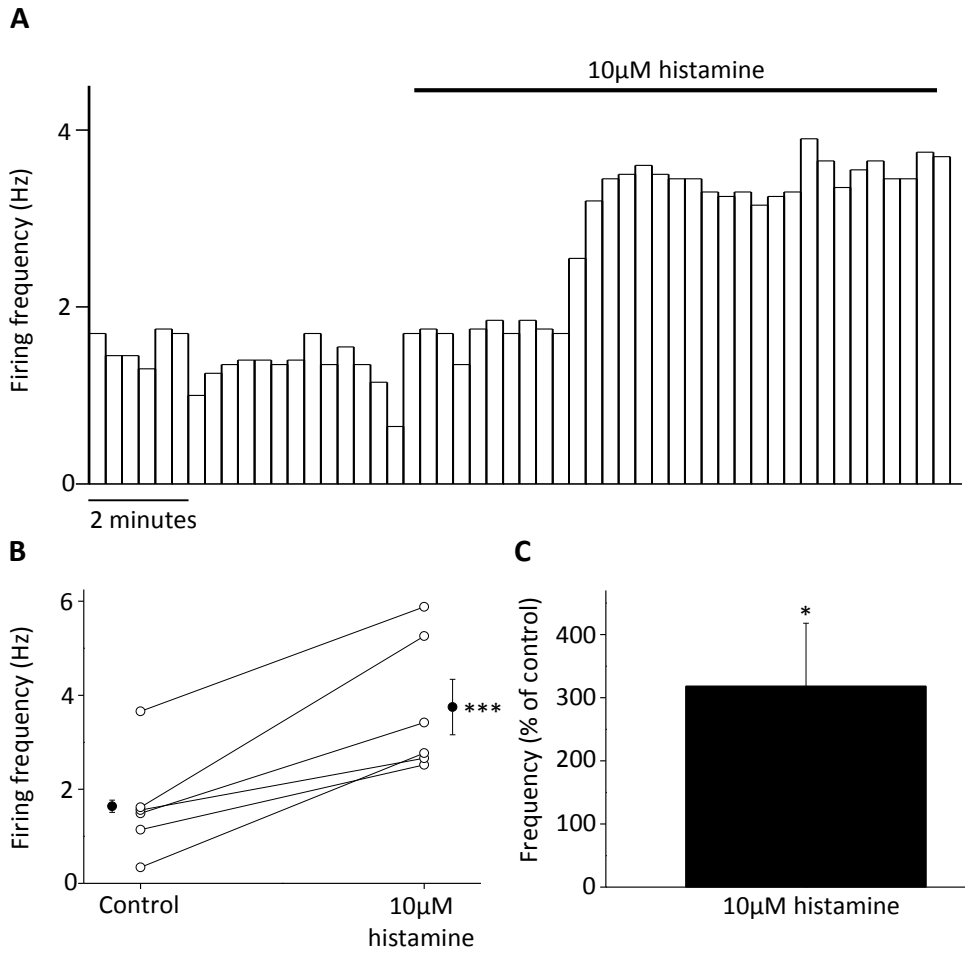

Figure 4.2. Histamine increases the firing of putative 5-HT neurons II. (A) A representative cell-attached recording of the firing frequency (20s bins) from a spontaneously firing neuron in the presence of 10μM histamine. (B) Firing frequency of individual putative 5-HT neurons (open circles) before (control) and after the application of histamine (10μM). The average firing frequency in control and in the presence of histamine is shown by the closed circles (mean ± SEM). (C) Bar graph showing the average effect of histamine when applied to spontaneously firing 5-HT neurons. Effect is displayed as the mean percentage of control firing frequency ± SEM. * $p < 0.05$, *** $p < 0.001$, paired Student's t-test.

control it can be seen that histamine caused a significant excitation (320%, $p < 0.05$, paired Student's t-test) of cell firing (Fig 4.2.C).

4.3 Histamine depolarises putative 5-HT neurons and increases their excitability

The whole-cell current-clamp technique was utilised to measure the membrane potential and input-output curve of putative 5-HT neurons in the absence and presence of bath applied histamine (10µM). In 2 cells the mean resting membrane potential was calculated to be -61mV (-56mV and -63mV). The bath application of histamine caused an average depolarisation of +7.8mV (+6mV and +10mV) and caused action potential firing (Fig.4.3.A). The effect of the bath application of histamine on the input-output relationship of these neurons was also investigated. A stimulus protocol was applied whereby a group of current steps (-40 to +120pA, 20pA increments, 400ms duration) were injected into the neuron three times per experimental condition and the resulting number of action potentials per step was determined (see 2.6.5). In both cells histamine shifted the input-output curve to the left i.e. increased cell excitability (Fig.4.3.B).

4.4 Histamine produces a large inward current in putative 5-HT neurons

In order to further investigate the role of histamine in the DRN I utilised the whole-cell voltage-clamp recording technique. Experiments were performed at a holding potential of -60mV with equal intracellular and extracellular chloride (see section 2.6.2). A representative voltage-clamp recording from a putative 5-HT neuron is illustrated in Fig 4.4.A. In this recording the bath application of 10µM histamine produced a large inward current which was associated with an increase in the baseline noise (RMS). A second representative voltage-camp recording is illustrated in Fig. 4.4.B. In this recording 300µM histamine was focally applied to the slice and was seen to cause a large inward current which was associated with an increase in baseline noise. In 95% (19 out of 20) of neurons the bath application of histamine caused an inward current with a mean of -36 ± 4pA ($p < 0.001$, paired Student's t-test) and an increase in RMS with a mean of 3 ± 0.5pA ($p < 0.001$, paired Student's t-test). In 90% (49 out of 54) of neurons the focal application of histamine produced an inward current with a mean of 17 ±

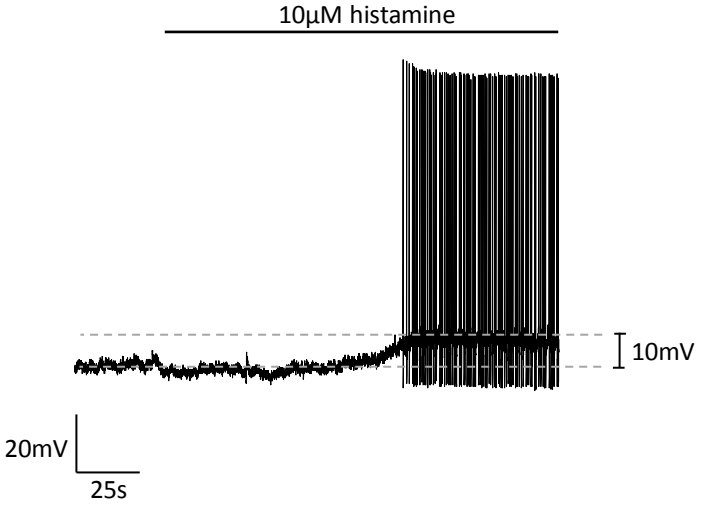

Figure 4.3.A Histamine depolarises putative 5-HT neurons. A representative current-clamp recording in which bath application of histamine (10µM) caused a depolarisation of the cell and initiation of action potential firing.

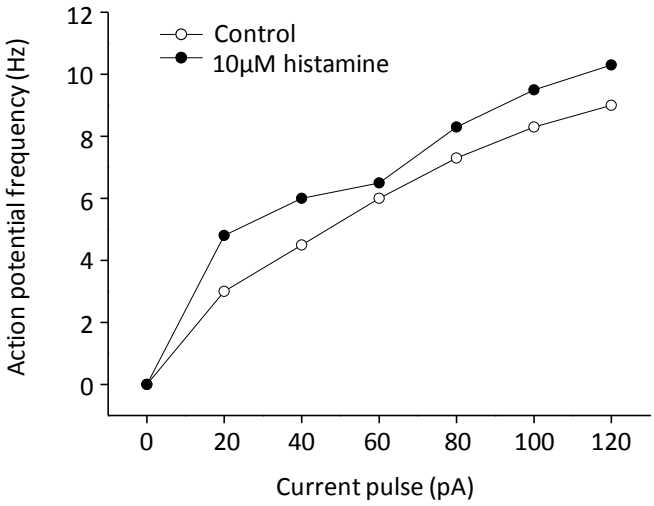

Figure 4.3.B. Histamine increases the excitability of putative 5-HT neurons. A plot of the current injected against the average action potential frequency of 2 responding neurons in each experimental condition. Note the leftward shift of the trace with bath application of histamine (10µM).

1pA ($p < 0.001$, paired Student's t- test) and an increase in RMS with a mean of 2 ± 0.1pA ($p < 0.001$, paired Student's t-test, Table 2.1).

4.5 Histamine mediates its effect via the H_1 receptor

Having demonstrated that histamine has an excitatory effect on putative 5-HT neurons within the DRN it was next important to identify which histamine receptor was responsible. As H_1, H_2 and H_3 receptor subtypes are known to be located in the DRN (Barbara *et al*., 2002; Drutel *et al*., 2001) putative 5-HT neurons were challenged with specific antagonists of each receptor subtype. Representative voltage-clamp (V_H = -60mV) recordings from putative 5-HT neurons are illustrated in Fig. 4.5. Histamine (300µM) was focally applied to each neuron (every 50s) and then a selective antagonist was bath applied. A total of 10 neurons were tested with the H_1R antagonist, histabudifen. Although histabudifen (20µM) caused a significant inhibition of the histamine-induced inward current ($p < 0.01$, paired Student's t-test) its effect was varied. In 2 cells there was complete inhibition of the histamine-induced current (Fig.4.5.A), in 7 cells there was partial inhibition and in 1 cell there was no effect. In order to assess whether the concentration of drug application was too low, three cells which were partially inhibited were challenged with a higher concentration of 60µM histabudifen. The higher concentration of histabudifen resulted in a complete inhibition of the histamine-induced current. It was thought that inconsistency in results obtained with histabudifen was due to a problem with the drug solubility and in light of this a second series of experiments was conducted with a different H_1R antagonist, oxatomide. Application of 100nM oxatomide completely inhibited the histamine-induced current in all cells tested (n = 4, data not shown). In order to investigate the role of H_2 and H_3 receptors, selective antagonists of each receptor were applied. The H_2 receptor antagonist, ranitidine (10µM) had no significant effect on the histamine-induced current ($p = 0.1$, n= 6, paired Student's test, Fig.4.5.B). Furthermore, the H_3 receptor antagonist, thioperamide had no significant effect on the histamine-induced current when applied at a concentration of 1µM ($p = 0.6$, n = 5 paired Student's t-test, Fig.4.5.C) or 10µM ($p = 0.8$, n = 3, paired Student's t-test).

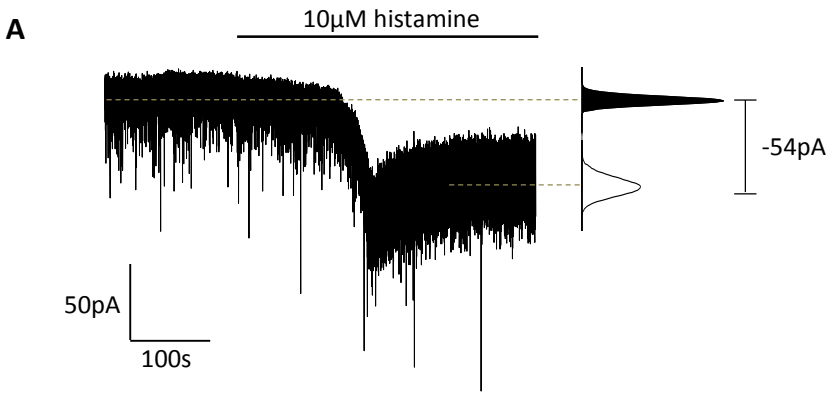

Figure 4.4.A The bath application of 10µM histamine to putative 5-HT neurons causes an inward current. A representative recording (V_H = -60mV) from a 5-HT neuron illustrating the inward current induced by bath application of 10µM histamine. The corresponding all points histogram and current shift is given to the right with the value of current shift.

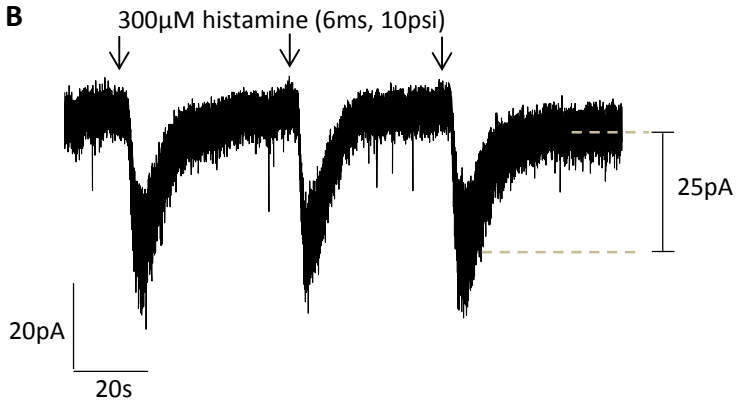

Figure 4.4.B. The focal application of 300µM histamine to putative 5-HT neurons causes an inward current. A representative recording (V_H = -60mV) from a 5-HT neuron illustrating the inward current induced by repetitive focal application of 300µM histamine (6ms and 10psi). The value of current shift is given to the right.

	Responding neurones	Mean Δ current ± SEM (range)	Mean Δ RMS ± SEM (range)
10µM histamine (bath application)	19/20 (95%)	-36 ± 4pA *** (-12 to -77pA)	3 ± 0.5pA *** (0 to 5.5pA)
300µM histamine (focal application)	49/54 (90%)	-17 ± 1pA *** (-6 to -51pA)	2 ± 0.1pA *** (1 to 4pA)

**Table 2.1. Bath and focal application of histamine causes an inward current associated with an increase in the baseline noise (RMS) in putative 5-HT neurons. *** $p < 0.001$, paired Student's t-test.

4.6 H_1Rs are constitutively active in the DRN

In vitro studies conducted over the last decade have revealed that H_1Rs can be functionally active in the absence of bound agonist i.e. constitutively or spontaneously active (Bakker *et al*., 2000; Leurs *et al*., 2002). The constitutive activity of a receptor can be revealed by the application of inverse agonists and neutral antagonists. Inverse agonists have negative efficacy (shifting the receptor equilibrium towards the inactive state) whereas neutral antagonists have zero efficacy (see section 1.2.2). Since the observation that H_1 antagonists can have negative efficacy, many have been reclassified as inverse agonists, raising important questions regarding the therapeutic applications of such ligands (Monczor *et al*., 2013).

Given the presence of functional H_1Rs in my DRN slices I wanted to investigate whether these receptors were constitutively active. In voltage-clamp recordings of neurons expressing

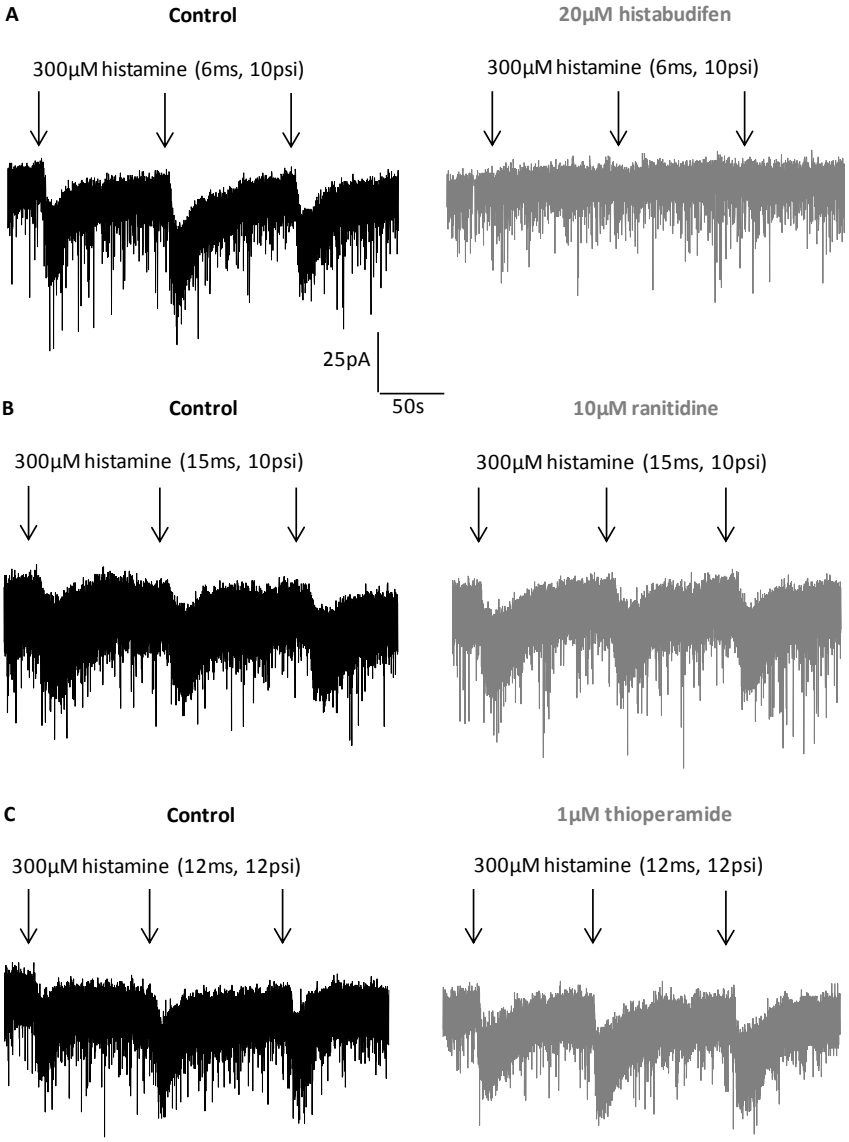

Figure 4.5 Histamine mediates its effects via the H_1 receptor. Representative recordings (V_H = -60mV) from putative 5-HT neurons illustrating the focal application of 300µM histamine during control (left) and during bath application of selective histamine receptor antagonists (right). (A) Bath application of 20µM histabudifen (H_1R antagonist) completely blocks the histamine-induced inward current. (B) Bath application of 10µM ranitidine (H_2R antagonist) has no effect on the histamine-induced current. (C) Bath application of 1µM thioperamide (H_3R

antagonist) also has no effect on the histamine-induced current. Note that all antagonist concentrations were selected based on an extensive literature search.

constitutively active H_1Rs, the inverse agonist induced closure of these receptors would be revealed as a shift in the holding current. The presence of these receptors in the DRN was investigated by bath applying two structurally distinct H_1 inverse agonists, mepyramine and dimethindene. These experiments were performed at a holding potential of -60mV with equal intracellular and extracellular chloride (see section 2.6.2). In the first series of experiments histamine (10µM) was bath applied to the slice followed by the bath application of mepyramine (300nM and 1µM). Bath application of histamine caused an average inward current of -38 ± 10pA, application of 300nM mepyramine caused an average outward current of 24 ± 7pA and application of 1µM mepyramine caused a further outward current shift of 18 ± 4pA (n = 6). Taken as a whole, 300nM is able to partially inhibit the histamine-induced current but it appears that 1µM mepyramine is required to fully inhibit the histamine effect. Voltage-clamp recordings from two putative 5-HT neurons illustrated in Fig.4.6 demonstrate the different responses to 300nM and 1µM mepyramine. In the first example 1µM mepyramine is required to completely inhibit the histamine-induced inward current (Fig.4.6 top) whereas in the second example 300nM causes complete inhibition and the subsequent application of 1µM mepyramine shifts the current further, beyond the control baseline (Fig.4.6 bottom). This shift in current above the control baseline suggested that there was a tonic histamine conductance present.

In order to assess the tonic histamine conductance further I focally applied 300µM histamine and bath applied mepyramine (300nM or 1µM) or dimethindene (100nM). In 3 cells the bath application of 300nM mepyramine completely inhibited the histamine-induced current and caused an average shift in the baseline current of +32 ± 18pA (Fig.4.7). A further 6 cells were challenged with 1µM mepyramine and this resulted in the inhibition of the histamine-induced current and average shift in the baseline current of +24 ± 3pA (Table 2.2). Application of 100nM dimethindene to 6 cells resulted in the inhibition of the histamine-induced current in every cell tested and an average shift in the baseline current of +28 ± 7pA in 5 of the cells tested (Table 2.2). Although this set of experiments strongly suggested the presence of a tonic H_1R conductance it could be argued that the exogenous application of histamine could account

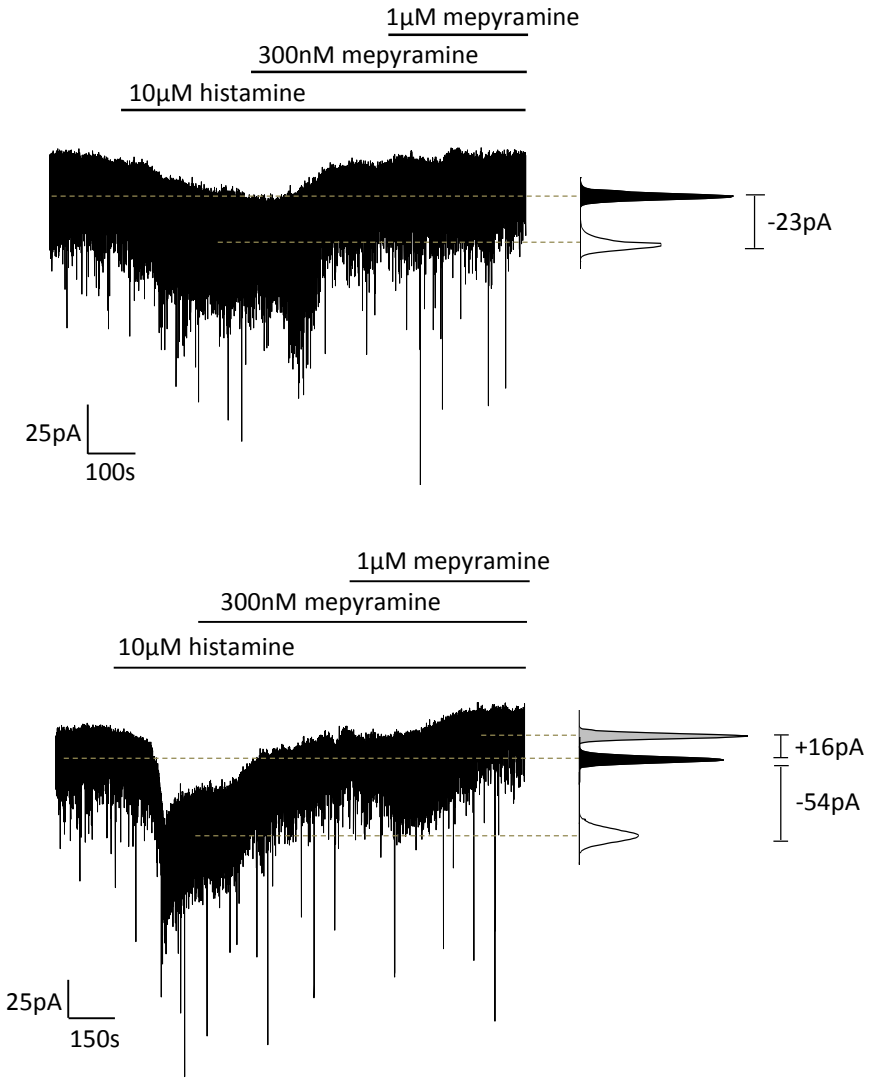

Figure 4.6. H_1 receptors are responsible for the histamine-induced inward current recorded from putative 5-HT neurons. Representative recordings (V_H = -60mV) from putative 5-HT neurons illustrating that the inward current induced by 10µM histamine is reversed by application of mepyramine (300nM and 1µM). The corresponding all points histograms are given to the right with the value of current shift. Note that in the 5-HT neuron illustrated in the top trace 1µM mepyramine only returns the current to the baseline whereas in the 5-HT neuron in the bottom trace application of 1µM mepyramine reveals a tonic histamine conductance.

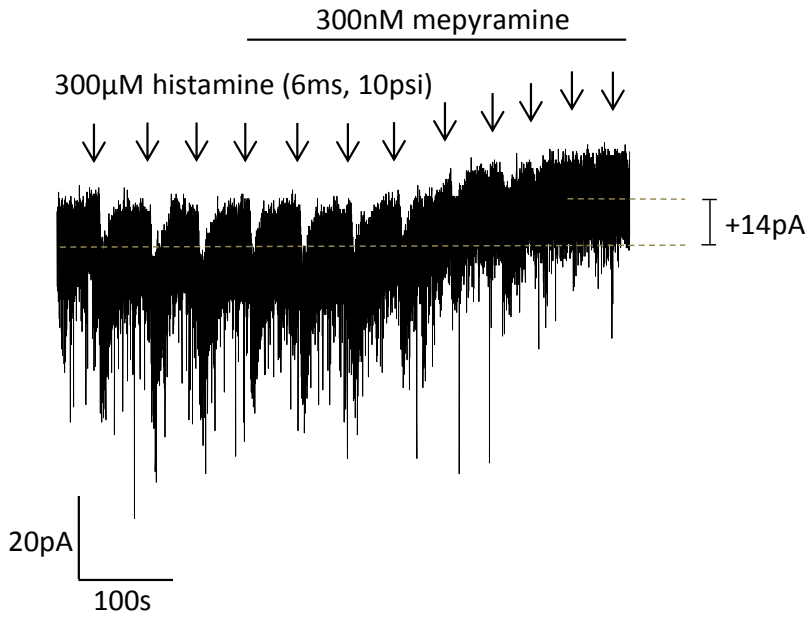

Figure 4.7. The bath application of 300nM mepyramine inhibits the histamine induced current and causes a shift in the holding current. A representative recording (V_H = -60mV) from a 5-HT neuron illustrating the focal application of 300µM histamine and subsequent bath application of 300nM mepyramine. Mepyramine inhibits the histamine induced current and in addition causes a shift in the baseline current (+14pA).

	Responding neurones	Mean Δ current ± SEM (range)	Mean Δ RMS ± SEM (range)
300nM mepyramine	3/3 (100%)	+32 ± 18pA (14 to 69pA)	-0.8 ± 0.8pA (0 to 5.5pA)
1µM mepyramine	7/7 (100%)	+24 ± 3pA *** (8 to 31pA)	-0.7 ± 0.1pA *** (-0.4 to -1.5pA)
100nM dimethindene	5/6 (83%)	+28 ± 7pA * (12 to 49pA)	-0.7 ± 0.4pA (0.2 to -1.9pA)

Table 2.2. Bath application of mepyramine and dimethendene causes a shift in the baseline current and a reduction in the baseline noise (RMS) in putative 5-HT neurons. * $p < 0.05$ and *** $p < 0.001$, paired Student's t-test.

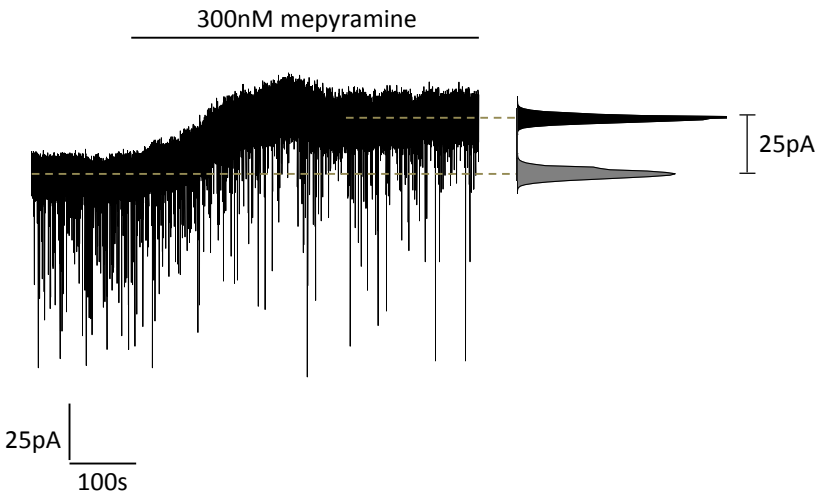

Figure 4.8. Putative 5-HT neurons in the DRN exhibit a tonic conductance mediated by H_1 receptors. A representative recording (V_H = -60mV) from a putative 5-HT neuron illustrating the shift current revealed by 1μM mepyramine. The corresponding all points histogram is shown to the right with the value of current shift.

	Responding neurones	Mean Δ current ± SEM (range)	Mean Δ RMS ± SEM (range)
1μM mepyramine	5/5 (100%)	20 ± 4pA *** (8 to 29pA) *	-0.1 ± 0.2pA (-0.7 to 0.5pA)
300nM mepyramine	5/8 (62.5%)	25 ± 7pA (8 to 50pA)	-0.6 ± 0.3pA (-1.7 to 0.3pA)
100nM mepyramine	1/4 (25%)	50 pA	0.2 pA

Table 2.3. A portion of putative 5-HT neurons exhibit a tonic conductance mediated by H_1 receptors. Application of 1μM mepyramine revealed 100% of neurons exhibited a tonic conductance with an average shift of 20 ± 4pA (mediated by H_1 receptors). Application of 300nM mepyramine revealed 62.5% of neurons exhibited a tonic conductance with an average shift of 25 ± 7pA whereas application of 100nM mepyramine revealed only 25% of neurons exhibit a tonic conductance. ***** $p < 0.05$ and ******* $p < 0.001$, paired Student's t-test.

for these observed effects. To further confirm that the measured conductance did not originate from exogenously applied histamine I bath applied mepyramine (100nM, 300nM or 1µM) in absence of any exogenously applied histamine. A representative voltage-clamp recording is illustrated in Fig 4.8. The bath application of 300nM mepyramine caused a shift in the baseline current of +25pA. A comparison of all three concentrations of mepyramine is illustrated in Table 2.3. It can be seen that 300nM and 1µM cause a similar magnitude of current shift however 100nM was only able to causes a current shift in 1/5 neurons. This confirms that H_1R are tonically active within the slice but it does address the origin of the tonic conductance i.e. whether it originates from constitutive activity or ambient levels of histamine. If ambient levels of histamine were responsible for the tonic conductance application of a neutral H_1R antagonist would produce similar results to those seen with the inverse agonists. In 5 cells tested the bath application of the neutral H_1R antagonist, oxatomide (100nM) caused no change in the holding current (Fig.4.9). Furthermore when mepyramine (1µM) was subsequently applied in the presence of oxatomide it was unable to produce any shift in the baseline current. These results indicate that H_1Rs are constitutively (spontaneously) active on putative 5-HT neurons present within the DRN. To the best of my knowledge this is the first demonstration of the constitutive activity of H_1Rs in the DRN.

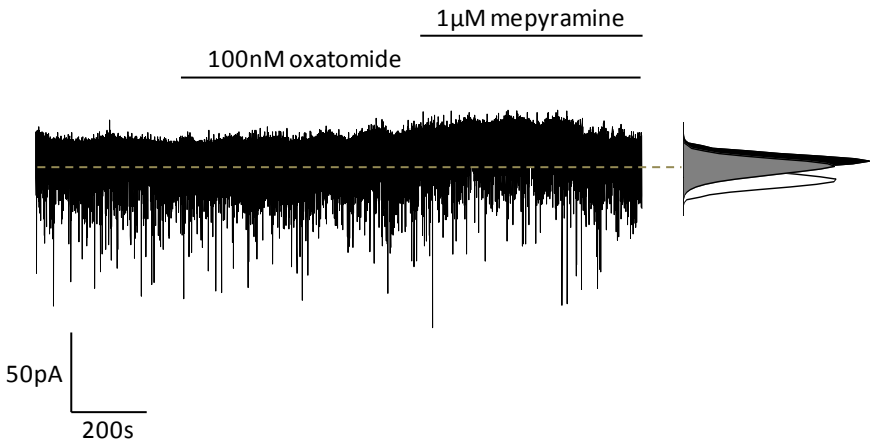

Figure 4.9. Bath application of 100nM oxatomide blocks the effect of mepyramine. A representative recording (V_H = -60mV) from a putative 5-HT neuron illustrating that the neutral antagonist oxatomide (100nM) has no effect on the baseline current and furthermore blocks the actions of mepyramine (1µM). The corresponding all points histogram is shown on the right: black (baseline), grey (oxatomide) and white (mepyramine).

4.7 H_1Rs are located on putative 5-HT neurons

H_1Rs have been found postsynaptically in numerous regions throughout the brain and there is evidence to suggest they may present postsynaptically within the DRN (Brown *et al*., 2002). In order to confirm the postsynaptic location of H_1Rs on putative neurons in the DRN I performed voltage-clamp recordings (V_H = -60mV) from neurons in the DRN in the absence and presence of voltage-dependent Na^+ channel blocker TTX. Bath application of 0.5μM TTX did not cause any change in the baseline current of neurons. In addition when histamine was bath applied in the presence of TTX it was still able to produce an inward current associated with an increase in the RMS (Fig.4.10). When the magnitude of the histamine-induced current is compared in the presence of TTX (n = 5) and absence of TTX (n = 19) there is no significant difference (Table 2.4). This suggests that the current originated locally from the activation of H_1Rs within the recorded cell. More evidence for the local activation of these receptors was provided when voltage-clamp recordings were performed with GDP-βS (a non-hydrolysable GDP analogue) substituted in the recording pipette. GDP-βS prevents G-protein coupled receptors from functioning correctly, as it was present within the recording pipette its action is limited to the neuron onto which it is patched. Under these recording conditions the focal application of histamine (300μM) failed to produced any change in the holding current (n = 8, Fig.4.11.A). Furthermore bath application of 1μM mepyramine failed to cause any change in the holding current (n = 4, Fig.4.11.B). These results demonstrate that H_1Rs are located on putative 5-HT neurons and that these G protein coupled receptors require GTP to function correctly.

4.8 H_1R inhibition causes a decrease in the input resistance of putative 5-HT neurons

In many neurons the activation of postsynaptic H_1Rs have been shown to cause a depolarisation and/or an increase in firing frequency. Several different mechanisms are thought to underlie this excitability including the block of a leak K^+ conductance (McCormick and Williamson, 1991; Reiner and Kamondi, 1994), activation of a TTX-insensitive Na^+ current (Gorelova and Reiner, 1996) and the activation of Ca^{2+}-activated cationic current (Smith and Armstrong, 1996).

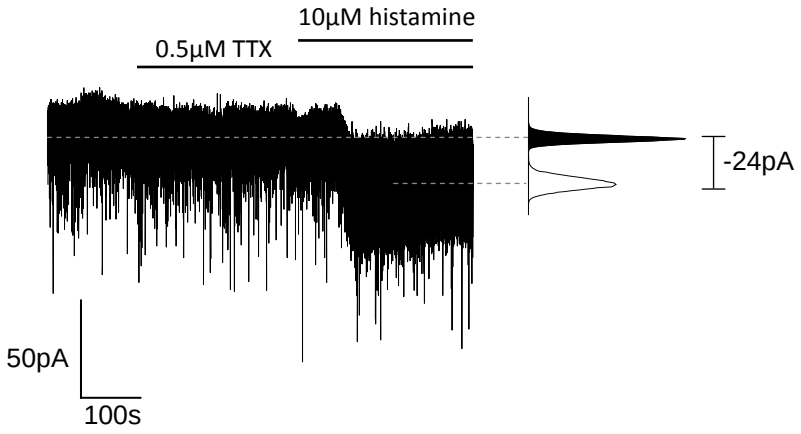

Figure 4.10. Bath application 0.5µM TTX has no effect on the baseline current and has no effect on histamine-induced current. A representative recording (V_H = -60mV) from a putative 5-HT neuron illustrating that TTX (0.5µM) has no effect on the baseline current. Furthermore TTX has no effect on the histamine-induced current produced by the bath application of histamine (10µM).

	Responding neurones	Mean Δ current ± SEM	Mean Δ RMS ± SEM
0.5µM TTX	0/5 (0%)	1 ± 4pA	-0.3 ± 0.2pA
10µM histamine (+ 0.5µM TTX)	5/5 (100%)	-36 ± 7pA *	3 ± 0.5pA ***
10µM histamine	19/20 (95%)	-36 ± 4pA ***	3 ± 0.5pA ***

Table 2.4. Application of 0.5µM TTX has no effect on putative 5-HT neurons and does not attenuate the histamine-induce current or increase in RMS. Bath application of TTX did not produce any effect on the holding current or RMS in any cells tested. When we compare the bath application of histamine (10µM) in the presence of TTX and in the absence of TTX we can see that blocking Na^+ dependent action potentials has no effect on the histamine-induced current. Furthermore when the bath application of histamine in the presence of TTX is compared to a separate group of cells devoid of TTX we can see the values are almost identical. ***** $p < 0.05$ and ******* $p < 0.001$, paired Student's t-test.

In 5-HT neurons in the DRN it is suggested that histamine activation of H_1Rs leads to activation of a mixed cationic conductance (Brown *et al.*, 2002). To further elucidate the H_1R mechanism within the DRN I performed whole-cell voltage-clamp recordings (V_H = -60mV) and assessed the neuronal input resistance in the absence and presence of bath applied mepyramine (see section 2.6.5). Neurons exhibited a mean input resistance of 308 ± 11MΩ (n = 3) and the bath application of 1μM mepyramine decreased the neuronal input resistance in all cells tested to 210 ± 14MΩ (see Fig.4.12). Given the decrease in input resistance observed with mepyramine it was thought that de-activation of H_1Rs may be linked to a leak potassium conductance. Preliminary voltage-ramp experiments were conducted in order to obtain an I-V plot, which I assumed would cross at the potassium equilibrium potential. Unfortunately technical problems prevented the completion of this set of data.

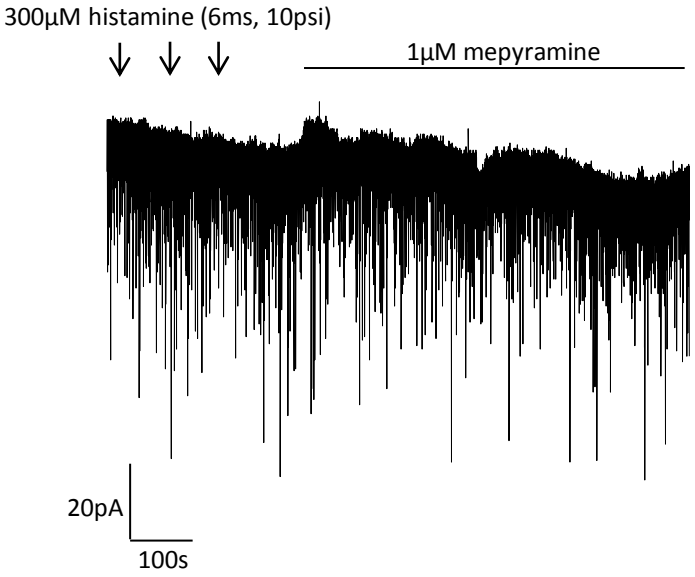

Figure 4.11. Inclusion of GDP-βS to the recording pipette prevents the histamine-induced current and tonic histamine conductance. A representative recording (V_H = 60mV) from a putative 5-HT neuron illustrating that when GDP-βS is included in the recording pipette histamine fails to produce a shift in the holding current and furthermore mepyramine (1μM) no longer has any effect on the baseline current

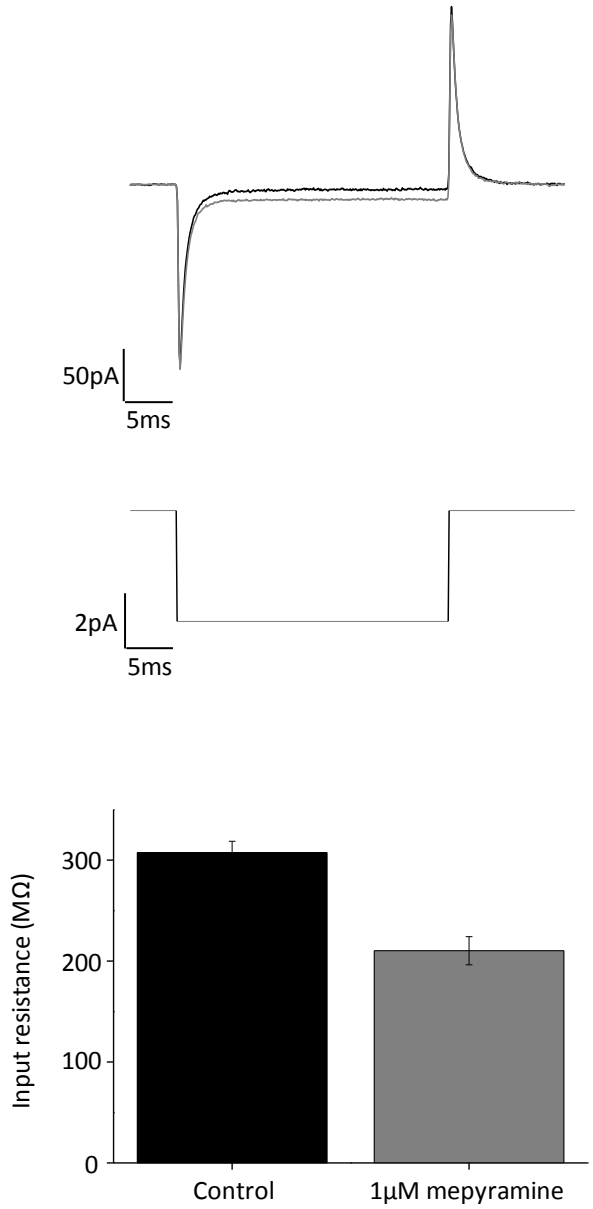

Figure 4.12. Bath application of mepyramine decreases the input resistance of putative 5-HT neurons. Measurement of input resistance in voltage-clamp mode before and after 1µM mepyramine application. Top: current shift of a 5-HT neuron induced by a hyperpolarising voltage step (-4mV). Not that the current shift is larger in the presence of mepyramine indicative of a decrease of input resistance (V = IR). Bottom: Bar graph illustrating the average input resistance in the absence and presence of mepyramine (n = 3). $p < 0.05$ paired Student's t-test.

4.9 Discussion

4.9.1 Histamine excites putative 5-HT neurons in the DRN

Extracellular single-unit recordings and cell-attached performed from putative 5-HT neurons in the DRN revealed that all of the neurons tested were excited by histamine. The histamine-induced excitation was reversed upon washout confirming that the observed effect was not an erroneous response. This reversible excitation is consistent with previous studies performed *in vitro* in rat brain slices. The first study demonstrated that histamine (50µM) produced a rapid excitation in 67% of neurons tested (Brown *et al*., 2002) and the second study demonstrated that histamine (3-30µM) produced an excitation in 84% of neurons in a concentration-dependent manner (Bárbara *et al*., 2002). The discrepancy between the percentages of responding neurons could be due to a species difference in the expression of histamine receptors. Hence, H_1 receptor expression might be lower in the rat DRN. Currently no study has been performed to map the expression pattern of histamine receptors in the DRN of either species, therefore this is just conjecture at this time.

Both bath application and local (spritz) application of histamine produced an inward current associated with an increase in baseline noise. These results are indicative of histamine causing receptors on the cell surface to open allowing ions to flow across the membrane. These data are also comparable to those obtained from 5-HT neurons in the rat DRN. The authors demonstrated that application of histamine (50µM) caused an inward current (-37 ± 9pA) associated with an increase in current noise and furthermore that histamine depolarised 5-HT neurons (Brown *et al*., 2002).

4.9.2 Histamine mediates it effect via the H_1 receptor

Whole-cell voltage-clamp experiments were performed in order to investigate which histamine receptor (H_1, H_2 or H_3) was responsible for the observed excitability in DRN 5-HT neurons. Bath application of two structurally distinct neutral H_1 receptor antagonists, histabudifen and oxatomide, inhibited the histamine-induced inward current. Whereas bath application of the

H_2 antagonist, ranitidine and H_3 antagonist, thioperamide failed to significantly attenuate the histamine response. These data are in keeping with previous work which demonstrated that the histamine-induced excitation of rat DRN 5-HT neurons could be inhibited by blocking H_1 receptors (Brown *et al*., 2002) whereas blocking H_2 receptors had no effect (Bárbara *et al*., 2002). However a very early study did demonstrate a role for H_2 receptors in the DRN. In this study microionophoretic application of histamine to DRN of aneasthetised rats produced a depression of cell firing in 240 serotonergic neurons tested (Lakoski & Aghajanian, 1983). This histamine-induced depression was shown to be attenuated by the H_2 antagonist, ranitidine but remained unaffected by inhibition of H_1 receptors. A follow up study also demonstrated that this histamine-induced depression could be attenuated by a second H_2 antagonist, cimetidine (Lakoski & Aghajanian, 1984). The authors demonstrated that the depression in firing caused by histamine could be antagonised by bicuculline and picrotoxin, suggesting a role for $GABA_A$ receptors in the observed histamine effect. It is possible that this observation could be species specific, although if this was the case it would be reasonable to assume that one or both of the more recent studies conducted in rats would have observed this effect. Neither reported any depressant effect. It is therefore possible that DRN 5-HT neurons are under regulatory control by both histamine receptors subtypes. H_1 receptors could directly activate 5-HT neurons through a postsynaptic mechanism whereas H_2 receptors could inhibit 5-HT neurons through an indirect mechanism involving GABAgergic neurons. As noted above, no study has investigated the expression pattern of histamine receptors therefore it remains to be elucidated whether H_2 receptors are located on GABAergic interneurons or afferents present in the DRN.

4.9.3 H_1 receptors are constitutively active in the DRN

Whole-cell voltage-clamp experiments were performed in order to investigate whether H_1 receptors in the DRN were constitutively (spontaneously) active. Bath application of two structurally distinct inverse agonists, mepyramine and dimethindene, not only inhibited the histamine-induced inward current observed in 5-HT neurons but also produced a shift in current beyond the baseline. Application of oxatomide to the slice failed to produce any change in the holding current and furthermore, inhibited the current shift produced by mepyramine. Taken together, these data indicate that H_1 receptors are constitutively active in the mouse DRN. Functional assays have revealed that H_1 receptors are constitutively active *in*

vitro (Bakker *et al*., 2000, 2001) however this is the first demonstration of constitutive activity in the DRN. This demonstration raises important questions as to the physiological role of constitutive H_1 receptor signalling in the DRN especially given the reclassification of a number of H_1 receptor antagonists as inverse agonists. This constitutive activity could represent a rate-limiting mechanism which would allow the histaminergic system to regulate DR 5-HT neurons irrespective of the level of histamine in the nucleus. It will be important to confirm the results presented here using an alternative method. Confirmation of constitutive H_1 receptor activity could be demonstrated by first depleting histamine from the slice (using a histidine decarboxylase inhibitor e.g. α-fluromethylhistidine) and then applying an inverse agonist.

The ability of GPCRs to achieve a constitutively (or spontaneously) active conformation was first demonstrated in delta opioid receptors (Costa & Hertz, 1989). Since this seminal study the constitutive activation of GPCRs is now well established, with recent reports suggesting that 80% of the classical GPCR antagonists have been reclassified as inverse agonists (Bond & Ijzerman, 2006) and that nearly all GPCRs display some constitutive activity (Khilnani & Khilnani, 2011). The clinical significance of constitutive receptor activity has been demonstrated in a number of diseases in which constitutively activated mutants exist. Mutations can lead to receptor under-activity (e.g. diabetes insipidus, retinitis pigmentosa and congenital night blindness), receptor over-activity (e.g. Leydig cell tumour and familial hypocalciuria) or alterations of coupling efficiency (e.g. allelic variants of human β-adrenoreceptors) (Spiegel & Weinstein, 2004). Inverse agonism at H_1 receptors may be a key component of the anti-allergic action of clinically used antihistamines (Khilnani & Khilnani, 2011). Cardiotoxic and anti-inflammatory effects of particular H_1 antihistamines are attributed to inverse agonism (Fitzimmons *et al*., 2004) Furthermore given the reciprocal regulation between the DRN and TMN during wakefulness it is more than likely that constitutive receptor activity would have a modulatory role during the emergence from waking. Most of the clinically available H_1 antihistamines are now know to be inverse agonists. Unfortunately no study to date has compared the effect of a H_1 inverse agonist and H_1 neutral antagonists on measured sleep parameters.

4.9.4 H_1 receptors are located on putative 5-HT neurons

After demonstrating the functional presence of constitutive H_1 receptor activity in the DRN the focus of the investigation turned to understanding where these receptors were located. Histamine was bath applied to cells under voltage-clamp. TTX was pre-applied to neurons but failed to alter the holding current or baseline noise, furthermore it failed to alter the histamine-induced current when these neurons were compared to TTX-free neurons. This suggested that histamine was not dependent on impulse flow from pre-synaptic neurons to exert its effect. In order to confirm that histamine was acting postsynaptically, GDP-βS was included in the intracellular solution. When GPCRs were blocked in the patched neuron histamine failed to produce any effect. Taken together these strongly suggest that H_1 receptors are located postsynaptically on serotonergic neurons i.e. the recorded neuron. This is the first compelling evidence that histamine receptors are located directly on 5-HT neurons in the DRN. A previous study inferred that H_1 receptors are located postsynaptically from electrophysiology data which compared the effects of histamine, phenylephrine and orexin in the DRN (Brown *et al.*, 2002). As described above it will be important to map the expression of histamine receptors further in the DRN to explore whether these neurons are expressed on 5-HT and non-5-HT neurons (e.g. GABAergic neurons). Histamine receptor expression could be mapped in the DRN using immunohistochemistry (with selective antibodies for each histamine receptor subtype) or by employing reverse-transcription polymerase chain reaction techniques to 5-HT cellular contents post-patching. Furthermore, it will be useful to know what effect, if any, histamine receptors have on non-serotonergic neurons in the DRN. Mice expressing green fluorescence protein specifically in GABA neurons (GAD67 strain of mice) are available and would quite easily enable researchers to assess what physiological role histamine has on these neurons.

4.9.5 Inhibition of H_1 receptors leads to a decrease in input resistance

Whole-cell voltage-clamp recordings were performed in order to elucidate ionic mechanisms by which histamine produced an increase in the excitability of DRN 5-HT neurons. Preliminary data show that application of mepyramine decreased the input resistance of 5-HT neurons, suggesting that the activation of a leak potassium conductance could be responsible. This data

should be interpreted with caution given the low number of experiments performed. In the future, voltage-clamp studies could be performed in order to assess whether voltage-ramps cross at the equilibrium potential. Furthermore, experiments should be performed to confirm that histamine produces the opposite effect to mepyramine i.e. decreases the input resistance of serotonergic cells.

Chapter 5:

Histaminergic regulation of dorsal raphe neurons *in vivo*

5.1 Introduction

As demonstrated by the experiments described in the previous section and in agreement with previous reports, histamine acts via the H_1 receptor to excite/depolarise presumed 5-HT neurons in the DRN (Barbara *et al*., 2002; Brown *et al*., 2002). In addition these experiments have suggested for the first time that H_1 receptors can be constitutively active in the DRN. To investigate the physiological role of H_1 receptors in the DRN further it was imperative that experiments were performed *in vivo*. Two approaches were taken; firstly single-unit recordings were made from DRN of anesthetised, head-restrained rats to assess if these receptors were functionally active and secondly EEG recordings were performed on freely moving animals to investigate the effect of H_1 receptor blockade on a number of sleep-wake parameters.

5.2 Mepyramine decreases the firing of putative 5-HT neurons in the DRN

Extracellular single-unit recordings were made from putative 5-HT neurons in the DRN of rats under urethane anaesthesia. A representative action potential can be seen in Figure 5.1. The majority of neurons (10/11) fired tri-phasic (positive-negative-positive), broad action potentials (3.2 ± 0.1ms, Fig.5.1.A1) in a highly regular pattering (CV of 0.4 ± 0.1, Fig.5.1.A2) and with low frequency (2.2 ± 0.4Hz, Fig.5.1.A3). One neuron fired bi-phasic (positive-negative), broad action potentials, a comparison of these neurons is illustrated in Figure.5.1.B. The observation of bi-phasic and tri-phasic, broad action potentials made in this study is consistent with previous recordings from 5-HT neurons in the DRN of rats under urethane anaesthesia (Allers and Sharp, 2003).

The effect of intravenous (i.v.) administration of mepyramine was tested in 13 cells (from 13 animals). A dose of 10mg/kg was selected based on previous studies however this proved fatal (n = 1). The dose was reduced to 3mg/kg but unfortunately this also proved fatal in some animals (1/3) therefore the non-lethal dose of 1mg/kg was selected for the study. A representative recording is illustrated in Figure.5.2. After a stable baseline (20 minutes) each animal received a vehicle treatment of 1ml/kg 0.9% NaCl (i.v.) and drug treatment of 1mg/kg

mepyramine (i.v.). It can be seen that the vehicle treatment does not alter the firing frequency of the neuron but subsequent administration of 1mg/kg mepyramine produces a rapid decrease in firing (Fig.5.2.A). When the firing frequency during vehicle treatment is compared with firing frequency during mepyramine treatment we can see there is a significant decrease across all cells tested (Fig.5.2.B). When expressed as a percentage of control it can be seen that 1mg/kg mepyramine caused a significant inhibition (56%, $p < 0.05$, paired Student's t-test) of cell firing across all 8 cells tested (Fig.5.2.C). In one instance the administration of 1mg/kg mepyramine produced an increase in the firing of the recorded neuron (25%, data not shown).

5.3 Mepyramine increases NREM sleep

Although the sedating properties of H_1 receptor inverse agonists/antagonists (antihistamines) are well known and drugs which enhance sleep by blocking H_1 receptors have been available over the counter for many years the precise mechanisms of action by which these agents cause drowsiness is unknown. I therefore performed EEG recording on freely moving rats in order to investigate the behavioural effect of mepyramine. Rats were intravenously administered 1mg/kg mepyramine or 1ml/kg vehicle (20% HBCD) at circadian time 5 (i.e. 5 hours after lights on). Measurements of sleep-wake characteristics were performed for 24 hours before (baseline) and 30 hours after drug treatment (see section 2.8.4). Animals were undisturbed for the duration of the study with the exception of 30mins at the time of dosing.

Intravenous administration of 1mg/kg mepyramine produced a significant decrease in the percentage of time spent awake and concurrently produced an increase in the percentage of NREM sleep in the first two hours after dosing ($p < 0.025$, ANCOVA, Fig.5.3). The latency to 60 seconds of continuous sleep was reduced from 36.9 ± 4.1 mins to 25.9 ± 2.8 mins after administration ($p < 0.025$ ANCOVA). The average length of sleep bout was also significantly increased in the first two hours after dosing ($p < 0.025$, ANCOVA, Fig.5.4). Mepyramine significantly increased the accumulated amount of NREM sleep after dosing ($p < 0.025$, ANCOVA, Figure 5.5) however mepyramine failed to have a significant effect on REM sleep at any time point (data not shown). In the first 7 hours after dosing (CT-5 to CT-12) mepyramine significantly increased the time animals were in NREM from 218.8 ± 4.4 minutes to 244.2 ± 4.4

minutes ($p < 0.001$, ANCOVA). It should also be noted that administration of mepyramine led to a decrease in the body temperature in the first hour after dosing (Fig.5.6).

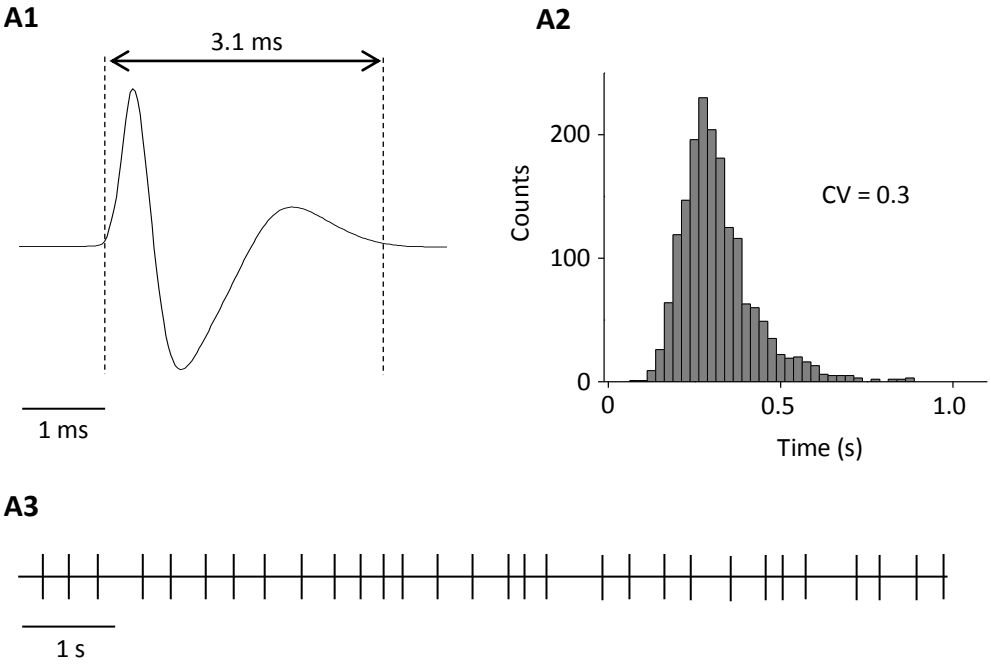

B

Neuron shape	n	Spike width (ms)	CV	Frequency (Hz)
Bi-phasic	1	3.7	0.4	4.4
Tri-phasic	10	3.2 ± 0.1 (2.7-4.0)	0.4 ± 0.1 (0.1-0.8)	2.2 ± 0.4 (0.5-3.3)

Figure 5.1. Extracellular single-unit recordings of 5-HT neurons in the DRN. (A1) A representative tri-phasic, broad-width action potential (spike) recorded from the DRN. (A2) A representative interevent-interval histogram (in 25ms bins) indicating a very regular firing pattern (CV = 0.3). (A3) A representative 10 second section of the spike train. (B) A table summarising the electrophysiological properties analysed to establish 5-HT neuronal identity. Values are displayed as the average ± SEM. Values in parentheses represent the range of values.

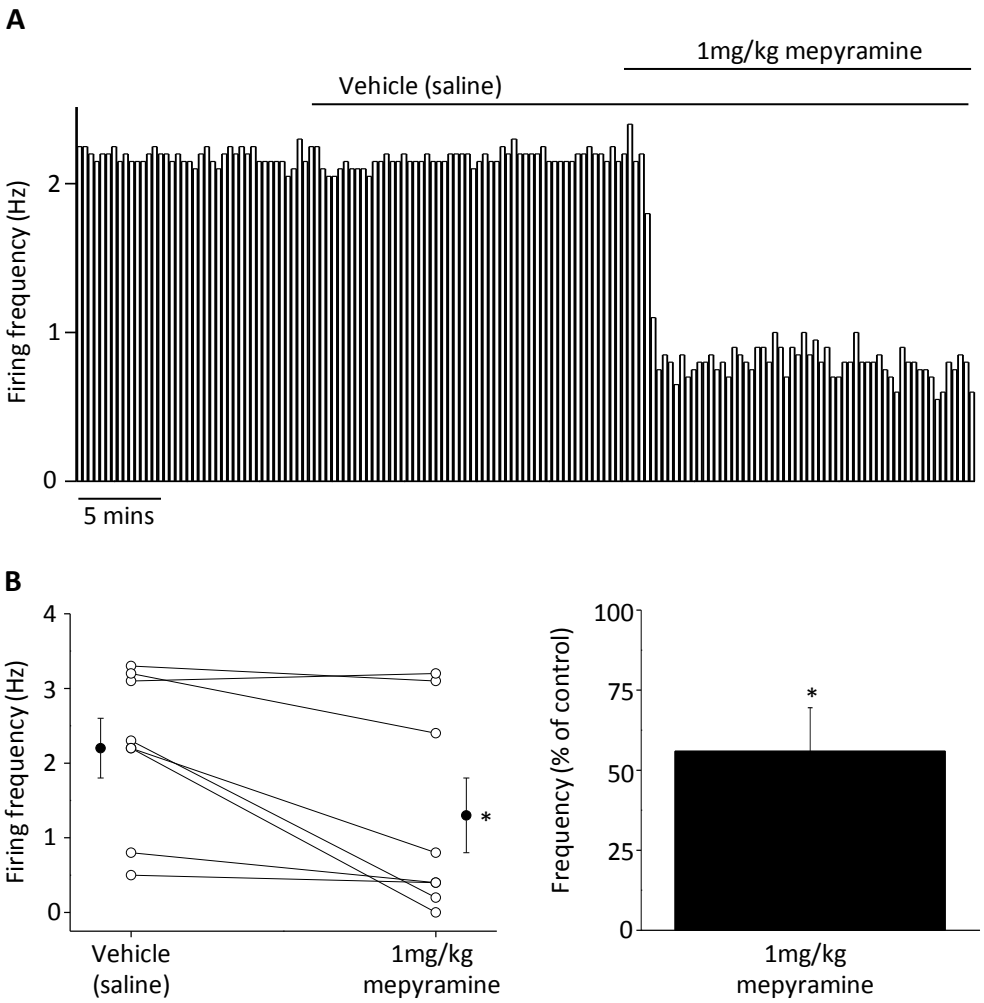

Figure 5.2. Mepyramine decreases the firing of neurons in the DRN. (A) A representative recording of the firing frequency (20s bins) from a spontaneously firing neuron in the presence of saline and 1mg/kg mepyramine. (B) Firing frequency of individual neurons (open circles) before (vehicle) and after the application of mepyramine (1mg/kg). The average firing frequency in vehicle and in the presence of histamine is shown by the closed circles (mean ± SEM). (C) Bar graph showing the average effect of histamine when applied to spontaneously firing neurons (n = 8). Effect is displayed as the mean percentage of control firing ± SEM. * $p < 0.05$, paired Student's t-test

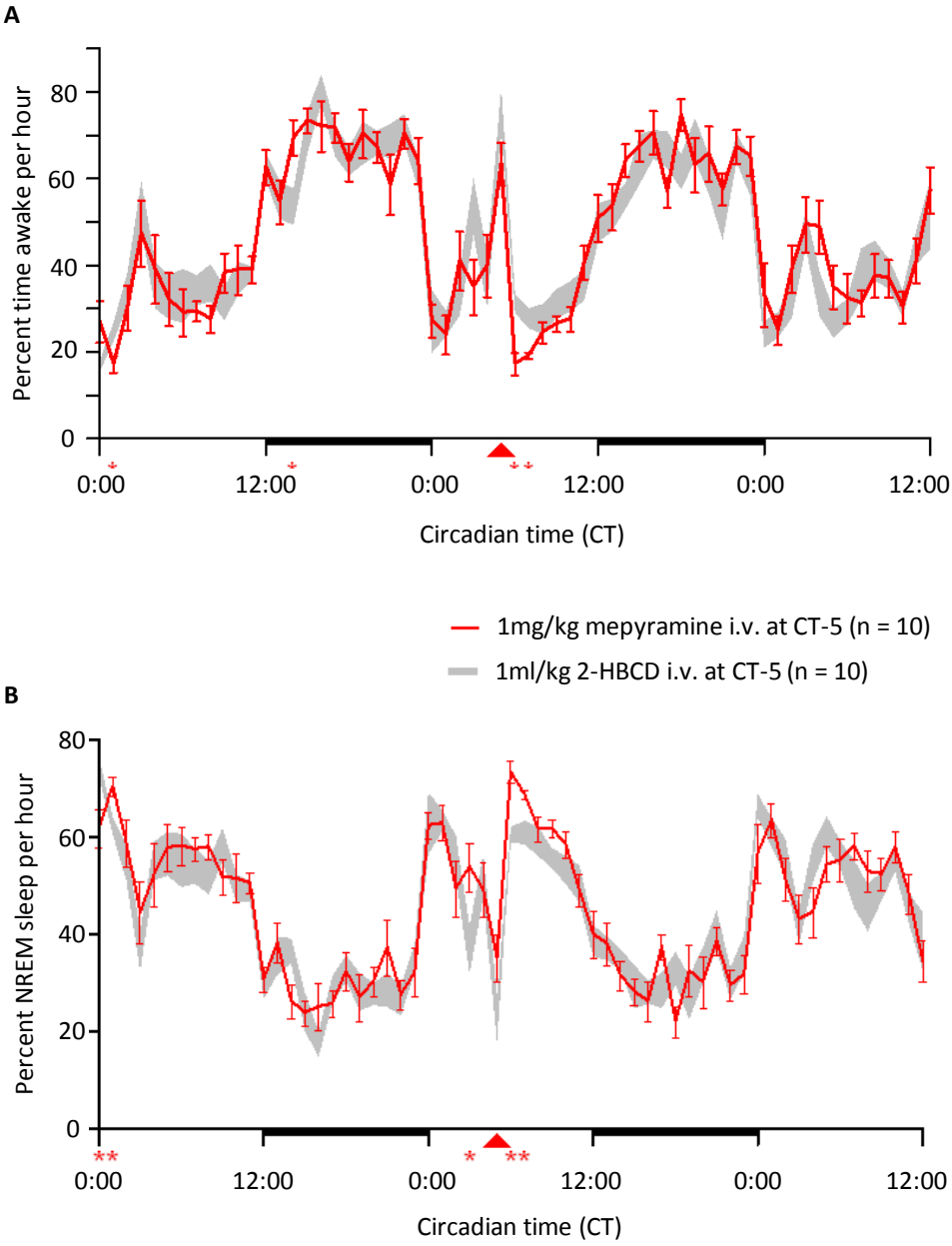

Figure 5.3. Mepyramine produces a decrease in the amount of wake time with a concurrent increase in NREM sleep after dosing. A plot of the percentage of wake (top) and NREM sleep (bottom) per hour illustrating rats administered intravenously with vehicle (1ml/kg 2-HBCD, grey, n = 10) and mepyramine (1mg/kg mepyramine, red, n = 10) at CT-5 (red triangle). Hourly values are represented as mean ± SEM.* $p < 0.025$, ANCOVA.

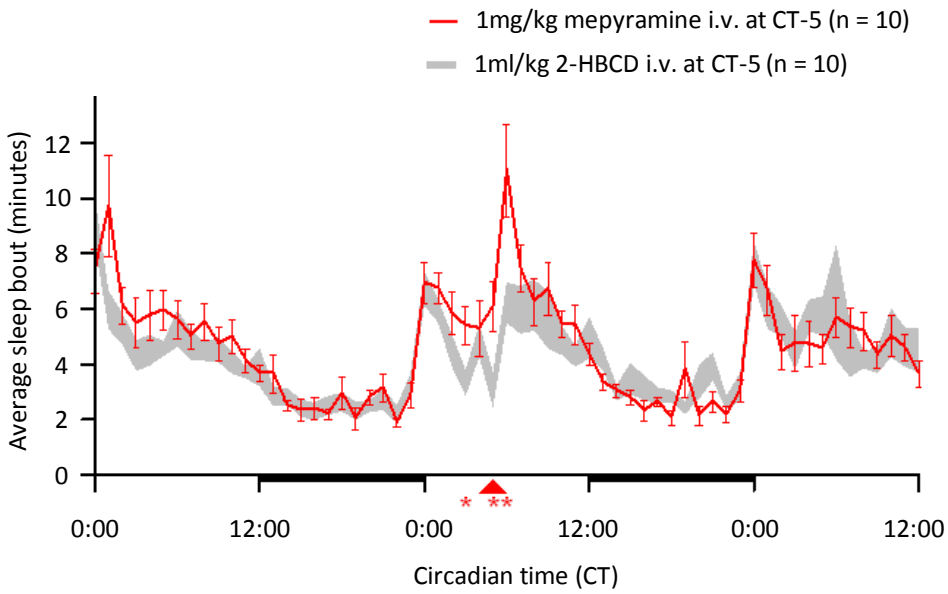

Figure 5.4. Mepyramine produces an acute increase in the aligned sleep bout. A plot illustrating the average duration of sleep bout in rats administered intravenously with vehicle (1ml/kg 2-HBCD, grey, n = 10) and mepyramine (1mg/kg mepyramine, red, n = 10) at CT-5 (red triangle). Hourly values are represented as mean ± SEM.* $p < 0.025$, ANCOVA.

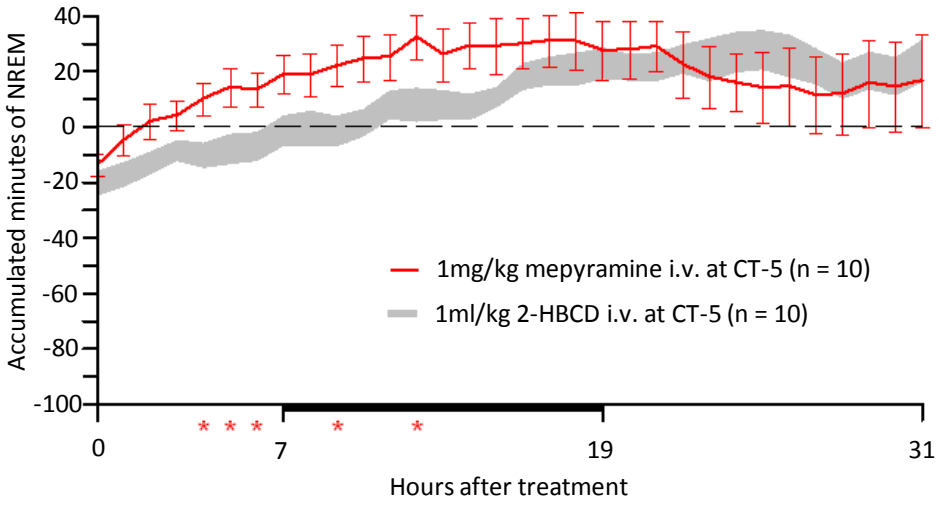

Figure 5.5. Mepyramine increases the amount of NREM sleep. A plot illustrating the accumulation of NREM sleep after rats were administered intravenously with vehicle (1ml/kg 2-HBCD, grey, n = 10) and mepyramine (1mg/kg mepyramine, red, n = 10). Hourly values are represented as mean ± SEM.* $p < 0.025$, ANCOVA.

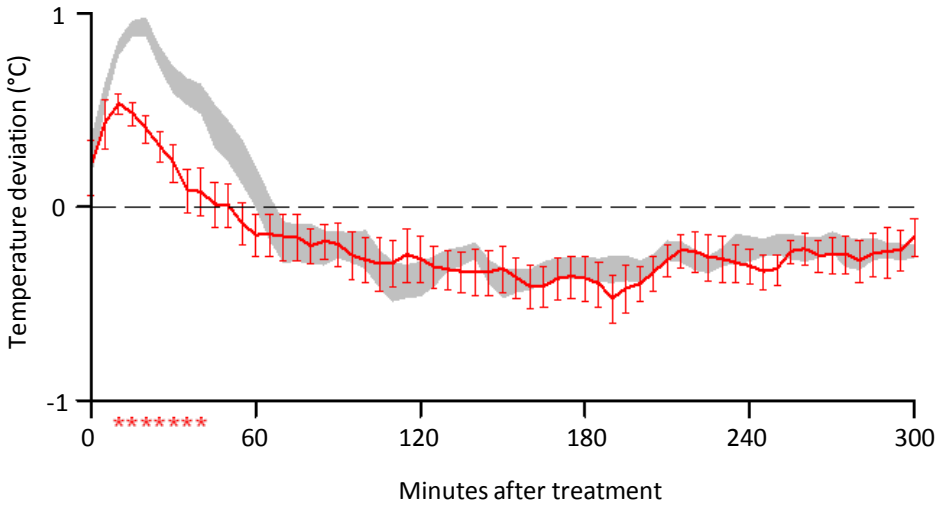

Figure 5.6. Mepyramine decreases body temperature. A plot illustrating the temperature deviation from the baseline mean. In rats administered intravenously with vehicle (1ml/kg 2-HBCD, grey, n = 10) and mepyramine (1mg/kg mepyramine, red, n = 10) at CT-5 (red triangle). Hourly values are represented as mean ± SEM.* $p < 0.025$, ANCOVA.

5.4 Discussion

5.4.1 Mepyramine decreases the firing of putative 5-HT neurons in the DRN

Intravenous administration of 1mg/kg mepyramine to rats under urethane anaesthesia produced a decrease in the firing of putative 5-HT neurons in the DRN. This result is consistent with data from a previous study which demonstrate that microiontophoretic application of mepyramine into the DRN of anesthetised rats had a depressant effect on 5-HT neurons (Lakoski and Aghajanian, 1983). In addition the results presented here are in keeping with a previous study in cats which demonstrated that infusion of mepyramine into the DRN suppressed the discharge of 5-HT neurons during wakefulness and slow wave sleep (Sakai and Crochet, 2000). When comparing the results from previous studies with the results presented here it is important to consider that mepyramine was administered by different routes i.e. locally into the DRN versus systemically. Therefore while previous studies could conclude that mepyramine was acting at H_1 receptors located within the DRN to depress 5-HT neurons, this same conclusion cannot be made based on the results presented in this section alone. If the results presented *in vivo* (Chapter 5) are combined with those obtained *in vitro* (Chapter 4) it could be concluded that mepyramine administered systemically acts predominantly via H_1 receptors in the DRN to produce its depressant effect, however the possibility that mepyramine could be acting at H_1 receptors located in other brain regions that impinge on the DRN cannot be ruled out.

In the present study the magnitude of mepyramine inhibition was highly variable, ranging from partial to full inhibition (6 - 100%). As the recordings were performed on rats under urethane anaesthesia it is conceivable that the level of urethane in the brain could affect the mepyramine response. The level of mepyramine in the brain will also be dependent on the pharmacokinetic profile of the drug and therefore will vary between animals, however the rapidity of the response suggests a very fast transport of drug into the brain following intravenous administration, and pharmacokinetic studies support high levels of drug measured in the brain following 1mg/kg i.v. (personal communication, Lilly). It has recently been shown *in vitro* that urethane can attenuate the response of 5-HT neurons in the DRN to various modulatory agents (McCardle and Gartside, 2012). Moreover the authors demonstrated that

the concentration of mepyramine could affect the magnitude of the attenuation in certain incidences. It would be pertinent in future studies to monitor the brain levels of urethane in order to extrapolate the affect that this has on the magnitude of mepyramine inhibition. While 1mg/kg mepyramine significantly inhibited the firing of the majority of neurons (6/8) it failed to have a significant effect on some (2/8). This is in keeping with the *in vitro* data which demonstrated the mepyramine had an inhibitory effect on most but not all of the neurons tested (section 4.6). It is most likely that neurons which failed to respond to mepyramine did not express H_1 receptors. These neurons may represent a subset population present in the DRN which are not regulated by histamine (at least via the H_1 receptor subtype). Similar findings were demonstrated in recordings made from the cat (Sakai and Crochet, 2000). In this study the authors went on to show that neurons which failed to respond to histamine and mepyramine were attenuated by the α_1-adrenoreceptor agonist, phenylephrine. The authors concluded that noradrenergic and histaminergic inputs target different populations of 5-HT neurons in the DRN.

It should also be noted here that in one neuron mepyramine produced a significant excitation of the baseline firing. This excitation was not seen in the *in vitro* data and likewise was not reported in any other study. While it is possible that this is an erroneous result it could also represent the presence of an indirect inhibitory effect of histamine in the DRN, possibly via GABAergic interneurons. However, it is important to note that that no histology was performed to confirm electrode placement in the DRN and no immunohistochemistry was carried out to confirm the neuronal identity of recorded neurons. In this study, putative serotonin neurons were selected based on their action potential shape (wide, bi- or tri-phasic waveform) and firing properties (slow, rhythmic discharge rates). As these characteristics do not guarantee 5-HT neuronal identity, it is possible that the neuron which was excited by mepyramine represents the response of a non-serotonergic neuron.

Taken together, these *in vivo* single-unit results demonstrate the functional activity of H_1 receptors in the DRN of rats. Future studies should investigate whether these receptors are constitutively active in the whole brain. This could be achieved by utilising neutral antagonists of the H_1 receptor e.g. oxatomide and histabudifen. These ligands have zero efficacy (whereas inverse agonists with negative efficacy) therefore if no effect was observed after their

administration one could propose that these receptors are constitutively active *in vivo*. These results demonstrate the heterogeneity of regulation in the DRN and exemplify just how complex the neuronal networks which control the sleep-wake cycle are. Lastly, these data highlight the need for post-hoc identification of the recording site (via staining or chemical/electrical lesioning) or better yet, the post-hoc identification of the neuron (using juxtacellular labelling).

5.4.2 Mepyramine increases NREM sleep

Intravenous administration of 1mg/kg mepyramine to rats produced a significant decrease in wakefulness and increase in NREM sleep in the two hours following dosing. In addition the length of the sleep bout was also significantly increased, however, no significant attenuation of REM sleep was observed. This acute attenuation of wakefulness and NREM sleep is consistent with a previous study in rats which demonstrated that interperitoneal (i.p.) administration of mepyramine during the light phase decreased wakefulness and increased NREM sleep in the two hours after dosing (Monti *et al*., 1986). The short duration of the mepyramine-induced sedation could be explained by its rapid metabolism and elimination from the rat. The plasma elimination half-life of 0.7mg/kg mepyramine has been calculated to be approximately 2.3 hours (Kelly and Slikker, 1987). The circadian time at which mepyramine was dosed will also affect the extent of sleep promoting activity, since the CT-5 time used here was the middle of the animals light period during which more naturally occurring sleep is present. In support of this, a previous study conducted within the laboratory demonstrated that i.p. administration of 20mg/kg mepyramine at CT-18 produced a more robust attenuation of NREM sleep (personal communication, Lilly) lasting up to four hours after dosing. Similar to results presented here, the average length of sleep bout was increased while REM sleep remained largely unaffected. The more robust increase in NREM sleep after CT-18 dosing is unsurprising given there is less naturally occurring sleep. A confounding factor here is the possibility that mepyramine may be more slowly absorbed and distributed differently when dosed i.p. (versus i.v. at CT-5). Unfortunately it was not possible to dose animals intravenously at CT-18 given the dark conditions, even red light would be permit i.v. dosing. A small but significant drop in body temperature was also observed after mepyramine administration. This

effect is observed with the application of other sedatives (personal communication) and is most likely related to the increase sleep and lack of movement just after drug dosing.

5.4.3 Clinical significance of H_1 inverse agonists on the sleep-wake cycle

Although originally classified as antagonists, all clinically available antihistamines are in fact inverse agonists (Leurs *et al*., 2002). Antihistamines are most frequently used as first line therapeutics for allergic disorders. Sedation is one of the most common side effects of prescription and over-the-counter antihistamines. Clinically available antihistamines have been divided into different classes depending on their sedative properties; sedative (first generation) and less sedative (second generation) (Yani *et al*., 1995, 2007). First generation antihistamines, which include diphenhydramine and chlorphenamine, produce the most profound sedation due to ease with which they cross the blood brain barrier (Goldberg *et al*., 1987). Second generation antihistamines, which include loratadine and fexofenadine, do not to cross the blood brain barrier as easily and hence produce much less sedation than the classical antihistamines (Izumi *et al*., 2008). The sedative properties of H_1 inverse agonists are obvious however the constitutive activity of H_1 receptors have not been demonstrated *in vivo*. It will therefore be important to assess the effect of H_1 neutral antagonists on sleep parameters, especially given the demonstration that H_1 receptors are constitutively active *in vitro* (section 4.6). Neutral H_1 antagonists may present a novel method by which sedation could be safely achieved in humans. Given the recent availability of selective neutral antagonists, it is only a matter of time before these studies are performed.

Conclusions and future directions

This study has characterised the regulation of serotonergic DR neurons by a number of different neurotransmitter systems including: serotonin, noradrenaline, orexin and histamine. Ninety-five percent of neurons were shown to be inhibited by 5-HT in a concentration-dependent manner, an observation in keeping with a plethora of evidence in the literature. An inhibitory role for 5-HT_2 receptors was demonstrated, an effect which could have been mediated by GABA directly on 5-HT neurons. Given the low experiment numbers reported

here, it would be pertinent in future to produce more data confirming the inhibitory role of 5-HT_2 receptors in the DRN. Phenylephrine was shown to excite serotonin neurons in the DRN suggesting an important regulatory role for α_1 adrenoreceptors. It will be interesting to investigate this excitatory drive further to assess whether it is specific to certain populations of 5-HT neurons located in the DRN. Orexins were shown to have a robust excitatory influence on serotonin neurons in the DRN. Patch-clamp electrophysiology revealed that orexin induced a large inward current in all neurons tested however the second messenger system and downstream receptor responsible for this effect was not determined. While some evidence is available to suggest the involvement of a TRP channel, future studies should aim to better characterise the cellular mechanisms responsible for the orexin-induced excitation. Histamine was shown to have a strong and robust excitatory effect on 5-HT neurons in the DRN. Patch-clamp recordings demonstrated that histamine depolarised neurons, caused a large inward current and increase in the baseline noise. Pharmacological studies revealed that H_1 receptors were primary responsible for the histamine effect. Patch clamp recordings also demonstrated that these receptors were located on 5-HT neurons and suggested for the first time that H_1 receptors are constitutively active in the DRN. Further evidence to confirm the constitutive activity of H_1 receptors *in vitro* is however needed. *In vivo* electrophysiology confirmed that H_1 receptors had an excitatory role in the DRN and demonstrated that these receptors are functionally active in the whole brain. Unfortunately the constitutive activity of H_1 receptors was not explored *in vivo*. It will be important to demonstrate whether H_1 receptors are constitutively active *in vivo*, especially as there is currently no report of this activity in the whole brain. EEG recordings revealed that inhibition of H_1 receptors led to an increase of NREM sleep. This is in keeping with scientific and clinical data but raises an important question as to whether constitutive H_1 receptor activity may play an important role in the increase of NREM sleep. Future studies should aim to investigate what effect neutral H_1 antagonists have on sleep parameters in order to ascertain if these compounds could have a more clinically significant therapeutic benefit over currently available sleep medications.

Collectively, the findings presented here demonstrate the regulation of serotonergic neurons in the DRN is multifactorial and highly complex. The data suggest for the first time the presence of constitutively active H_1 receptors in the DRN. This constitutive receptor activity could have important implications for drug discovery. Combination sleep therapies which

target both the histamine and serotonin systems (e.g. H_1/5-HT_2 antagonists) could have less desirable efficacy than one may expect from their individual sedative actions.

References

ABRAMS, J. K., JOHNSON, P. L., HOLLIS, J. H. & LOWRY, C. A. 2004. Anatomic and functional topography of the dorsal raphe nucleus. *Ann N Y Acad Sci,* 1018**,** 46-57.

ADELL, A., CELADA, P. & ARTIGAS, F. 2001. The role of 5-HT1B receptors in the regulation of serotonin cell firing and release in the rat brain. *J Neurochem,* 79**,** 172-82.

AGHAJANIAN, G. K. 1985. Modulation of a transient outward current in serotonergic neurones by alpha 1-adrenoceptors. *Nature,* 315**,** 501-3.

AGHAJANIAN, G. K., FOOTE, W. E. & SHEARD, M. H. 1968. Lysergic acid diethylamide: sensitive neuronal units in the midbrain raphe. *Science,* 161**,** 706-8.

AGHAJANIAN, G. K. & LAKOSKI, J. M. 1984. Hyperpolarization of serotonergic neurons by serotonin and LSD: studies in brain slices showing increased K+ conductance. *Brain Res,* 305**,** 181-5.

AGHAJANIAN, G. K. & VANDERMAELEN, C. P. 1982. Intracellular identification of central noradrenergic and serotonergic neurons by a new double labeling procedure. *J Neurosci,* 2**,** 1786-92.

AGHAJANIAN, G. K. & VANDERMAELEN, C. P. 1982. Intracellular recordings from serotonergic dorsal raphe neurons: pacemaker potentials and the effect of LSD. *Brain Res,* 238**,** 463-9.

AKERSTEDT, T. 1998. Is there an optimal sleep-wake pattern in shift work? *Scand J Work Environ Health,* 24 Suppl 3**,** 18-27.

AKERSTEDT, T. & FOLKARD, S. 1997. The three-process model of alertness and its extension to performance, sleep latency, and sleep length. *Chronobiol Int,* 14**,** 115-23.

ALEXANDER, S. P., MATHIE, A. & PETERS, J. A. 2011. Guide to Receptors and Channels (GRAC), 5th edition. *Br J Pharmacol,* 164 Suppl 1**,** S1-324.

ALHOLA, P. & POLO-KANTOLA, P. 2007. Sleep deprivation: Impact on cognitive performance. *Neuropsychiatr Dis Treat,* 3**,** 553-67.

ALLERS, K. A. & SHARP, T. 2003. Neurochemical and anatomical identification of fast- and slow-firing neurones in the rat dorsal raphe nucleus using juxtacellular labelling methods in vivo. *Neuroscience,* 122**,** 193-204.

AL-SHAMMA, H. A., ANDERSON, C., CHUANG, E., LUTHRINGER, R., GROTTICK, A. J., HAUSER, E.,

MORGAN, M., SHANAHAN, W., TEEGARDEN, B. R., THOMSEN, W. J. & BEHAN, D. 2010. Nelotanserin, a novel selective human 5-hydroxytryptamine2A inverse agonist for the treatment of insomnia. *J Pharmacol Exp Ther,* 332**,** 281-90.

AMICI, R., SANFORD, L. D., KEARNEY, K., MCINERNEY, B., ROSS, R. J., HORNER, R. L. & MORRISON, A. R. 2004. A serotonergic (5-HT2) receptor mechanism in the laterodorsal tegmental nucleus participates in regulating the pattern of rapid-eye-movement sleep occurrence in the rat. *Brain Res,* 996**,** 9-18.

ARARAGI, N., MLINAR, B., BACCINI, G., GUTKNECHT, L., LESCH, K. P. & CORRADETTI, R. 2013. Conservation of 5-HT1A receptor-mediated autoinhibition of serotonin (5-HT) neurons in mice with altered 5-HT homeostasis. *Front Pharmacol,* 4**,** 97.

ARRANG, J. M., GARBARG, M. & SCHWARTZ, J. C. 1987. Autoinhibition of histamine synthesis mediated by presynaptic H3-receptors. *Neuroscience,* 23**,** 149-57.

ASERINSKY, E. & KLEITMAN, N. 1953. Regularly occurring periods of eye motility, and concomitant phenomena, during sleep. *Science,* 118**,** 273-4.

AZNAVOUR, N., RBAH, L., LEGER, L., BUDA, C., SASTRE, J. P., IMHOF, A., CHARNAY, Y. & ZIMMER, L. 2006. A comparison of in vivo and in vitro neuroimaging of 5-HT 1A receptor binding sites in the cat brain. *J Chem Neuroanat,* 31**,** 226-32.

BAKKER, R. A., SCHOONUS, S. B., SMIT, M. J., TIMMERMAN, H. & LEURS, R. 2001. Histamine H(1)-receptor activation of nuclear factor-kappa B: roles for G beta gamma- and G alpha(q/11)-subunits in constitutive and agonist-mediated signaling. *Mol Pharmacol,* 60**,** 1133-42.

BAKKER, R. A., WIELAND, K., TIMMERMAN, H. & LEURS, R. 2000. Constitutive activity of the histamine H(1) receptor reveals inverse agonism of histamine H(1) receptor antagonists. *Eur J Pharmacol,* 387**,** R5-7.

BARABAN, J. M. & AGHAJANIAN, G. K. 1980. Suppression of firing activity of 5-HT neurons in the dorsal raphe by alpha-adrenoceptor antagonists. *Neuropharmacology,* 19**,** 355-63.

BARABAN, J. M. & AGHAJANIAN, G. K. 1981. Noradrenergic innervation of serotonergic neurons in the dorsal raphe: demonstration by electron microscopic autoradiography. *Brain Res,* 204**,** 1-11.

BARBARA, A., ACEVES, J. & ARIAS-MONTANO, J. A. 2002. Histamine H1 receptors in rat dorsal raphe nucleus: pharmacological characterisation and linking to increased neuronal activity. *Brain Res,* 954**,** 247-55.

BARNES, W. G. & HOUGH, L. B. 2002. Membrane-bound histamine N-methyltransferase in mouse brain: possible role in the synaptic inactivation of neuronal histamine. *J*

Neurochem, 82**,** 1262-71.

BAUDRY, M., MARTRES, M. P. & SCHWARTZ, J. C. 1975. H1 and H2 receptors in the histamine-induced accumulation of cyclic AMP in guinea pig brain slices. *Nature,* 253**,** 362-4.

BECK, S. G., PAN, Y. Z., AKANWA, A. C. & KIRBY, L. G. 2004. Median and dorsal raphe neurons are not electrophysiologically identical. *J Neurophysiol,* 91**,** 994-1005.

BELIN, M. F., NANOPOULOS, D., DIDIER, M., AGUERA, M., STEINBUSCH, H., VERHOFSTAD, A., MAITRE, M. & PUJOL, J. F. 1983. Immunohistochemical evidence for the presence of gamma-aminobutyric acid and serotonin in one nerve cell. A study on the raphe nuclei of the rat using antibodies to glutamate decarboxylase and serotonin. *Brain Res,* 275**,** 329-39.

BERNARDIS, L. L. & BELLINGER, L. L. 1996. The lateral hypothalamic area revisited: ingestive behavior. *Neurosci Biobehav Rev,* 20**,** 189-287.

BIANCHI, M. T., CLARK, A. G. & FISHER, J. L. 2011. The wake-promoting transmitter histamine preferentially enhances alpha-4 subunit-containing GABAA receptors. *Neuropharmacology,* 61**,** 747-52.

BJORVATN, B., FAGERLAND, S., EID, T. & URSIN, R. 1997. Sleep/waking effects of a selective 5-HT1A receptor agonist given systemically as well as perfused in the dorsal raphe nucleus in rats. *Brain Res,* 770**,** 81-8.

BLANDINA, P., GIORGETTI, M., BARTOLINI, L., CECCHI, M., TIMMERMAN, H., LEURS, R., PEPEU, G. & GIOVANNINI, M. G. 1996. Inhibition of cortical acetylcholine release and cognitive performance by histamine H3 receptor activation in rats. *Br J Pharmacol,* 119**,** 1656-64.

BOESS, F. G. & MARTIN, I. L. 1994. Molecular biology of 5-HT receptors. *Neuropharmacology,* 33**,** 275-317.

BOISSARD, R., GERVASONI, D., SCHMIDT, M. H., BARBAGLI, B., FORT, P. & LUPPI, P. H. 2002. The rat ponto-medullary network responsible for paradoxical sleep onset and maintenance: a combined microinjection and functional neuroanatomical study. *Eur J Neurosci,* 16**,** 1959-73.

BOND, R. A. & IJZERMAN, A. P. 2006. Recent developments in constitutive receptor activity and inverse agonism, and their potential for GPCR drug discovery. *Trends Pharmacol Sci,* 27**,** 92-6.

BONNAVION, P., BERNARD, J. F., HAMON, M., ADRIEN, J. & FABRE, V. 2010. Heterogeneous distribution of the serotonin 5-HT(1A) receptor mRNA in chemically identified neurons of the mouse rostral brainstem: Implications for the role of serotonin in the regulation

of wakefulness and REM sleep. *J Comp Neurol,* 518**,** 2744-70.

BOOTHMAN, L. J., ALLERS, K. A., RASMUSSEN, K. & SHARP, T. 2003. Evidence that central 5-HT2A and 5-HT2B/C receptors regulate 5-HT cell firing in the dorsal raphe nucleus of the anaesthetised rat. *Br J Pharmacol,* 139**,** 998-1004.

BOOTHMAN, L. J. & SHARP, T. 2005. A role for midbrain raphe gamma aminobutyric acid neurons in 5-hydroxytryptamine feedback control. *Neuroreport,* 16**,** 891-6.

BORBELY, A. A. 1982. A two process model of sleep regulation. *Hum Neurobiol,* 1**,** 195-204.

BOSCHERT, U., AMARA, D. A., SEGU, L. & HEN, R. 1994. The mouse 5-hydroxytryptamine1B receptor is localized predominantly on axon terminals. *Neuroscience,* 58**,** 167-82.

BOSSENMEYER-POURIE, C., LIEVRE, V., GROJEAN, S., KOZIEL, V., PILLOT, T. & DAVAL, J. L. 2002. Sequential expression patterns of apoptosis- and cell cycle-related proteins in neuronal response to severe or mild transient hypoxia. *Neuroscience,* 114**,** 869-82.

BOUTREL, B., MONACA, C., HEN, R., HAMON, M. & ADRIEN, J. 2002. Involvement of 5-HT1A receptors in homeostatic and stress-induced adaptive regulations of paradoxical sleep: studies in 5-HT1A knock-out mice. *J Neurosci,* 22**,** 4686-92.

BRAESTRUP, C., SCHMIECHEN, R., NEEF, G., NIELSEN, M. & PETERSEN, E. N. 1982. Interaction of convulsive ligands with benzodiazepine receptors. *Science,* 216**,** 1241-3.

BROWN, R. E. & HAAS, H. L. 1999. On the mechanism of histaminergic inhibition of glutamate release in the rat dentate gyrus. *J Physiol,* 515 (Pt 3)**,** 777-86.

BROWN, R. E., MCKENNA, J. T., WINSTON, S., BASHEER, R., YANAGAWA, Y., THAKKAR, M. M. & MCCARLEY, R. W. 2008. Characterization of GABAergic neurons in rapid-eye-movement sleep controlling regions of the brainstem reticular formation in GAD67-green fluorescent protein knock-in mice. *Eur J Neurosci,* 27**,** 352-63.

BROWN, R. E., SERGEEVA, O., ERIKSSON, K. S. & HAAS, H. L. 2001. Orexin A excites serotonergic neurons in the dorsal raphe nucleus of the rat. *Neuropharmacology,* 40**,** 457-9.

BROWN, R. E., SERGEEVA, O. A., ERIKSSON, K. S. & HAAS, H. L. 2002. Convergent excitation of dorsal raphe serotonin neurons by multiple arousal systems (orexin/hypocretin, histamine and noradrenaline). *J Neurosci,* 22**,** 8850-9.

BURLHIS, T. M. & AGHAJANIAN, G. K. 1987. Pacemaker potentials of serotonergic dorsal raphe neurons: contribution of a low-threshold Ca2+ conductance. *Synapse,* 1**,** 582-8.

CALIZO, L. H., AKANWA, A., MA, X., PAN, Y. Z., LEMOS, J. C., CRAIGE, C., HEEMSTRA, L. A. & BECK, S. G. 2011. Raphe serotonin neurons are not homogenous: electrophysiological, morphological and neurochemical evidence. *Neuropharmacology,* 61**,** 524-43.

CERRITO, F. & RAITERI, M. 1979. Evidence for an autoreceptor-mediated presynaptic control of serotonin release in central nerve endings [proceedings]. *Br J Pharmacol,* 67**,** 424P-425P.

CERRITO, F. & RAITERI, M. 1979. Serotonin release is modulated by presynaptic autoreceptors. *Eur J Pharmacol,* 57**,** 427-30.

CHAZOT, P. L., HANN, V., WILSON, C., LEES, G. & THOMPSON, C. L. 2001. Immunological identification of the mammalian H3 histamine receptor in the mouse brain. *Neuroreport,* 12**,** 259-62.

CHEMELLI, R. M., WILLIE, J. T., SINTON, C. M., ELMQUIST, J. K., SCAMMELL, T., LEE, C., RICHARDSON, J. A., WILLIAMS, S. C., XIONG, Y., KISANUKI, Y., FITCH, T. E., NAKAZATO, M., HAMMER, R. E., SAPER, C. B. & YANAGISAWA, M. 1999. Narcolepsy in orexin knockout mice: molecular genetics of sleep regulation. *Cell,* 98**,** 437-51.

CHOU, T. C., BJORKUM, A. A., GAUS, S. E., LU, J., SCAMMELL, T. E. & SAPER, C. B. 2002. Afferents to the ventrolateral preoptic nucleus. *J Neurosci,* 22**,** 977-90.

CLARK, C. T., WEISSBACH, H. & UDENFRIEND, S. 1954. 5-Hydroxytryptophan decarboxylase: preparation and properties. *J Biol Chem,* 210**,** 139-48.

COMMONS, K. G. 2009. Locally collateralizing glutamate neurons in the dorsal raphe nucleus responsive to substance P contain vesicular glutamate transporter 3 (VGLUT3). *J Chem Neuroanat,* 38**,** 273-81.

COMMONS, K. G., BECK, S. G. & BEY, V. W. 2005. Two populations of glutamatergic axons in the rat dorsal raphe nucleus defined by the vesicular glutamate transporters 1 and 2. *Eur J Neurosci,* 21**,** 1577-86.

COMMONS, K. G., CONNOLLEY, K. R. & VALENTINO, R. J. 2003. A neurochemically distinct dorsal raphe-limbic circuit with a potential role in affective disorders. *Neuropsychopharmacology,* 28**,** 206-15.

COSTA, T. & HERZ, A. 1989. Antagonists with negative intrinsic activity at delta opioid receptors coupled to GTP-binding proteins. *Proc Natl Acad Sci U S A,* 86**,** 7321-5.

CRAWFORD, L. K., CRAIGE, C. P. & BECK, S. G. 2010. Increased intrinsic excitability of lateral wing serotonin neurons of the dorsal raphe: a mechanism for selective activation in stress circuits. *J Neurophysiol,* 103**,** 2652-63.

CRUNELLI, V., FORDA, S., BROOKS, P. A., WILSON, K. C., WISE, J. C. & KELLY, J. S. 1983. Passive membrane properties of neurones in the dorsal raphe and periaqueductal grey recorded in vitro. *Neurosci Lett,* 40**,** 263-8.

DAAN, S., BEERSMA, D. G. & BORBELY, A. A. 1984. Timing of human sleep: recovery process gated by a circadian pacemaker. *Am J Physiol,* 246**,** R161-83.

DAHLSTROM, A. & FUXE, K. 1964. Localization of monoamines in the lower brain stem. *Experientia,* 20**,** 398-9.

DATE, Y., UETA, Y., YAMASHITA, H., YAMAGUCHI, H., MATSUKURA, S., KANGAWA, K., SAKURAI, T., YANAGISAWA, M. & NAKAZATO, M. 1999. Orexins, orexigenic hypothalamic peptides, interact with autonomic, neuroendocrine and neuroregulatory systems. *Proc Natl Acad Sci U S A,* 96**,** 748-53.

DATTA, S. 1997. Cellular basis of pontine ponto-geniculo-occipital wave generation and modulation. *Cell Mol Neurobiol,* 17**,** 341-65.

DAVIES, P. A., WANG, W., HALES, T. G. & KIRKNESS, E. F. 2003. A novel class of ligand-gated ion channel is activated by Zn2+. *J Biol Chem,* 278**,** 712-7.

DE ESCH, I. J., THURMOND, R. L., JONGEJAN, A. & LEURS, R. 2005. The histamine H4 receptor as a new therapeutic target for inflammation. *Trends Pharmacol Sci,* 26**,** 462-9.

DE LEAN, A., STADEL, J. M. & LEFKOWITZ, R. J. 1980. A ternary complex model explains the agonist-specific binding properties of the adenylate cyclase-coupled beta-adrenergic receptor. *J Biol Chem,* 255**,** 7108-17.

DE LECEA, L., KILDUFF, T. S., PEYRON, C., GAO, X., FOYE, P. E., DANIELSON, P. E., FUKUHARA, C., BATTENBERG, E. L., GAUTVIK, V. T., BARTLETT, F. S., 2ND, FRANKEL, W. N., VAN DEN POL, A. N., BLOOM, F. E., GAUTVIK, K. M. & SUTCLIFFE, J. G. 1998. The hypocretins: hypothalamus-specific peptides with neuroexcitatory activity. *Proc Natl Acad Sci U S A,* 95**,** 322-7.

DEMENT, W. & KLEITMAN, N. 1957. Cyclic variations in EEG during sleep and their relation to eye movements, body motility, and dreaming. *Electroencephalogr Clin Neurophysiol,* 9**,** 673-90.

DENG, D. R., DJALALI, S., HOLTJE, M., GROSSE, G., STROH, T., VOIGT, I., KUSSEROW, H., THEURING, F., AHNERT-HILGER, G. & HORTNAGL, H. 2007. Embryonic and postnatal development of the serotonergic raphe system and its target regions in 5-HT1A receptor deletion or overexpressing mouse mutants. *Neuroscience,* 147**,** 388-402.

DESCARRIES, L., WATKINS, K. C., GARCIA, S. & BEAUDET, A. 1982. The serotonin neurons in nucleus raphe dorsalis of adult rat: a light and electron microscope radioautographic

study. *J Comp Neurol,* 207**,** 239-54.

DOUCET, E., POHL, M., FATTACCINI, C. M., ADRIEN, J., MESTIKAWY, S. E. & HAMON, M. 1995. In situ hybridization evidence for the synthesis of 5-HT1B receptor in serotoninergic neurons of anterior raphe nuclei in the rat brain. *Synapse,* 19**,** 18-28.

DRUTEL, G., PEITSARO, N., KARLSTEDT, K., WIELAND, K., SMIT, M. J., TIMMERMAN, H., PANULA, P. & LEURS, R. 2001. Identification of rat H3 receptor isoforms with different brain expression and signaling properties. *Mol Pharmacol,* 59**,** 1-8.

EASTON, A., MEERLO, P., BERGMANN, B. & TUREK, F. W. 2004. The suprachiasmatic nucleus regulates sleep timing and amount in mice. *Sleep,* 27**,** 1307-18.

EGAN, C. T., HERRICK-DAVIS, K. & TEITLER, M. 1998. Creation of a constitutively activated state of the 5-hydroxytryptamine2A receptor by site-directed mutagenesis: inverse agonist activity of antipsychotic drugs. *J Pharmacol Exp Ther,* 286**,** 85-90.

ERICSON, H., WATANABE, T. & KOHLER, C. 1987. Morphological analysis of the tuberomammillary nucleus in the rat brain: delineation of subgroups with antibody against L-histidine decarboxylase as a marker. *J Comp Neurol,* 263**,** 1-24.

ERIKSSON, K. S., SERGEEVA, O., BROWN, R. E. & HAAS, H. L. 2001. Orexin/hypocretin excites the histaminergic neurons of the tuberomammillary nucleus. *J Neurosci,* 21**,** 9273-9.

EVRARD, A., LAPORTE, A. M., CHASTANET, M., HEN, R., HAMON, M. & ADRIEN, J. 1999. 5-HT1A and 5-HT1B receptors control the firing of serotoninergic neurons in the dorsal raphe nucleus of the mouse: studies in 5-HT1B knock-out mice. *Eur J Neurosci,* 11**,** 3823-31.

FALCK, B., HILLARP, N. A., THIEME, G. & TORP, A. 1982. Fluorescence of catechol amines and related compounds condensed with formaldehyde. *Brain Res Bull,* 9**,** xi-xv.

FAY, R. & KUBIN, L. 2001. 5-HT(2A) receptor-like protein is present in small neurons located in rat mesopontine cholinergic nuclei, but absent from cholinergic neurons. *Neurosci Lett,* 314**,** 77-81.

FINK, K. B. & GOTHERT, M. 2007. 5-HT receptor regulation of neurotransmitter release. *Pharmacol Rev,* 59**,** 360-417.

FITZPATRICK, P. F. 1999. Tetrahydropterin-dependent amino acid hydroxylases. *Annu Rev Biochem,* 68**,** 355-81.

FLEMING, J. V., FAJARDO, I., LANGLOIS, M. R., SANCHEZ-JIMENEZ, F. & WANG, T. C. 2004. The C-terminus of rat L-histidine decarboxylase specifically inhibits enzymic activity and disrupts pyridoxal phosphate-dependent interactions with L-histidine substrate

analogues. *Biochem J,* 381**,** 769-78.

FOLKARD, S. & AKERSTEDT, T. 1992. *Sleep, arousal, and performance : a tribute to Bob Wilkinson,* Boston, Birkhäuser.

FORNAL, C. A., LITTO, W. J., METZLER, C. W., MARROSU, F., TADA, K. & JACOBS, B. L. 1994. Single-unit responses of serotonergic dorsal raphe neurons to 5-HT1A agonist and antagonist drug administration in behaving cats. *J Pharmacol Exp Ther,* 270**,** 1345-58.

FORNAL, C. A., METZLER, C. W., GALLEGOS, R. A., VEASEY, S. C., MCCREARY, A. C. & JACOBS, B. L. 1996. WAY-100635, a potent and selective 5-hydroxytryptamine1A antagonist, increases serotonergic neuronal activity in behaving cats: comparison with (S)-WAY-100135. *J Pharmacol Exp Ther,* 278**,** 752-62.

FOULKES, W. D. 1962. Dream reports from different stages of sleep. *J Abnorm Soc Psychol,* 65**,** 14-25.

FRANK, M. G., STRYKER, M. P. & TECOTT, L. H. 2002. Sleep and sleep homeostasis in mice lacking the 5-HT2c receptor. *Neuropsychopharmacology,* 27**,** 869-73.

FREDRIKSSON, R., LAGERSTROM, M. C., LUNDIN, L. G. & SCHIOTH, H. B. 2003. The G-protein-coupled receptors in the human genome form five main families. Phylogenetic analysis, paralogon groups, and fingerprints. *Mol Pharmacol,* 63**,** 1256-72.

FREMEAU, R. T., JR., BURMAN, J., QURESHI, T., TRAN, C. H., PROCTOR, J., JOHNSON, J., ZHANG, H., SULZER, D., COPENHAGEN, D. R., STORM-MATHISEN, J., REIMER, R. J., CHAUDHRY, F. A. & EDWARDS, R. H. 2002. The identification of vesicular glutamate transporter 3 suggests novel modes of signaling by glutamate. *Proc Natl Acad Sci U S A,* 99**,** 14488-93.

FU, W., LE MAITRE, E., FABRE, V., BERNARD, J. F., DAVID XU, Z. Q. & HOKFELT, T. 2010. Chemical neuroanatomy of the dorsal raphe nucleus and adjacent structures of the mouse brain. *J Comp Neurol,* 518**,** 3464-94.

GALLAGER, D. W. & AGHAJANIAN, G. K. 1976. Effect of antipsychotic drugs on the firing of dorsal raphe cells. II. Reversal by picrotoxin. *Eur J Pharmacol,* 39**,** 357-64.

GALLOPIN, T., FORT, P., EGGERMANN, E., CAULI, B., LUPPI, P. H., ROSSIER, J., AUDINAT, E., MUHLETHALER, M. & SERAFIN, M. 2000. Identification of sleep-promoting neurons in vitro. *Nature,* 404**,** 992-5.

GALLOPIN, T., LUPPI, P. H., RAMBERT, F. A., FRYDMAN, A. & FORT, P. 2004. Effect of the wake-promoting agent modafinil on sleep-promoting neurons from the ventrolateral preoptic nucleus: an in vitro pharmacologic study. *Sleep,* 27**,** 19-25.

GAO, B., FRITSCHY, J. M., BENKE, D. & MOHLER, H. 1993. Neuron-specific expression of GABAA-receptor subtypes: differential association of the alpha 1- and alpha 3-subunits with serotonergic and GABAergic neurons. *Neuroscience,* 54**,** 881-92.

GARBARG, M. & SCHWARTZ, J. C. 1988. Synergism between histamine H1- and H2-receptors in the cAMP response in guinea pig brain slices: effects of phorbol esters and calcium. *Mol Pharmacol,* 33**,** 38-43.

GARRATT, J. C., CRESPI, F., MASON, R. & MARSDEN, C. A. 1991. Effects of idazoxan on dorsal raphe 5-hydroxytryptamine neuronal function. *Eur J Pharmacol,* 193**,** 87-93.

GARRATT, J. C., KIDD, E. J., WRIGHT, I. K. & MARSDEN, C. A. 1991. Inhibition of 5-hydroxytryptamine neuronal activity by the 5-HT agonist, DOI. *Eur J Pharmacol,* 199**,** 349-55.

GARTSIDE, S. E., UMBERS, V., HAJOS, M. & SHARP, T. 1995. Interaction between a selective 5-HT1A receptor antagonist and an SSRI in vivo: effects on 5-HT cell firing and extracellular 5-HT. *Br J Pharmacol,* 115**,** 1064-70.

GERASHCHENKO, D., KOHLS, M. D., GRECO, M., WALEH, N. S., SALIN-PASCUAL, R., KILDUFF, T. S., LAPPI, D. A. & SHIROMANI, P. J. 2001. Hypocretin-2-saporin lesions of the lateral hypothalamus produce narcoleptic-like sleep behavior in the rat. *J Neurosci,* 21**,** 7273-83.

GERVASONI, D., PANCONI, E., HENNINOT, V., BOISSARD, R., BARBAGLI, B., FORT, P. & LUPPI, P. H. 2002. Effect of chronic treatment with milnacipran on sleep architecture in rats compared with paroxetine and imipramine. *Pharmacol Biochem Behav,* 73**,** 557-63.

GERVASONI, D., PEYRON, C., RAMPON, C., BARBAGLI, B., CHOUVET, G., URBAIN, N., FORT, P. & LUPPI, P. H. 2000. Role and origin of the GABAergic innervation of dorsal raphe serotonergic neurons. *J Neurosci,* 20**,** 4217-25.

GISSELMANN, G., PUSCH, H., HOVEMANN, B. T. & HATT, H. 2002. Two cDNAs coding for histamine-gated ion channels in D. melanogaster. *Nat Neurosci,* 5**,** 11-2.

GOCHO, Y., SAKAI, A., YANAGAWA, Y., SUZUKI, H. & SAITOW, F. 2013. Electrophysiological and pharmacological properties of GABAergic cells in the dorsal raphe nucleus. *J Physiol Sci,* 63**,** 147-54.

GOLDBERG, M. J., SPECTOR, R. & CHIANG, C. K. 1987. Transport of diphenhydramine in the central nervous system. *J Pharmacol Exp Ther,* 240**,** 717-22.

GONG, H., MCGINTY, D., GUZMAN-MARIN, R., CHEW, K. T., STEWART, D. & SZYMUSIAK, R. 2004. Activation of c-fos in GABAergic neurones in the preoptic area during sleep and in response to sleep deprivation. *J Physiol,* 556**,** 935-46.

GONG, H., SZYMUSIAK, R., KING, J., STEININGER, T. & MCGINTY, D. 2000. Sleep-related c-Fos protein expression in the preoptic hypothalamus: effects of ambient warming. *Am J Physiol Regul Integr Comp Physiol,* 279**,** R2079-88.

GOODFELLOW, N. M., BAILEY, C. D. & LAMBE, E. K. 2012. The native serotonin 5-HT(5A) receptor: electrophysiological characterization in rodent cortex and 5-HT(1A)-mediated compensatory plasticity in the knock-out mouse. *J Neurosci,* 32**,** 5804-9.

GORELOVA, N. & REINER, P. B. 1996. Histamine depolarizes cholinergic septal neurons. *J Neurophysiol,* 75**,** 707-14.

GUREVICH, V. V. & GUREVICH, E. V. 2008. How and why do GPCRs dimerize? *Trends Pharmacol Sci,* 29**,** 234-40.

HAAS, H. & PANULA, P. 2003. The role of histamine and the tuberomamillary nucleus in the nervous system. *Nat Rev Neurosci,* 4**,** 121-30.

HAAS, H. L., SERGEEVA, O. A. & SELBACH, O. 2008. Histamine in the nervous system. *Physiol Rev,* 88**,** 1183-241.

HADDJERI, N., LAVOIE, N. & BLIER, P. 2004. Electrophysiological evidence for the tonic activation of 5-HT(1A) autoreceptors in the rat dorsal raphe nucleus. *Neuropsychopharmacology,* 29**,** 1800-6.

HAGAN, C. E., MCDEVITT, R. A., LIU, Y., FURAY, A. R. & NEUMAIER, J. F. 2012. 5-HT(1B) autoreceptor regulation of serotonin transporter activity in synaptosomes. *Synapse,* 66**,** 1024-34.

HAJ-DAHMANE, S. & SHEN, R. Y. 2005. The wake-promoting peptide orexin-B inhibits glutamatergic transmission to dorsal raphe nucleus serotonin neurons through retrograde endocannabinoid signaling. *J Neurosci,* 25**,** 896-905.

HAJOS, M., HOFFMANN, W. E., TETKO, I. V., HYLAND, B., SHARP, T. & VILLA, A. E. 2001. Different tonic regulation of neuronal activity in the rat dorsal raphe and medial prefrontal cortex via 5-HT(1A) receptors. *Neurosci Lett,* 304**,** 129-32.

HALLANGER, A. E., LEVEY, A. I., LEE, H. J., RYE, D. B. & WAINER, B. H. 1987. The origins of cholinergic and other subcortical afferents to the thalamus in the rat. *J Comp Neurol,* 262**,** 105-24.

HARDIE, R. C. 1989. A histamine-activated chloride channel involved in neurotransmission at a photoreceptor synapse. *Nature,* 339**,** 704-6.

HASSANI, O. K., LEE, M. G. & JONES, B. E. 2009. Melanin-concentrating hormone neurons

discharge in a reciprocal manner to orexin neurons across the sleep-wake cycle. *Proc Natl Acad Sci U S A,* 106**,** 2418-22.

HENNY, P. & JONES, B. E. 2008. Projections from basal forebrain to prefrontal cortex comprise cholinergic, GABAergic and glutamatergic inputs to pyramidal cells or interneurons. *Eur J Neurosci,* 27**,** 654-70.

HERRICK-DAVIS, K. 2013. Functional significance of serotonin receptor dimerization. *Exp Brain Res,* 230**,** 375-86.

HERRICK-DAVIS, K., GRINDE, E. & MAZURKIEWICZ, J. E. 2004. Biochemical and biophysical characterization of serotonin 5-HT2C receptor homodimers on the plasma membrane of living cells. *Biochemistry,* 43**,** 13963-71.

HERRICK-DAVIS, K., GRINDE, E. & TEITLER, M. 2000. Inverse agonist activity of atypical antipsychotic drugs at human 5-hydroxytryptamine2C receptors. *J Pharmacol Exp Ther,* 295**,** 226-32.

HERRING, W. J., SNYDER, E., BUDD, K., HUTZELMANN, J., SNAVELY, D., LIU, K., LINES, C., ROTH, T. & MICHELSON, D. 2012. Orexin receptor antagonism for treatment of insomnia: a randomized clinical trial of suvorexant. *Neurology,* 79**,** 2265-74.

HINDMARCH, I. & SHAMSI, Z. 1999. Antihistamines: models to assess sedative properties, assessment of sedation, safety and other side-effects. *Clin Exp Allergy,* 29 Suppl 3**,** 133-42.

HOANG, Q. V., BAJIC, D., YANAGISAWA, M., NAKAJIMA, S. & NAKAJIMA, Y. 2003. Effects of orexin (hypocretin) on GIRK channels. *J Neurophysiol,* 90**,** 693-702.

HOEVER, P., DE HAAS, S. L., DORFFNER, G., CHIOSSI, E., VAN GERVEN, J. M. & DINGEMANSE, J. 2012. Orexin receptor antagonism: an ascending multiple-dose study with almorexant. *J Psychopharmacol,* 26**,** 1071-80.

HOEVER, P., DORFFNER, G., BENES, H., PENZEL, T., DANKER-HOPFE, H., BARBANOJ, M. J., PILLAR, G., SALETU, B., POLO, O., KUNZ, D., ZEITLHOFER, J., BERG, S., PARTINEN, M., BASSETTI, C. L., HOGL, B., EBRAHIM, I. O., HOLSBOER-TRACHSLER, E., BENGTSSON, H., PEKER, Y., HEMMETER, U. M., CHIOSSI, E., HAJAK, G. & DINGEMANSE, J. 2012. Orexin receptor antagonism, a new sleep-enabling paradigm: a proof-of-concept clinical trial. *Clin Pharmacol Ther,* 91**,** 975-85.

HOYER, D., HANNON, J. P. & MARTIN, G. R. 2002. Molecular, pharmacological and functional diversity of 5-HT receptors. *Pharmacol Biochem Behav,* 71**,** 533-54.

IDZIKOWSKI, C., MILLS, F. J. & GLENNARD, R. 1986. 5-Hydroxytryptamine-2 antagonist increases human slow wave sleep. *Brain Res,* 378**,** 164-8.

IZUMI, N., MIZUGUCHI, H., UMEHARA, H., OGINO, S. & FUKUI, H. 2008. Evaluation of efficacy and sedative profiles of H(1) antihistamines by large-scale surveillance using the visual analogue scale (VAS). *Allergol Int,* 57**,** 257-63.

JACOBS, B. L. & AZMITIA, E. C. 1992. Structure and function of the brain serotonin system. *Physiol Rev,* 72**,** 165-229.

JANKOWSKI, M. P. & SESACK, S. R. 2004. Prefrontal cortical projections to the rat dorsal raphe nucleus: ultrastructural features and associations with serotonin and gamma-aminobutyric acid neurons. *J Comp Neurol,* 468**,** 518-29.

JEGO, S., GLASGOW, S. D., HERRERA, C. G., EKSTRAND, M., REED, S. J., BOYCE, R., FRIEDMAN, J., BURDAKOV, D. & ADAMANTIDIS, A. R. 2013. Optogenetic identification of a rapid eye movement sleep modulatory circuit in the hypothalamus. *Nat Neurosci,* 16**,** 1637-43.

JEONG, H. J., LAM, K., MITCHELL, V. A. & VAUGHAN, C. W. 2013. Serotonergic modulation of neuronal activity in rat midbrain periaqueductal gray. *J Neurophysiol,* 109**,** 2712-9.

JONES, B. E. 2004. Activity, modulation and role of basal forebrain cholinergic neurons innervating the cerebral cortex. *Prog Brain Res,* 145**,** 157-69.

JONNAKUTY, C. & GRAGNOLI, C. 2008. What do we know about serotonin? *J Cell Physiol,* 217**,** 301-6.

JOUVET, M. 1968. Insomnia and decrease of cerebral 5-hydroxytryptamine after destruction of the raphe system in the cat. *Adv Pharmacol,* 6**,** 265-79.

JOUVET, M. 1969. Biogenic amines and the states of sleep. *Science,* 163**,** 32-41.

JOUVET, M. 1972. The role of monoamines and acetylcholine-containing neurons in the regulation of the sleep-waking cycle. *Ergeb Physiol,* 64**,** 166-307.

JUDGE, S. J. & GARTSIDE, S. E. 2006. Firing of 5-HT neurones in the dorsal and median raphe nucleus in vitro shows differential alpha1-adrenoceptor and 5-HT1A receptor modulation. *Neurochem Int,* 48**,** 100-7.

JUDGE, S. J., INGRAM, C. D. & GARTSIDE, S. E. 2004. GABA receptor modulation of 5-HT neuronal firing: characterization and effect of moderate in vivo variations in glucocorticoid levels. *Neurochem Int,* 45**,** 1057-65.

KARLIN, A. 1967. On the application of "a plausible model" of allosteric proteins to the receptor for acetylcholine. *J Theor Biol,* 16**,** 306-20.

KARTERIS, E., MACHADO, R. J., CHEN, J., ZERVOU, S., HILLHOUSE, E. W. & RANDEVA, H. S. 2005. Food deprivation differentially modulates orexin receptor expression and signaling in rat hypothalamus and adrenal cortex. *Am J Physiol Endocrinol Metab,* 288**,** E1089-100.

KATAYAMA, J., YAKUSHIJI, T. & AKAIKE, N. 1997. Characterization of the K+ current mediated by 5-HT1A receptor in the acutely dissociated rat dorsal raphe neurons. *Brain Res,* 745**,** 283-92.

KELLY, D. W. & SLIKKER, W., JR. 1987. The metabolism and elimination of pyrilamine maleate in the rat. *Drug Metab Dispos,* 15**,** 460-5.

KHILNANI, G. & KHILNANI, A. K. 2011. Inverse agonism and its therapeutic significance. *Indian J Pharmacol,* 43**,** 492-501.

KIDD, E. J., GARRATT, J. C. & MARSDEN, C. A. 1991. Effects of repeated treatment with 1-(2,5-dimethoxy-4-iodophenyl)-2-aminopropane (DOI) on the autoregulatory control of dorsal raphe 5-HT neuronal firing and cortical 5-HT release. *Eur J Pharmacol,* 200**,** 131-9.

KIM, M. A., LEE, H. S., LEE, B. Y. & WATERHOUSE, B. D. 2004. Reciprocal connections between subdivisions of the dorsal raphe and the nuclear core of the locus coeruleus in the rat. *Brain Res,* 1026**,** 56-67.

KIRBY, L. G., PERNAR, L., VALENTINO, R. J. & BECK, S. G. 2003. Distinguishing characteristics of serotonin and non-serotonin-containing cells in the dorsal raphe nucleus: electrophysiological and immunohistochemical studies. *Neuroscience,* 116**,** 669-83.

KIYASOVA, V., BONNAVION, P., SCOTTO-LOMASSESE, S., FABRE, V., SAHLY, I., TRONCHE, F., DENERIS, E., GASPAR, P. & FERNANDEZ, S. P. 2013. A subpopulation of serotonergic neurons that do not express the 5-HT1A autoreceptor. *ACS Chem Neurosci,* 4**,** 89-95.

KOBILKA, B. K. 2007. G protein coupled receptor structure and activation. *Biochim Biophys Acta,* 1768**,** 794-807.

KOELLA, W. P., FELDSTEIN, A. & CZICMAN, J. S. 1968. The effect of para-chlorophenylalanine on the sleep of cats. *Electroencephalogr Clin Neurophysiol,* 25**,** 481-90.

KOHLMEIER, K. A., WATANABE, S., TYLER, C. J., BURLET, S. & LEONARD, C. S. 2008. Dual orexin actions on dorsal raphe and laterodorsal tegmentum neurons: noisy cation current activation and selective enhancement of Ca2+ transients mediated by L-type calcium channels. *J Neurophysiol,* 100**,** 2265-81.

KOLLONITSCH, J., PERKINS, L. M., PATCHETT, A. A., DOLDOURAS, G. A., MARBURG, S., DUGGAN, D. E., MAYCOCK, A. L. & ASTER, S. D. 1978. Selective inhibitors of biosynthesis of aminergic neurotransmitters. *Nature,* 274**,** 906-8.

KREBS-THOMSON, K., PAULUS, M. P. & GEYER, M. A. 1998. Effects of hallucinogens on locomotor and investigatory activity and patterns: influence of 5-HT2A and 5-HT2C receptors. *Neuropsychopharmacology,* 18**,** 339-51.

KROUT, K. E., BELZER, R. E. & LOEWY, A. D. 2002. Brainstem projections to midline and intralaminar thalamic nuclei of the rat. *J Comp Neurol,* 448**,** 53-101.

LAKOSKI, J. M. & AGHAJANIAN, G. K. 1983. Effects of histamine, H1- and H2-receptor antagonists on the activity of serotonergic neurons in the dorsal raphe nucleus. *J Pharmacol Exp Ther,* 227**,** 517-23.

LAKOSKI, J. M., GALLAGER, D. W. & AGHAJANIAN, G. K. 1984. Histamine-induced depression of serotoninergic dorsal raphe neurons: antagonism by cimetidine, a reevaluation. *Eur J Pharmacol,* 103**,** 153-6.

LAUDER, J. M. & BLOOM, F. E. 1974. Ontogeny of monoamine neurons in the locus coeruleus, Raphe nuclei and substantia nigra of the rat. I. Cell differentiation. *J Comp Neurol,* 155**,** 469-81.

LEE, H. S., KIM, M. A., VALENTINO, R. J. & WATERHOUSE, B. D. 2003. Glutamatergic afferent projections to the dorsal raphe nucleus of the rat. *Brain Res,* 963**,** 57-71.

LEE, H. S., LEE, B. Y. & WATERHOUSE, B. D. 2005. Retrograde study of projections from the tuberomammillary nucleus to the dorsal raphe and the locus coeruleus in the rat. *Brain Res,* 1043**,** 65-75.

LEE, H. S., PARK, S. H., SONG, W. C. & WATERHOUSE, B. D. 2005. Retrograde study of hypocretin-1 (orexin-A) projections to subdivisions of the dorsal raphe nucleus in the rat. *Brain Res,* 1059**,** 35-45.

LEE, S. B., CHANG, B. J. & LEE, H. S. 2008. Organization of histamine-immunoreactive, tuberomammillary neurons projecting to the dorsal tier of the substantia nigra compacta in the rat. *Brain Res,* 1203**,** 79-88.

LEFF, P. 1995. The two-state model of receptor activation. *Trends Pharmacol Sci,* 16**,** 89-97.

LEMOS, J. C., PAN, Y. Z., MA, X., LAMY, C., AKANWA, A. C. & BECK, S. G. 2006. Selective 5-HT receptor inhibition of glutamatergic and GABAergic synaptic activity in the rat dorsal and median raphe. *Eur J Neurosci,* 24**,** 3415-30.

LEURS, R., CHURCH, M. K. & TAGLIALATELA, M. 2002. H1-antihistamines: inverse agonism, anti-inflammatory actions and cardiac effects. *Clin Exp Allergy,* 32**,** 489-98.

LEVINE, E. S. & JACOBS, B. L. 1992. Neurochemical afferents controlling the activity of

serotonergic neurons in the dorsal raphe nucleus: microiontophoretic studies in the awake cat. *J Neurosci,* 12**,** 4037-44.

LIM, A. S., LOZANO, A. M., MORO, E., HAMANI, C., HUTCHISON, W. D., DOSTROVSKY, J. O., LANG, A. E., WENNBERG, R. A. & MURRAY, B. J. 2007. Characterization of REM-sleep associated ponto-geniculo-occipital waves in the human pons. *Sleep,* 30**,** 823-7.

LIU, R., JOLAS, T. & AGHAJANIAN, G. 2000. Serotonin 5-HT(2) receptors activate local GABA inhibitory inputs to serotonergic neurons of the dorsal raphe nucleus. *Brain Res,* 873**,** 34-45.

LIU, R. J., LAMBE, E. K. & AGHAJANIAN, G. K. 2005. Somatodendritic autoreceptor regulation of serotonergic neurons: dependence on L-tryptophan and tryptophan hydroxylase-activating kinases. *Eur J Neurosci,* 21**,** 945-58.

LIU, R. J., VAN DEN POL, A. N. & AGHAJANIAN, G. K. 2002. Hypocretins (orexins) regulate serotonin neurons in the dorsal raphe nucleus by excitatory direct and inhibitory indirect actions. *J Neurosci,* 22**,** 9453-64.

LJUBIC-THIBAL, V., MORIN, A., DIKSIC, M. & HAMEL, E. 1999. Origin of the serotonergic innervation to the rat dorsolateral hypothalamus: retrograde transport of cholera toxin and upregulation of tryptophan hydroxylase mRNA expression following selective nerve terminals lesion. *Synapse,* 32**,** 177-86.

LO, C. C., CHOU, T., PENZEL, T., SCAMMELL, T. E., STRECKER, R. E., STANLEY, H. E. & IVANOV, P. 2004. Common scale-invariant patterns of sleep-wake transitions across mammalian species. *Proc Natl Acad Sci U S A,* 101**,** 17545-8.

LOWRY, C. A., EVANS, A. K. & GASSER, P. J. 2007. *Serotonin : molecular, functional and clinical aspects,* Boston, MA, Birkhaeuser Verlag AG, Boston/Basel/Berlin.

LU, J., BJORKUM, A. A., XU, M., GAUS, S. E., SHIROMANI, P. J. & SAPER, C. B. 2002. Selective activation of the extended ventrolateral preoptic nucleus during rapid eye movement sleep. *J Neurosci,* 22**,** 4568-76.

LU, J., SHERMAN, D., DEVOR, M. & SAPER, C. B. 2006. A putative flip-flop switch for control of REM sleep. *Nature,* 441**,** 589-94.

LUPPI, P. H., GERVASONI, D., VERRET, L., GOUTAGNY, R., PEYRON, C., SALVERT, D., LEGER, L. & FORT, P. 2006. Paradoxical (REM) sleep genesis: the switch from an aminergic-cholinergic to a GABAergic-glutamatergic hypothesis. *J Physiol Paris,* 100**,** 271-83.

MAGUIRE, E. P., MITCHELL, E. A., GREIG, S. J., CORTEEN, N., BALFOUR, D. J., SWINNY, J. D., LAMBERT, J. J. & BELELLI, D. 2014. Extrasynaptic glycine receptors of rodent dorsal raphe serotonergic neurons: a sensitive target for ethanol.

Neuropsychopharmacology, 39**,** 1232-44.

MANNING, K. A., WILSON, J. R. & UHLRICH, D. J. 1996. Histamine-immunoreactive neurons and their innervation of visual regions in the cortex, tectum, and thalamus in the primate Macaca mulatta. *J Comp Neurol,* 373**,** 271-82.

MANNS, I. D., MAINVILLE, L. & JONES, B. E. 2001. Evidence for glutamate, in addition to acetylcholine and GABA, neurotransmitter synthesis in basal forebrain neurons projecting to the entorhinal cortex. *Neuroscience,* 107**,** 249-63.

MARCUS, J. N., ASCHKENASI, C. J., LEE, C. E., CHEMELLI, R. M., SAPER, C. B., YANAGISAWA, M. & ELMQUIST, J. K. 2001. Differential expression of orexin receptors 1 and 2 in the rat brain. *J Comp Neurol,* 435**,** 6-25.

MARTINEZ-MIR, M. I., POLLARD, H., MOREAU, J., ARRANG, J. M., RUAT, M., TRAIFFORT, E., SCHWARTZ, J. C. & PALACIOS, J. M. 1990. Three histamine receptors (H1, H2 and H3) visualized in the brain of human and non-human primates. *Brain Res,* 526**,** 322-7.

MC, I. W. & PAGE, I. H. 1959. The metabolism of serotonin (5-hydroxytryptamine). *J Biol Chem,* 234**,** 858-64.

MCCARDLE, C. E. & GARTSIDE, S. E. 2012. Effects of general anaesthetics on 5-HT neuronal activity in the dorsal raphe nucleus. *Neuropharmacology,* 62**,** 1787-96.

MCCORMICK, D. A. & WILLIAMSON, A. 1989. Convergence and divergence of neurotransmitter action in human cerebral cortex. *Proc Natl Acad Sci U S A,* 86**,** 8098-102.

MCCORMICK, D. A. & WILLIAMSON, A. 1991. Modulation of neuronal firing mode in cat and guinea pig LGNd by histamine: possible cellular mechanisms of histaminergic control of arousal. *J Neurosci,* 11**,** 3188-99.

MCGINTY, D. J. & HARPER, R. M. 1976. Dorsal raphe neurons: depression of firing during sleep in cats. *Brain Res,* 101**,** 569-75.

MCGREW, L., CHANG, M. S. & SANDERS-BUSH, E. 2002. Phospholipase D activation by endogenous 5-hydroxytryptamine 2C receptors is mediated by Galpha13 and pertussis toxin-insensitive Gbetagamma subunits. *Mol Pharmacol,* 62**,** 1339-43.

MCKENNA, D. J. & SAAVEDRA, J. M. 1987. Autoradiography of LSD and 2,5-dimethoxyphenylisopropylamine psychotomimetics demonstrates regional, specific cross-displacement in the rat brain. *Eur J Pharmacol,* 142**,** 313-5.

MERICA, H. & FORTUNE, R. D. 2004. State transitions between wake and sleep, and within the ultradian cycle, with focus on the link to neuronal activity. *Sleep Med Rev,* 8**,** 473-85.

MERICKEL, A. & EDWARDS, R. H. 1995. Transport of histamine by vesicular monoamine transporter-2. *Neuropharmacology,* 34**,** 1543-7.

MICHELSEN, K. A., SCHMITZ, C. & STEINBUSCH, H. W. 2007. The dorsal raphe nucleus--from silver stainings to a role in depression. *Brain Res Rev,* 55**,** 329-42.

MILLER, J. D., FARBER, J., GATZ, P., ROFFWARG, H. & GERMAN, D. C. 1983. Activity of mesencephalic dopamine and non-dopamine neurons across stages of sleep and walking in the rat. *Brain Res,* 273**,** 133-41.

MOHAMMAD-ZADEH, L. F., MOSES, L. & GWALTNEY-BRANT, S. M. 2008. Serotonin: a review. *J Vet Pharmacol Ther,* 31**,** 187-99.

MOLINOFF, P. B. & AXELROD, J. 1971. Biochemistry of catecholamines. *Annu Rev Biochem,* 40**,** 465-500.

MOLLEMAN, A. 2002. *Patch Clamping: An Introductory Guide to Patch Clamp Electrophysiology*, Wiley.

MOLLEMAN, A. 2003. *Patch clamping : an introductory guide to patch clamp electrophysiology,* New York, J. Wiley.

MONCZOR, F., FERNANDEZ, N., FITZSIMONS, C. P., SHAYO, C. & DAVIO, C. 2013. Antihistaminergics and inverse agonism: Potential therapeutic applications. *Eur J Pharmacol,* 715**,** 26-32.

MONOD, J., WYMAN, J. & CHANGEUX, J. P. 1965. On the Nature of Allosteric Transitions: A Plausible Model. *J Mol Biol,* 12**,** 88-118.

MONTI, J. M. 2010. The role of dorsal raphe nucleus serotonergic and non-serotonergic neurons, and of their receptors, in regulating waking and rapid eye movement (REM) sleep. *Sleep Med Rev,* 14**,** 319-27.

MONTI, J. M. 2011. Serotonin control of sleep-wake behavior. *Sleep Med Rev,* 15**,** 269-81.

MONTI, J. M. & JANTOS, H. 1992. Dose-dependent effects of the 5-HT1A receptor agonist 8-OH-DPAT on sleep and wakefulness in the rat. *J Sleep Res,* 1**,** 169-175.

MONTI, J. M. & JANTOS, H. 1994. Stereoselective antagonism by the pindolol enantiomers of 8-OH-DPAT-induced changes of sleep and wakefulness. *Neuropharmacology,* 33**,** 705-8.

MONTI, J. M. & JANTOS, H. 2003. Differential effects of the 5-HT1A receptor agonist flesinoxan given locally or systemically on REM sleep in the rat. *Eur J Pharmacol,* 478**,** 121-30.

MONTI, J. M. & JANTOS, H. 2006. Effects of activation and blockade of 5-HT2A/2C receptors in the dorsal raphe nucleus on sleep and waking in the rat. *Prog Neuropsychopharmacol Biol Psychiatry,* 30**,** 1189-95.

MONTI, J. M. & JANTOS, H. 2006. Effects of the serotonin 5-HT2A/2C receptor agonist DOI and of the selective 5-HT2A or 5-HT2C receptor antagonists EMD 281014 and SB-243213, respectively, on sleep and waking in the rat. *Eur J Pharmacol,* 553**,** 163-70.

MONTI, J. M. & JANTOS, H. 2011. Effects of the 5-HT(6) receptor antagonists SB-399885 and RO-4368554 and of the 5-HT(2A) receptor antagonist EMD 281014 on sleep and wakefulness in the rat during both phases of the light-dark cycle. *Behav Brain Res,* 216**,** 381-8.

MONTI, J. M., JANTOS, H. & MONTI, D. 2002. Increased REM sleep after intra-dorsal raphe nucleus injection of flesinoxan or 8-OHDPAT: prevention with WAY 100635. *Eur Neuropsychopharmacol,* 12**,** 47-55.

MONTI, J. M., PELLEJERO, T. & JANTOS, H. 1986. Effects of H1- and H2-histamine receptor agonists and antagonists on sleep and wakefulness in the rat. *J Neural Transm,* 66**,** 1-11.

MORAIRTY, S. R., HEDLEY, L., FLORES, J., MARTIN, R. & KILDUFF, T. S. 2008. Selective 5HT2A and 5HT6 receptor antagonists promote sleep in rats. *Sleep,* 31**,** 34-44.

MORIKAWA, H., MANZONI, O. J., CRABBE, J. C. & WILLIAMS, J. T. 2000. Regulation of central synaptic transmission by 5-HT(1B) auto- and heteroreceptors. *Mol Pharmacol,* 58**,** 1271-8.

MORUZZI, G. & MAGOUN, H. W. 1949. Brain stem reticular formation and activation of the EEG. *Electroencephalogr Clin Neurophysiol,* 1**,** 455-73.

MOSKO, S. S. & JACOBS, B. L. 1976. Recording of dorsal raphe unit activity in vitro. *Neurosci Lett,* 2**,** 195-200.

NAMBU, T., SAKURAI, T., MIZUKAMI, K., HOSOYA, Y., YANAGISAWA, M. & GOTO, K. 1999. Distribution of orexin neurons in the adult rat brain. *Brain Res,* 827**,** 243-60.

NEBIGIL, C. G., ETIENNE, N., SCHAERLINGER, B., HICKEL, P., LAUNAY, J. M. & MAROTEAUX, L. 2001. Developmentally regulated serotonin 5-HT2B receptors. *Int J Dev Neurosci,* 19**,** 365-72.

NEU, D., KAJOSCH, H., PEIGNEUX, P., VERBANCK, P., LINKOWSKI, P. & LE BON, O. 2011. Cognitive impairment in fatigue and sleepiness associated conditions. *Psychiatry Res,* 189**,** 128-34.

NEWMAN-TANCREDI, A., CUSSAC, D., MARINI, L., TOUZARD, M. & MILLAN, M. J. 2003. h5-HT(1B) receptor-mediated constitutive Galphai3-protein activation in stably transfected Chinese hamster ovary cells: an antibody capture assay reveals protean efficacy of 5-HT. *Br J Pharmacol,* 138**,** 1077-84.

NICHOLS, D. E. & NICHOLS, C. D. 2008. Serotonin receptors. *Chem Rev,* 108**,** 1614-41.

OLDHAM, W. M. & HAMM, H. E. 2008. Heterotrimeric G protein activation by G-protein-coupled receptors. *Nat Rev Mol Cell Biol,* 9**,** 60-71.

PALACIOS, J. M., WAMSLEY, J. K. & KUHAR, M. J. 1981. The distribution of histamine H1-receptors in the rat brain: an autoradiographic study. *Neuroscience,* 6**,** 15-37.

PALCHAUDHURI, M. & FLUGGE, G. 2005. 5-HT1A receptor expression in pyramidal neurons of cortical and limbic brain regions. *Cell Tissue Res,* 321**,** 159-72.

PAN, Z. Z., GRUDT, T. J. & WILLIAMS, J. T. 1994. Alpha 1-adrenoceptors in rat dorsal raphe neurons: regulation of two potassium conductances. *J Physiol,* 478 Pt 3**,** 437-47.

PANULA, P., PIRVOLA, U., AUVINEN, S. & AIRAKSINEN, M. S. 1989. Histamine-immunoreactive nerve fibers in the rat brain. *Neuroscience,* 28**,** 585-610.

PATEL, P. D., PONTRELLO, C. & BURKE, S. 2004. Robust and tissue-specific expression of TPH2 versus TPH1 in rat raphe and pineal gland. *Biol Psychiatry,* 55**,** 428-33.

PAXINOS, G. & FRANKLIN, K. B. J. 2008. *The Mouse Brain in Stereotaxic Coordinates*, Elsevier Academic Press.

PAXINOS, G. & WATSON, C. 2005. *The rat brain in stereotaxic coordinates*, Elsevier Academic Press.

PAZOS, A., CORTES, R. & PALACIOS, J. M. 1985. Quantitative autoradiographic mapping of serotonin receptors in the rat brain. II. Serotonin-2 receptors. *Brain Res,* 346**,** 231-49.

PENINGTON, N. J., KELLY, J. S. & FOX, A. P. 1993. Whole-cell recordings of inwardly rectifying K+ currents activated by 5-HT1A receptors on dorsal raphe neurones of the adult rat. *J Physiol,* 469**,** 387-405.

PERKINS, K. L. 2006. Cell-attached voltage-clamp and current-clamp recording and stimulation techniques in brain slices. *J Neurosci Methods,* 154**,** 1-18.

PETERS, J. A., COOPER, M. A., CARLAND, J. E., LIVESEY, M. R., HALES, T. G. & LAMBERT, J. J. 2010. Novel structural determinants of single channel conductance and ion selectivity in 5-hydroxytryptamine type 3 and nicotinic acetylcholine receptors. *J Physiol,* 588**,**

587-96.

PEYRON, C., LUPPI, P. H., FORT, P., RAMPON, C. & JOUVET, M. 1996. Lower brainstem catecholamine afferents to the rat dorsal raphe nucleus. *J Comp Neurol,* 364**,** 402-413.

PEYRON, C., PETIT, J. M., RAMPON, C., JOUVET, M. & LUPPI, P. H. 1998. Forebrain afferents to the rat dorsal raphe nucleus demonstrated by retrograde and anterograde tracing methods. *Neuroscience,* 82**,** 443-68.

PEYRON, C., TIGHE, D. K., VAN DEN POL, A. N., DE LECEA, L., HELLER, H. C., SUTCLIFFE, J. G. & KILDUFF, T. S. 1998. Neurons containing hypocretin (orexin) project to multiple neuronal systems. *J Neurosci,* 18**,** 9996-10015.

PILLOT, C., HERON, A., COCHOIS, V., TARDIVEL-LACOMBE, J., LIGNEAU, X., SCHWARTZ, J. C. & ARRANG, J. M. 2002. A detailed mapping of the histamine H(3) receptor and its gene transcripts in rat brain. *Neuroscience,* 114**,** 173-93.

POLLARD, H., MOREAU, J., ARRANG, J. M. & SCHWARTZ, J. C. 1993. A detailed autoradiographic mapping of histamine H3 receptors in rat brain areas. *Neuroscience,* 52**,** 169-89.

POPA, D., LENA, C., FABRE, V., PRENAT, C., GINGRICH, J., ESCOURROU, P., HAMON, M. & ADRIEN, J. 2005. Contribution of 5-HT2 receptor subtypes to sleep-wakefulness and respiratory control, and functional adaptations in knock-out mice lacking 5-HT2A receptors. *J Neurosci,* 25**,** 11231-8.

PORTAS, C. M., BJORVATN, B., FAGERLAND, S., GRONLI, J., MUNDAL, V., SORENSEN, E. & URSIN, R. 1998. On-line detection of extracellular levels of serotonin in dorsal raphe nucleus and frontal cortex over the sleep/wake cycle in the freely moving rat. *Neuroscience,* 83**,** 807-14.

PORTAS, C. M. & MCCARLEY, R. W. 1994. Behavioral state-related changes of extracellular serotonin concentration in the dorsal raphe nucleus: a microdialysis study in the freely moving cat. *Brain Res,* 648**,** 306-12.

PORTAS, C. M., THAKKAR, M., RAINNIE, D. & MCCARLEY, R. W. 1996. Microdialysis perfusion of 8-hydroxy-2-(di-n-propylamino)tetralin (8-OH-DPAT) in the dorsal raphe nucleus decreases serotonin release and increases rapid eye movement sleep in the freely moving cat. *J Neurosci,* 16**,** 2820-8.

PUDOVKINA, O. L., CREMERS, T. I. & WESTERINK, B. H. 2003. Regulation of the release of serotonin in the dorsal raphe nucleus by alpha1 and alpha2 adrenoceptors. *Synapse,* 50**,** 77-82.

RAPPORT, M. M., GREEN, A. A. & PAGE, I. H. 1948. Serum vasoconstrictor, serotonin; isolation

and characterization. *J Biol Chem,* 176**,** 1243-51.

RASMUSSEN, K., HEYM, J. & JACOBS, B. L. 1984. Activity of serotonin-containing neurons in nucleus centralis superior of freely moving cats. *Exp Neurol,* 83**,** 302-17.

RASMUSSEN, K., MCCREARY, A. C. & SHANKS, E. A. 2004. Attenuation of the effects of fluoxetine on serotonergic neuronal activity by pindolol in rats. *Neurosci Lett,* 355**,** 1-4.

RAVNA, A. W., SYLTE, I. & DAHL, S. G. 2009. Structure and localisation of drug binding sites on neurotransmitter transporters. *J Mol Model,* 15**,** 1155-64.

RECHTSCHAFFEN, A. & SIEGEL, J. 2012. *Principles of neural science,* New York, McGraw-Hill.

REINER, P. B. & KAMONDI, A. 1994. Mechanisms of antihistamine-induced sedation in the human brain: H1 receptor activation reduces a background leakage potassium current. *Neuroscience,* 59**,** 579-88.

REPPERT, S. M. & WEAVER, D. R. 2002. Coordination of circadian timing in mammals. *Nature,* 418**,** 935-41.

RIAD, M., GARCIA, S., WATKINS, K. C., JODOIN, N., DOUCET, E., LANGLOIS, X., EL MESTIKAWY, S., HAMON, M. & DESCARRIES, L. 2000. Somatodendritic localization of 5-HT1A and preterminal axonal localization of 5-HT1B serotonin receptors in adult rat brain. *J Comp Neurol,* 417**,** 181-94.

RICHELSON, E. 1978. Histamine H1 receptor-mediated guanosine 3',5'-monophosphate formation by cultured mouse neuroblastoma cells. *Science,* 201**,** 69-71.

RODRIGUEZ, J. J., NORISTANI, H. N., HOOVER, W. B., LINLEY, S. B. & VERTES, R. P. 2011. Serotonergic projections and serotonin receptor expression in the reticular nucleus of the thalamus in the rat. *Synapse,* 65**,** 919-28.

RYE, D. B., SAPER, C. B., LEE, H. J. & WAINER, B. H. 1987. Pedunculopontine tegmental nucleus of the rat: cytoarchitecture, cytochemistry, and some extrapyramidal connections of the mesopontine tegmentum. *J Comp Neurol,* 259**,** 483-528.

SAKAI, K. 2011. Sleep-waking discharge profiles of dorsal raphe nucleus neurons in mice. *Neuroscience,* 197**,** 200-24.

SAKAI, K. & CROCHET, S. 2000. Serotonergic dorsal raphe neurons cease firing by disfacilitation during paradoxical sleep. *Neuroreport,* 11**,** 3237-41.

SAKAI, K. & CROCHET, S. 2001. Differentiation of presumed serotonergic dorsal raphe neurons in relation to behavior and wake-sleep states. *Neuroscience,* 104**,** 1141-55.

SAKAI, K. & JOUVET, M. 1980. Brain stem PGO-on cells projecting directly to the cat dorsal lateral geniculate nucleus. *Brain Res,* 194**,** 500-5.

SAKURAI, T., AMEMIYA, A., ISHII, M., MATSUZAKI, I., CHEMELLI, R. M., TANAKA, H., WILLIAMS, S. C., RICHARDSON, J. A., KOZLOWSKI, G. P., WILSON, S., ARCH, J. R., BUCKINGHAM, R. E., HAYNES, A. C., CARR, S. A., ANNAN, R. S., MCNULTY, D. E., LIU, W. S., TERRETT, J. A., ELSHOURBAGY, N. A., BERGSMA, D. J. & YANAGISAWA, M. 1998. Orexins and orexin receptors: a family of hypothalamic neuropeptides and G protein-coupled receptors that regulate feeding behavior. *Cell,* 92**,** 573-85.

SALIM, K., FENTON, T., BACHA, J., URIEN-RODRIGUEZ, H., BONNERT, T., SKYNNER, H. A., WATTS, E., KERBY, J., HEALD, A., BEER, M., MCALLISTER, G. & GUEST, P. C. 2002. Oligomerization of G-protein-coupled receptors shown by selective co-immunoprecipitation. *J Biol Chem,* 277**,** 15482-5.

SAMAMA, P., COTECCHIA, S., COSTA, T. & LEFKOWITZ, R. J. 1993. A mutation-induced activated state of the beta 2-adrenergic receptor. Extending the ternary complex model. *J Biol Chem,* 268**,** 4625-36.

SANFORD, L. D., ROSS, R. J., SEGGOS, A. E., MORRISON, A. R., BALL, W. A. & MANN, G. L. 1994. Central administration of two 5-HT receptor agonists: effect on REM sleep initiation and PGO waves. *Pharmacol Biochem Behav,* 49**,** 93-100.

SAPER, C. B., CHOU, T. C. & SCAMMELL, T. E. 2001. The sleep switch: hypothalamic control of sleep and wakefulness. *Trends Neurosci,* 24**,** 726-31.

SAPER, C. B., FULLER, P. M., PEDERSEN, N. P., LU, J. & SCAMMELL, T. E. 2010. Sleep state switching. *Neuron,* 68**,** 1023-42.

SAPER, C. B. & LEVISOHN, D. 1983. Afferent connections of the median preoptic nucleus in the rat: anatomical evidence for a cardiovascular integrative mechanism in the anteroventral third ventricular (AV3V) region. *Brain Res,* 288**,** 21-31.

SAPER, C. B., SCAMMELL, T. E. & LU, J. 2005. Hypothalamic regulation of sleep and circadian rhythms. *Nature,* 437**,** 1257-63.

SARAS, A., GISSELMANN, G., VOGT-EISELE, A. K., ERLKAMP, K. S., KLETKE, O., PUSCH, H. & HATT, H. 2008. Histamine action on vertebrate GABAA receptors: direct channel gating and potentiation of GABA responses. *J Biol Chem,* 283**,** 10470-5.

SARI, Y. 2004. Serotonin1B receptors: from protein to physiological function and behavior. *Neurosci Biobehav Rev,* 28**,** 565-82.

SATOH, K. & FIBIGER, H. C. 1986. Cholinergic neurons of the laterodorsal tegmental nucleus: efferent and afferent connections. *J Comp Neurol,* 253**,** 277-302.

SCHLICKER, E., WERTHWEIN, S. & ZENTNER, J. 1999. Histamine H3 receptor-mediated inhibition of noradrenaline release in the human brain. *Fundam Clin Pharmacol,* 13**,** 120-2.

SELBACH, O., BROWN, R. E. & HAAS, H. L. 1997. Long-term increase of hippocampal excitability by histamine and cyclic AMP. *Neuropharmacology,* 36**,** 1539-48.

SELBACH, O., BROWN, R. E. & HAAS, H. L. 1997. Long-term increase of hippocampal excitability by histamine and cyclic AMP. *Neuropharmacology,* 36**,** 1539-48.

SERGEEVA, O. A., KOROTKOVA, T. M., SCHERER, A., BROWN, R. E. & HAAS, H. L. 2003. Co-expression of non-selective cation channels of the transient receptor potential canonical family in central aminergic neurones. *J Neurochem,* 85**,** 1547-52.

SERRATS, J., MENGOD, G. & CORTES, R. 2005. Expression of serotonin 5-HT2C receptors in GABAergic cells of the anterior raphe nuclei. *J Chem Neuroanat,* 29**,** 83-91.

SHARPLEY, A. L., ELLIOTT, J. M., ATTENBURROW, M. J. & COWEN, P. J. 1994. Slow wave sleep in humans: role of 5-HT2A and 5-HT2C receptors. *Neuropharmacology,* 33**,** 467-71.

SHEN, R. Y. & ANDRADE, R. 1998. 5-Hydroxytryptamine2 receptor facilitates GABAergic neurotransmission in rat hippocampus. *J Pharmacol Exp Ther,* 285**,** 805-12.

SHERIN, J. E., ELMQUIST, J. K., TORREALBA, F. & SAPER, C. B. 1998. Innervation of histaminergic tuberomammillary neurons by GABAergic and galaninergic neurons in the ventrolateral preoptic nucleus of the rat. *J Neurosci,* 18**,** 4705-21.

SHERIN, J. E., SHIROMANI, P. J., MCCARLEY, R. W. & SAPER, C. B. 1996. Activation of ventrolateral preoptic neurons during sleep. *Science,* 271**,** 216-9.

SHIKANAI, H., YOSHIDA, T., KONNO, K., YAMASAKI, M., IZUMI, T., OHMURA, Y., WATANABE, M. & YOSHIOKA, M. 2012. Distinct neurochemical and functional properties of GAD67-containing 5-HT neurons in the rat dorsal raphe nucleus. *J Neurosci,* 32**,** 14415-26.

SMIT, M. J., LEURS, R., ALEWIJNSE, A. E., BLAUW, J., VAN NIEUW AMERONGEN, G. P., VAN DE VREDE, Y., ROOVERS, E. & TIMMERMAN, H. 1996. Inverse agonism of histamine H2 antagonist accounts for upregulation of spontaneously active histamine H2 receptors. *Proc Natl Acad Sci U S A,* 93**,** 6802-7.

SMITH, B. N. & ARMSTRONG, W. E. 1996. The ionic dependence of the histamine-induced depolarization of vasopressin neurones in the rat supraoptic nucleus. *J Physiol,* 495 (Pt 2)**,** 465-78.

SMITH, B. N. & ARMSTRONG, W. E. 1996. The ionic dependence of the histamine-induced

depolarization of vasopressin neurones in the rat supraoptic nucleus. *J Physiol,* 495 (Pt 2)**,** 465-78.

SMITH, D. A. & GALLAGER, D. W. 1989. Electrophysiological and biochemical characterization of the development of alpha 1-adrenergic and 5-HT1 receptors associated with dorsal raphe neurons. *Brain Res Dev Brain Res,* 46**,** 173-86.

SOIZA-REILLY, M., ANDERSON, W. B., VAUGHAN, C. W. & COMMONS, K. G. 2013. Presynaptic gating of excitation in the dorsal raphe nucleus by GABA. *Proc Natl Acad Sci U S A,* 110**,** 15800-5.

SOIZA-REILLY, M. & COMMONS, K. G. 2011. Glutamatergic drive of the dorsal raphe nucleus. *J Chem Neuroanat,* 41**,** 247-55.

SORENSEN, E., GRONLI, J., BJORVATN, B., BJORKUM, A. & URSIN, R. 2001. Sleep and waking following microdialysis perfusion of the selective 5-HT1A receptor antagonist p-MPPI into the dorsal raphe nucleus in the freely moving rat. *Brain Res,* 897**,** 122-30.

SOTELO, C., CHOLLEY, B., EL MESTIKAWY, S., GOZLAN, H. & HAMON, M. 1990. Direct Immunohistochemical Evidence of the Existence of 5-HT1A Autoreceptors on Serotoninergic Neurons in the Midbrain Raphe Nuclei. *Eur J Neurosci,* 2**,** 1144-1154.

SPIEGEL, A. M. & WEINSTEIN, L. S. 2004. Inherited diseases involving g proteins and g protein-coupled receptors. *Annu Rev Med,* 55**,** 27-39.

SPROUSE, J. S. & AGHAJANIAN, G. K. 1986. (-)-Propranolol blocks the inhibition of serotonergic dorsal raphe cell firing by 5-HT1A selective agonists. *Eur J Pharmacol,* 128**,** 295-8.

SPROUSE, J. S. & AGHAJANIAN, G. K. 1987. Electrophysiological responses of serotoninergic dorsal raphe neurons to 5-HT1A and 5-HT1B agonists. *Synapse,* 1**,** 3-9.

STAMFORD, J. A., DAVIDSON, C., MCLAUGHLIN, D. P. & HOPWOOD, S. E. 2000. Control of dorsal raphe 5-HT function by multiple 5-HT(1) autoreceptors: parallel purposes or pointless plurality? *Trends Neurosci,* 23**,** 459-65.

STANTON, J. A. & BEER, M. S. 1997. Characterisation of a cloned human 5-HT1A receptor cell line using [35S]GTP gamma S binding. *Eur J Pharmacol,* 320**,** 267-75.

STEINBUSCH, H. W. 1981. Distribution of serotonin-immunoreactivity in the central nervous system of the rat-cell bodies and terminals. *Neuroscience,* 6**,** 557-618.

STEININGER, T. L., GONG, H., MCGINTY, D. & SZYMUSIAK, R. 2001. Subregional organization of preoptic area/anterior hypothalamic projections to arousal-related monoaminergic cell groups. *J Comp Neurol,* 429**,** 638-53.

STERIADE, M. 1994. Sleep oscillations and their blockage by activating systems. *J Psychiatry Neurosci,* 19**,** 354-8.

STERIADE, M. 2005. Sleep, epilepsy and thalamic reticular inhibitory neurons. *Trends Neurosci,* 28**,** 317-24.

STERIADE, M., DATTA, S., PARE, D., OAKSON, G. & CURRO DOSSI, R. C. 1990. Neuronal activities in brain-stem cholinergic nuclei related to tonic activation processes in thalamocortical systems. *J Neurosci,* 10**,** 2541-59.

STEVENS, D. R., ERIKSSON, K. S., BROWN, R. E. & HAAS, H. L. 2001. The mechanism of spontaneous firing in histamine neurons. *Behav Brain Res,* 124**,** 105-12.

STRECKER, R. E., MORAIRTY, S., THAKKAR, M. M., PORKKA-HEISKANEN, T., BASHEER, R., DAUPHIN, L. J., RAINNIE, D. G., PORTAS, C. M., GREENE, R. W. & MCCARLEY, R. W. 2000. Adenosinergic modulation of basal forebrain and preoptic/anterior hypothalamic neuronal activity in the control of behavioral state. *Behav Brain Res,* 115**,** 183-204.

SZYMUSIAK, R., ALAM, N., STEININGER, T. L. & MCGINTY, D. 1998. Sleep-waking discharge patterns of ventrolateral preoptic/anterior hypothalamic neurons in rats. *Brain Res,* 803**,** 178-88.

TAKAHASHI, K., KAYAMA, Y., LIN, J. S. & SAKAI, K. 2010. Locus coeruleus neuronal activity during the sleep-waking cycle in mice. *Neuroscience,* 169**,** 1115-26.

TAKAHASHI, K., LIN, J. S. & SAKAI, K. 2006. Neuronal activity of histaminergic tuberomammillary neurons during wake-sleep states in the mouse. *J Neurosci,* 26**,** 10292-8.

TAKAHASHI, K., LIN, J. S. & SAKAI, K. 2008. Neuronal activity of orexin and non-orexin waking-active neurons during wake-sleep states in the mouse. *Neuroscience,* 153**,** 860-70.

TAKAHASHI, K., LIN, J. S. & SAKAI, K. 2009. Characterization and mapping of sleep-waking specific neurons in the basal forebrain and preoptic hypothalamus in mice. *Neuroscience,* 161**,** 269-92.

TAKAHASHI, K., WANG, Q. P., GUAN, J. L., KAYAMA, Y., SHIODA, S. & KOYAMA, Y. 2005. State-dependent effects of orexins on the serotonergic dorsal raphe neurons in the rat. *Regul Pept,* 126**,** 43-7.

TANAKA, H., HAYASHI, M. & HORI, T. 2000. Topographical characteristics of slow wave activities during the transition from wakefulness to sleep. *Clin Neurophysiol,* 111**,** 417-27.

TAO, R., MA, Z., MCKENNA, J. T., THAKKAR, M. M., WINSTON, S., STRECKER, R. E. & MCCARLEY, R. W. 2006. Differential effect of orexins (hypocretins) on serotonin release in the dorsal and median raphe nuclei of freely behaving rats. *Neuroscience,* 141**,** 1101-5.

TRIARHOU, L. C. 2006. The percipient observations of Constantin von Economo on encephalitis lethargica and sleep disruption and their lasting impact on contemporary sleep research. *Brain Res Bull,* 69**,** 244-58.

TRIVEDI, P., YU, H., MACNEIL, D. J., VAN DER PLOEG, L. H. & GUAN, X. M. 1998. Distribution of orexin receptor mRNA in the rat brain. *FEBS Lett,* 438**,** 71-5.

TRULSON, M. E. & CRISP, T. 1984. Role of norepinephrine in regulating the activity of serotonin-containing dorsal raphe neurons. *Life Sci,* 35**,** 511-5.

TRULSON, M. E. & CRISP, T. 1986. Do serotonin-containing dorsal raphe neurons possess autoreceptors? *Exp Brain Res,* 62**,** 579-86.

UNNO, K., OZAKI, T., MOHAMMAD, S., TSUNO, S., IKEDA-SAGARA, M., HONDA, K. & IKEDA, M. 2012. First and second generation H(1) histamine receptor antagonists produce different sleep-inducing profiles in rats. *Eur J Pharmacol,* 683**,** 179-85.

URBAIN, N., CREAMER, K. & DEBONNEL, G. 2006. Electrophysiological diversity of the dorsal raphe cells across the sleep-wake cycle of the rat. *J Physiol,* 573**,** 679-95.

USCHAKOV, A., GONG, H., MCGINTY, D. & SZYMUSIAK, R. 2007. Efferent projections from the median preoptic nucleus to sleep- and arousal-regulatory nuclei in the rat brain. *Neuroscience,* 150**,** 104-20.

VANDERMAELEN, C. P. & AGHAJANIAN, G. K. 1983. Electrophysiological and pharmacological characterization of serotonergic dorsal raphe neurons recorded extracellularly and intracellularly in rat brain slices. *Brain Res,* 289**,** 109-19.

VERTES, R. P. 1991. A PHA-L analysis of ascending projections of the dorsal raphe nucleus in the rat. *J Comp Neurol,* 313**,** 643-68.

VERTES, R. P. & CRANE, A. M. 1997. Distribution, quantification, and morphological characteristics of serotonin-immunoreactive cells of the supralemniscal nucleus (B9) and pontomesencephalic reticular formation in the rat. *J Comp Neurol,* 378**,** 411-24.

VERTES, R. P. & KOCSIS, B. 1994. Projections of the dorsal raphe nucleus to the brainstem: PHA-L analysis in the rat. *J Comp Neurol,* 340**,** 11-26.

WAFFORD, K. A. & EBERT, B. 2008. Emerging anti-insomnia drugs: tackling sleeplessness and the quality of wake time. *Nat Rev Drug Discov,* 7**,** 530-40.

WALTHER, D. J., PETER, J. U., BASHAMMAKH, S., HORTNAGL, H., VOITS, M., FINK, H. & BADER, M. 2003. Synthesis of serotonin by a second tryptophan hydroxylase isoform. *Science,* 299**,** 76.

WANG, Q. P., GUAN, J. L., MATSUOKA, T., HIRAYANA, Y. & SHIODA, S. 2003. Electron microscopic examination of the orexin immunoreactivity in the dorsal raphe nucleus. *Peptides,* 24**,** 925-30.

WANG, Q. P., KOYAMA, Y., GUAN, J. L., TAKAHASHI, K., KAYAMA, Y. & SHIODA, S. 2005. The orexinergic synaptic innervation of serotonin- and orexin 1-receptor-containing neurons in the dorsal raphe nucleus. *Regul Pept,* 126**,** 35-42.

WASELUS, M., VALENTINO, R. J. & VAN BOCKSTAELE, E. J. 2011. Collateralized dorsal raphe nucleus projections: a mechanism for the integration of diverse functions during stress. *J Chem Neuroanat,* 41**,** 266-80.

WEISS, J. M., MORGAN, P. H., LUTZ, M. W. & KENAKIN, T. P. 1996. The cubic ternary complex receptor-occupancy model. III. resurrecting efficacy. *J Theor Biol,* 181**,** 381-97.

WILLIAMS, J. T., COLMERS, W. F. & PAN, Z. Z. 1988. Voltage- and ligand-activated inwardly rectifying currents in dorsal raphe neurons in vitro. *J Neurosci,* 8**,** 3499-506.

WOOLF, N. J. & BUTCHER, L. L. 1989. Cholinergic systems in the rat brain: IV. Descending projections of the pontomesencephalic tegmentum. *Brain Res Bull,* 23**,** 519-40.

WRIGHT, I. K., GARRATT, J. C. & MARSDEN, C. A. 1990. Effects of a selective 5-HT2 agonist, DOI, on 5-HT neuronal firing in the dorsal raphe nucleus and 5-HT release and metabolism in the frontal cortex. *Br J Pharmacol,* 99**,** 221-2.

XU, Z. Q. & HOKFELT, T. 1997. Expression of galanin and nitric oxide synthase in subpopulations of serotonin neurons of the rat dorsal raphe nucleus. *J Chem Neuroanat,* 13**,** 169-87.

YANAI, K., RYU, J. H., WATANABE, T., IWATA, R., IDO, T., SAWAI, Y., ITO, K. & ITOH, M. 1995. Histamine H1 receptor occupancy in human brains after single oral doses of histamine H1 antagonists measured by positron emission tomography. *Br J Pharmacol,* 116**,** 1649-55.

YANAI, K. & TASHIRO, M. 2007. The physiological and pathophysiological roles of neuronal histamine: an insight from human positron emission tomography studies. *Pharmacol Ther,* 113**,** 1-15.

YOSHIDA, K., MCCORMACK, S., ESPANA, R. A., CROCKER, A. & SCAMMELL, T. E. 2006. Afferents to the orexin neurons of the rat brain. *J Comp Neurol,* 494**,** 845-61.